Supplement S1

December 15, 2021

1 Step-wise comparison AoB2015

The results from Schymanski et al. (2015) are used as a benchmark and starting point from the current analysis. Several adjustmens have been made in the general set-up of the model, the effects of these choices are assessed in a stepwise approach:

0. Benchmark data
1. Reproducing benchmark results
2. reproducing the optimization of SCE
3. Change atmospheric CO_2 to MaunaLoa records
4. Change soil layer thickness
5. Change atmospheric pressure from fixed to variable
6. Optimize rooting depth grasses as optimizable property
7. Update the weatherdata with new SILO-data
8. Updated and extended meteorological data
9. New hydrology
10. New soils
11. New soil parameters and hydrology

The starting points are therefore the parameters and settings used by Schymanski et al. (2015). From there, one change is included at a time, to see the specific influence of this change.

1.1 Reproducing benchmark results

Here, the vegetation properties are not re-optimized and the outputs of the optimization of Schymanski et al. (2015) are used. Both model runs should therefore produce the same results.

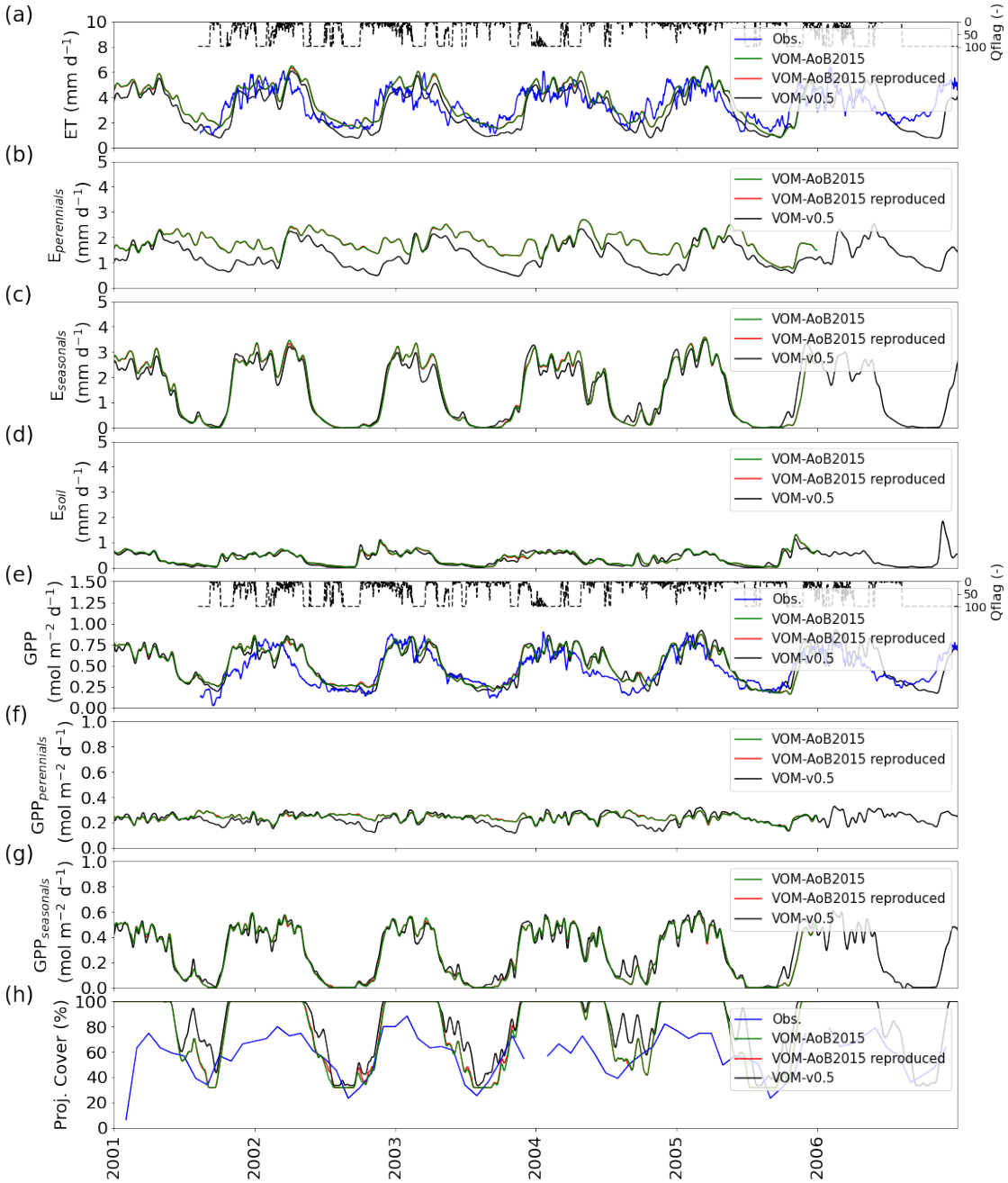

Figure S1.1. *Comparison for Howard Springs from 2001-2006 (subset from 1980-2017) between the results of Schymanski et al. (2015) (VOM-AoB2015, green) and a reproduction of those results (VOM-AoB2015 reproduced,red) based on the best run of the SCE-algorithm from Schymanski et al. (2015), and the new VOM-v0.5 modelling results (black), for a) ET, b) transpiration perennials (trees), c) transpiration seasonals (grasses), d) soil evaporation, e) GPP, f) GPP perennials (trees), g) GPP seasonals (grasses), all smoothed with a moving average of 7 days, and h) projective cover. The daily average quality flags of the fluxtower observations are shown in dashed lines with a value of 100 when a day is completely gap-filled and 1 when it is observed.*

These smoothed results are similar between the reproduced runs, and the original results of Schymanski et al. (2015), but there is a small a shift in time due to leap years, that were not accounted for by Schymanski et al. (2015).

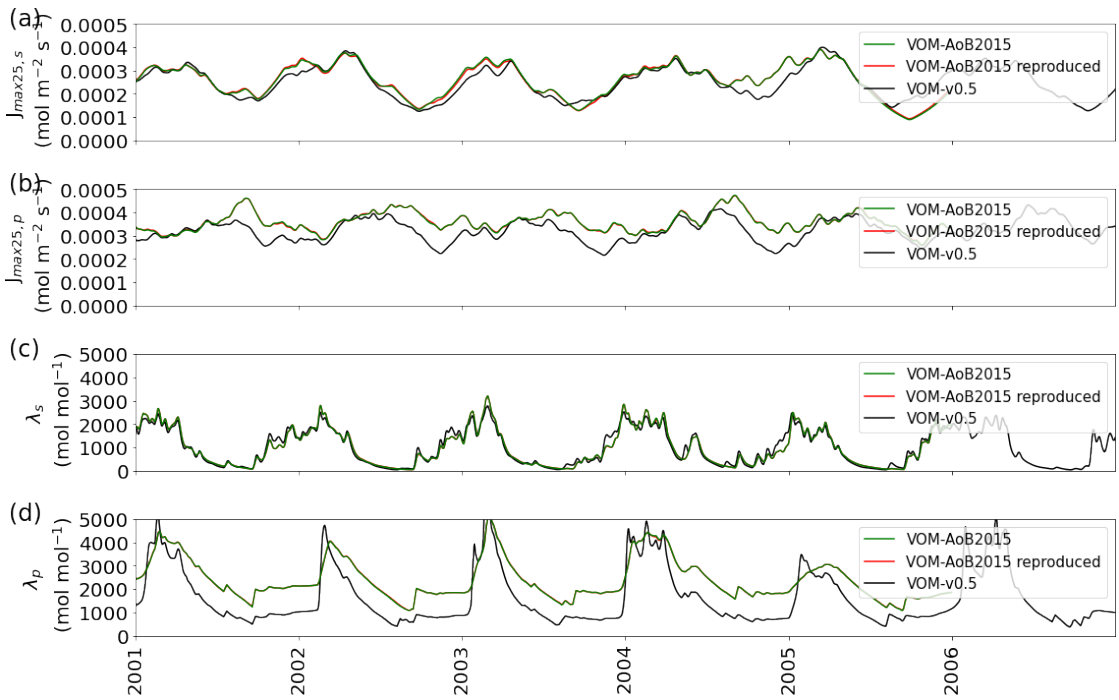

Figure S1.2. *Comparison for Howard Springs from 2001-2006 (subset from 1980-2017) between the results of Schymanski et al. (2015) (VOM-AoB2015, green) and a reproduction of those results (VOM-AoB2015 reproduced,red) based on the best run of the SCE-algorithm from Schymanski et al. (2015), and the new VOM-v0.5 modelling results (black), for a) the electron transport capacity at 25 ^oC for seasonal grasses ($J_{max25,s}$), b) the electron transport capacity at 25 ^oC for perennials trees ($J_{max25,p}$), d) transpiration seasonals (grasses), d) the daily slope (λ_s) between assimilation and transpiration of the seasonal grasses, e) the daily slope (λ_p) between assimilation and transpiration of the perennials (trees).*

These smoothed results are similar between the reproduced runs, and the original results of Schymanski et al. (2015), but there is a small a shift in time due to leap years, that were not accounted for by Schymanski et al. (2015).

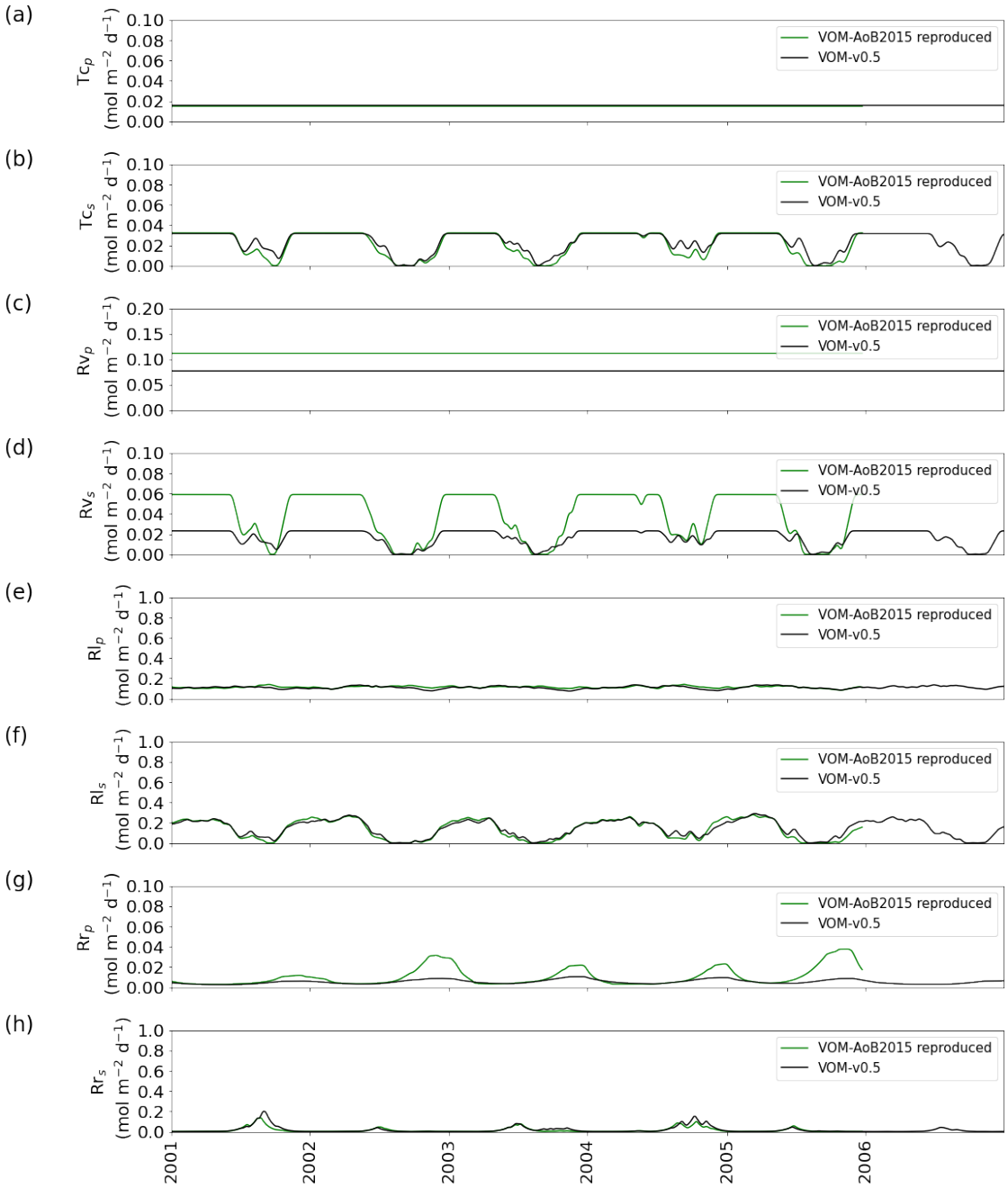

Figure S1.3. *Comparison for Howard Springs from 2001-2006 (subset from 1980-2017) between the reproduced results of Schymanski et al. (2015) (VOM-AoB2015 reproduced, green) based on the best run of the SCE-algorithm from Schymanski et al. (2015), and the new VOM-v0.5 modelling results (black), for a) the foliage turnover costs perennial trees (Tc_p), b) the foliage turnover costs seasonal grasses (Tc_s), c) the water transport costs for perennial trees (Rv_p), d) the water transport costs for seasonal grasses (Rv_s), e) leaf respiration perennial trees (Rl_p), f)leaf respiration seasonal grasses (Rl_s), g) root respiration perennial trees (Rr_p), h) root respiration seasonal grasses (Rr_s), all smoothed with a moving average of 7 days, and h) projective cover.Note that the original results*

of Schymanski et al. (2015) are not shown, as these variables were not produced as outputs, but only the reproduced values are shown.

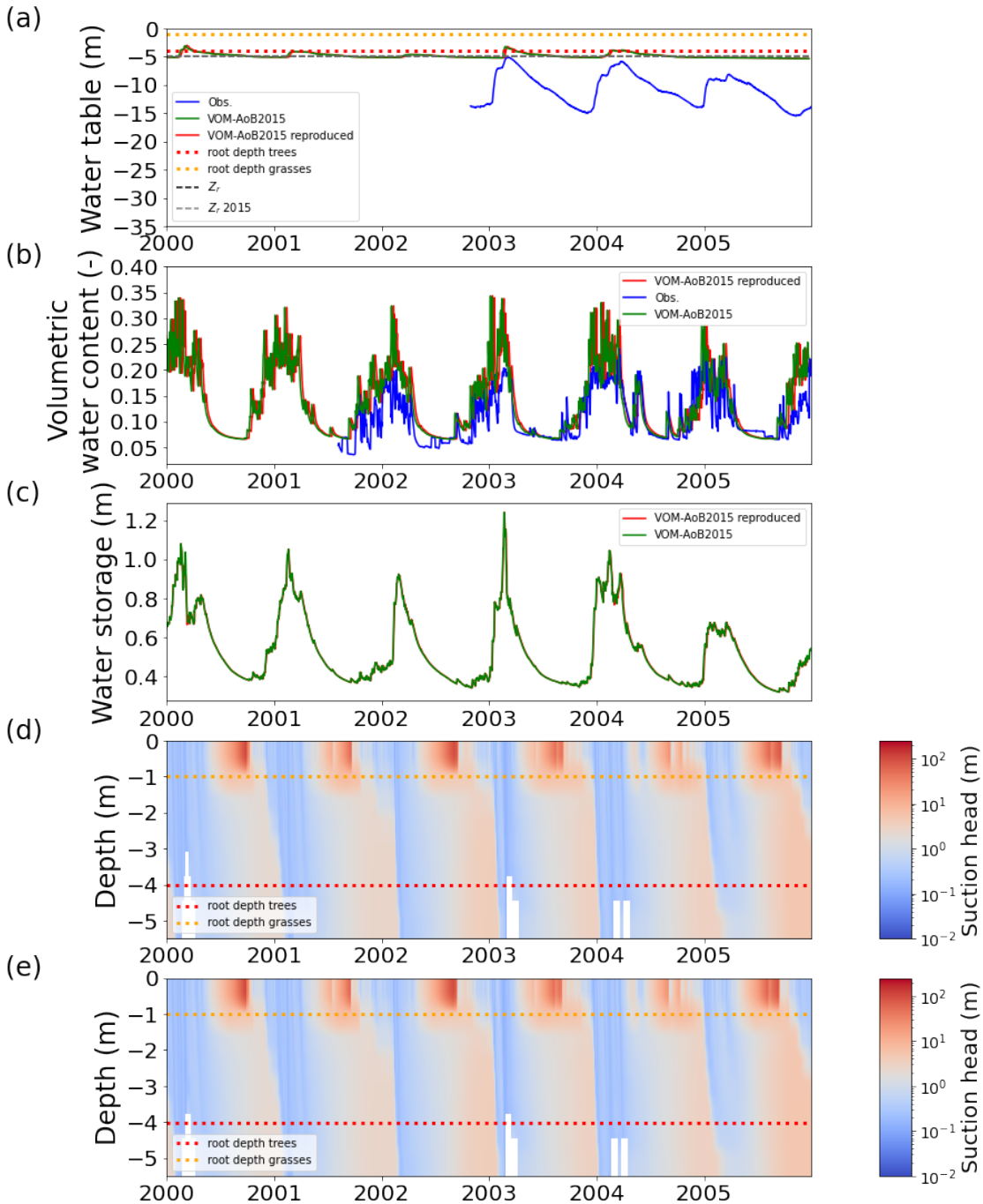

Figure S1.4. *Results for Howard Springs with a) groundwater depths, with dashed lines representing the bedrock depth, dotted lines the rooting depths (trees in red and grasses in orange), the reproduced results of Schymanski et al. (2015) in red (VOM-AoB2015 reproduced), the results of Schymanski et al. (2015) in green (VOM-AoB2015), and observations of three different boreholes*

in the vicinity of the study site in blue (Government Northern Territory, Australia, 2018). The soil moisture saturation in the upper soil layer is shown for Howard Springs in b) with the reproduced results of Schymanski et al. (2015) in red (VOM-AoB2015 reproduced), the results of Schymanski et al. (2015) in green (VOM-AoB2015) and soil moisture measurements at 5 cm depth at the flux tower sites in blue. The total water storage in the root zone is shown in c) for the reproduced results of Schymanski et al. (2015) (red) and the results of Schymanski et al. (2015) in green. The matrix suction heads are shown in d) for the reproduced model runs of the VOM, whereas e) displays the water suction heads of Schymanski et al. (2015).

Concluding remarks

The results of Schymanski et al. (2015) were largely reproduced with a new version of the VOM, as shown in Figures S1.1-S1.4. Differences in the fluxes and other time series are neglible, and the new version of the VOM provides a good starting point of the new study.

1.2 Reproducing the optimization

The vegetation properties are re-optimized with the same settings, and the inputs and parameter ranges kept the same as for the model runs by Schymanski et al. (2015). These simulations should therefore give rather similar results, but not exactly the same.

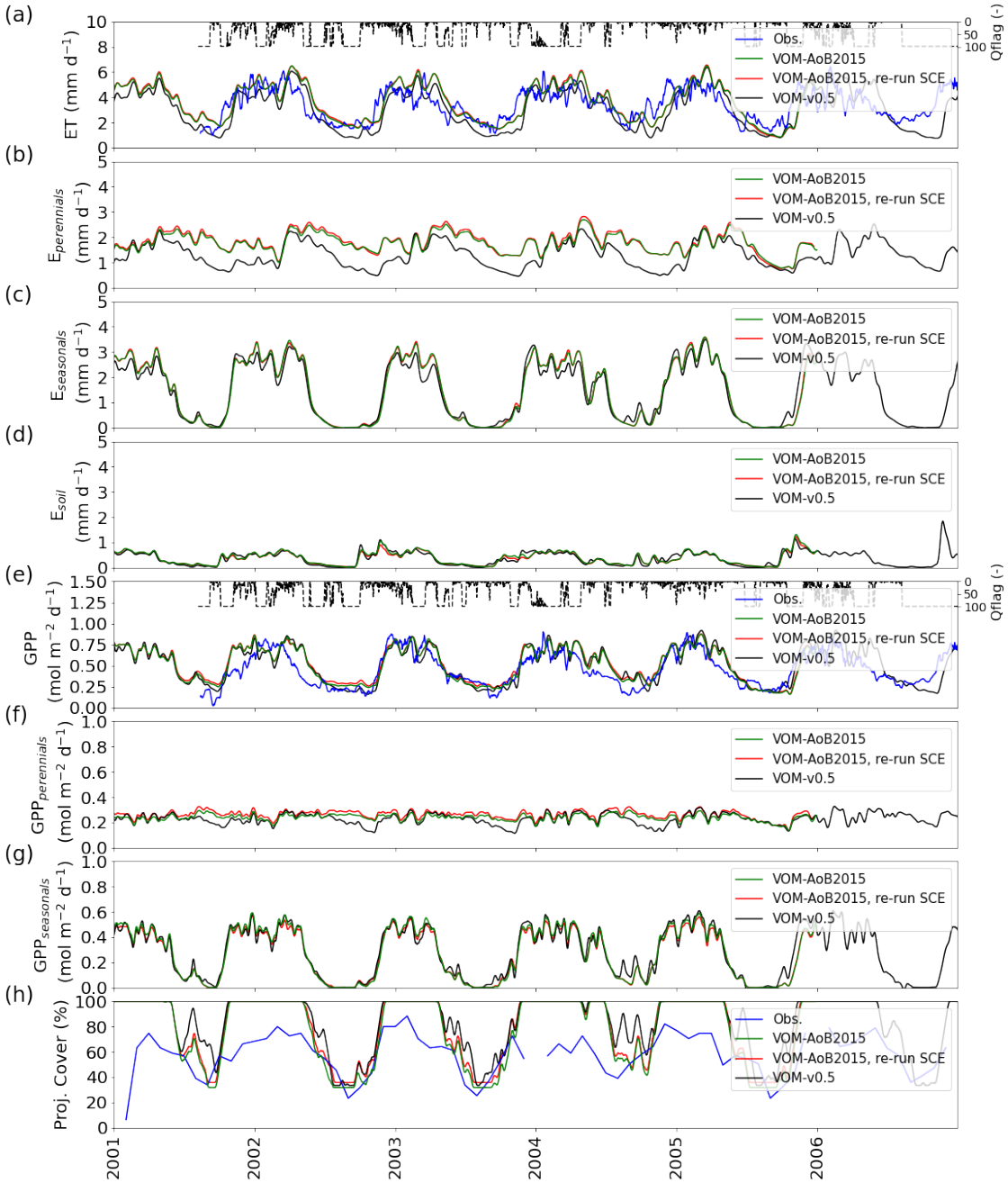

Figure S1.5. *Comparison for Howard Springs from 2001-2006 (subset from 1980-2017) between the results of Schymanski et al. (2015) (VOM-AoB2015, green) and a reproduction of those results (VOM-AoB2015, re-run SCE, red) based on re-running the SCE-algorithm, and the new VOM-v0.5 modelling results (black), for a) ET, b) transpiration perennials (trees), c) transpiration seasonals (grasses), d) soil evaporation, e) GPP, f) GPP perennials (trees), g) GPP seasonals (grasses), all smoothed with a moving average of 7 days, and h) projective cover. The daily average quality flags of the fluxtower observations are shown in dashed lines with a value of 100 when a day is completely gap-filled and 1 when it is observed.*

Only minor differences occur for the different model runs, with the biggest differences for the vegetation cover.

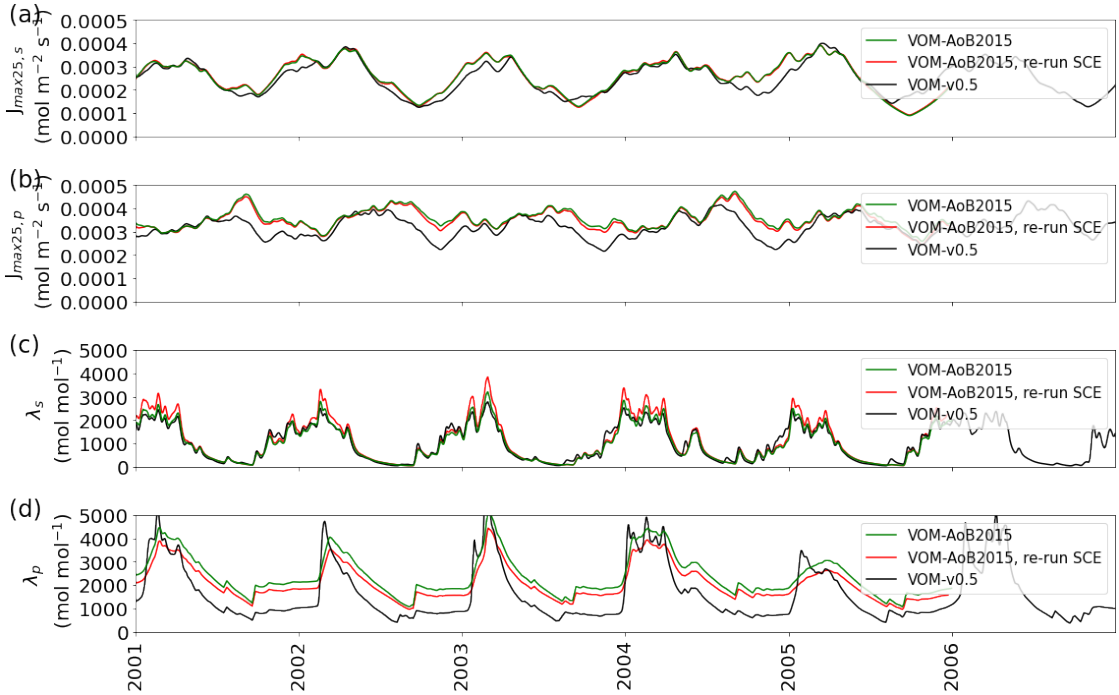

Figure S1.6. *Comparison for Howard Springs from 2001-2006 (subset from 1980-2017) between the results of Schymanski et al. (2015) (VOM-AoB2015, green) and a reproduction of those results (VOM-AoB2015, re-run SCE, red) based on re-running the SCE-algorithm, and the new VOM-v0.5 modelling results (black), for a) the electron transport capacity at 25 ^oC for seasonal grasses ($J_{max25,s}$), b) the electron transport capacity at 25 ^oC for perennials trees ($J_{max25,p}$), d) transpiration seasonals (grasses), d) the daily slope (λ_s) between assimilation and transpiration of the seasonal grasses, e) the daily slope (λ_p) between assimilation and transpiration of the perennials (trees).*

Results are similar between the reproduced runs, and the original results of Schymanski et al. (2015), but the values for λ_p are slightly increased for the new optimization.

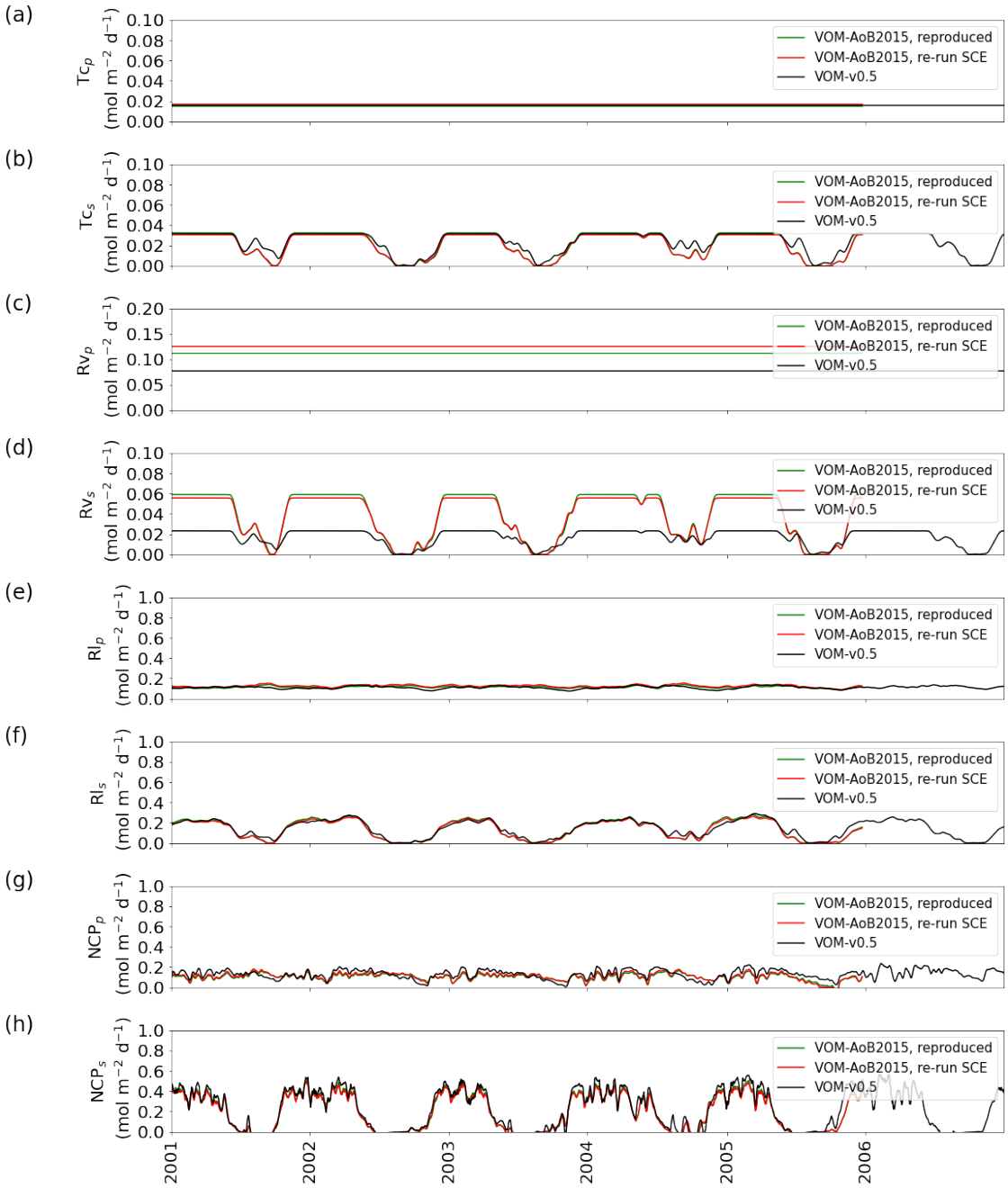

Figure S1.7. *Comparison for Howard Springs from 2001-2006 (subset from 1980-2017) between the reproduced results of Schymanski et al. (2015) (VOM-AoB2015, reproduced, green) and a reproduction of those results (VOM-AoB2015, re-run SCE, red) based on re-running the SCE-algorithm, and the new VOM-v0.5 modelling results (black), for a) the foliage turnover costs perennial trees (Tc_p), b) the foliage turnover costs seasonal grasses (Tc_s), c) the water transport costs for perennial trees (Rv_p), d) the water transport costs for seasonal grasses (Rv_s), e) leaf respiration perennial trees (Rl_p), f)leaf respiration seasonal grasses (Rl_s), g) root respiration perennial trees (Rr_p), h) root respiration seasonal grasses (Rr_s), all smoothed with a moving average of 7 days, and h)*

projective cover. Note that the original results of Schymanski et al. (2015) are not shown, as these variables were not produced as outputs, but only the reproduced values are shown.

The differences between the reproduced results and the results of the re-run optimization remain rather small.

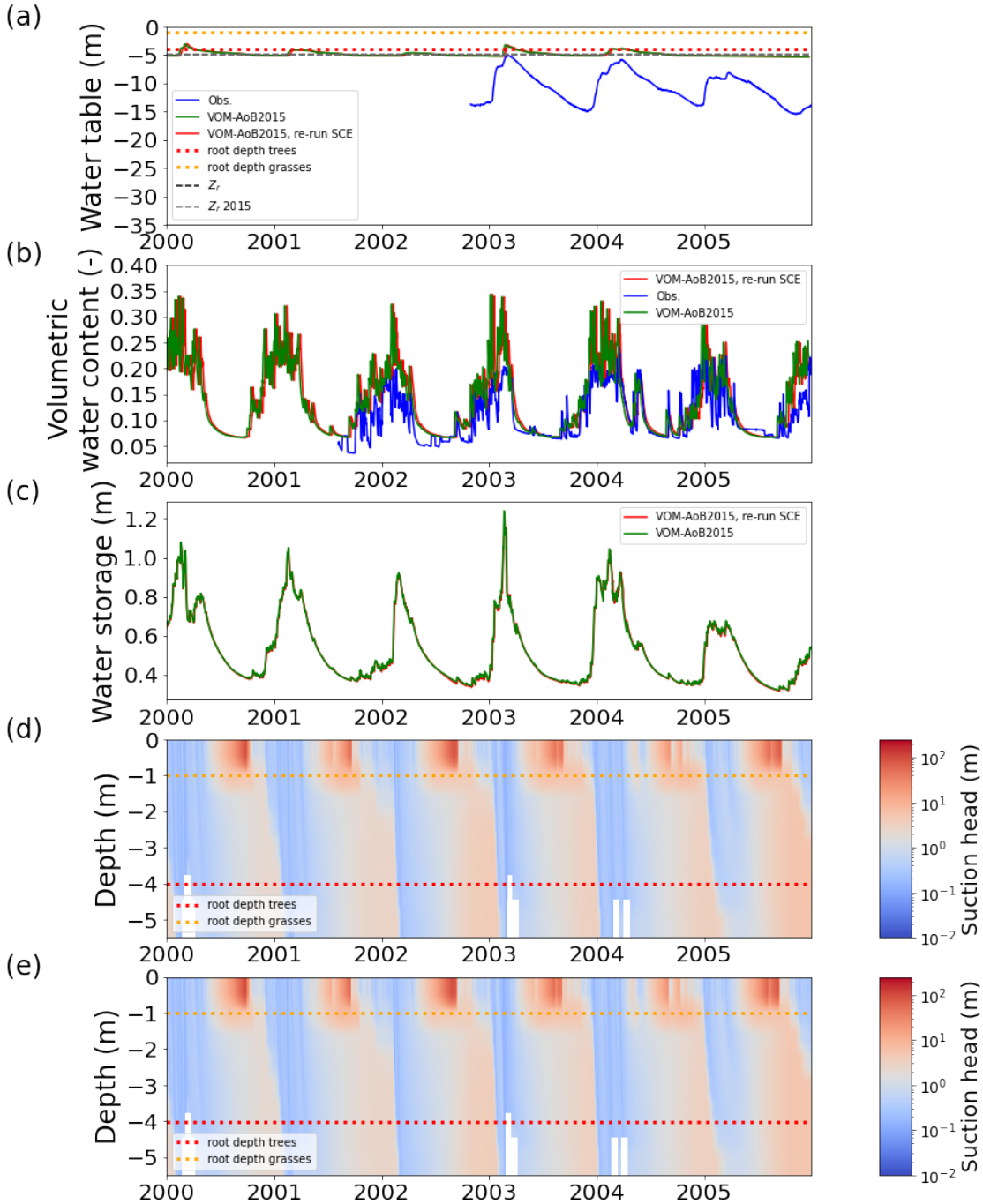

Figure S1.8. *Results for Howard Springs with a) groundwater depths, with dashed lines representing the bedrock depth, dotted lines the rooting depths (trees in red and grasses in orange), the reproduced results (based on re-running the SCE-algorithm) of Schymanski et al. (2015) in red (VOM-AoB2015, re-run SCE), the results of Schymanski et al. (2015) in green (VOM-AoB2015), and observations of three different boreholes in the vicinity of the study site in blue (Government Northern Territory, Australia, 2018). The soil moisture saturation in the upper soil layer is shown for Howard Springs in b) with the reproduced results of Schymanski et al. (2015) in red (VOM-AoB2015, re-run SCE), the results of Schymanski et al. (2015) in green (VOM-AoB2015) and soil moisture measurements at 5 cm depth at the flux tower sites in blue. The total water storage in the root zone is shown in c) for the reproduced results of Schymanski et al. (2015) (OM-AoB2015, re-run SCE, red) and the results of Schymanski et al. (2015) in green (VOM-AoB2015). The water suction heads are shown in d) for the reproduced model runs of the VOM, whereas e) displays the water suction heads of Schymanski et al. (2015).*

The differences are also here rather small between the original results of Schymanski et al. (2015), and the results of the re-run optimization.

Concluding remarks

The results of Schymanski et al. (2015) were also largely reproduced with a new version of the VOM and re-running the optimization with the same settings as Schymanski et al. (2015), as shown in Figures S1.5-S1.8. Therefore, the convergence of the SCE-algorithm towards similar values as Schymanski et al. (2015) also confirms that the new version of the VOM provides a good starting point of the new study.

1.3 Change of atmospheric CO_2-values

The model runs of Schymanski et al. (2015) used fixed atmospheric CO_2-values at 317 ppm, whereas the new runs use variable CO_2-levels based on data from the Mauna Loa records.

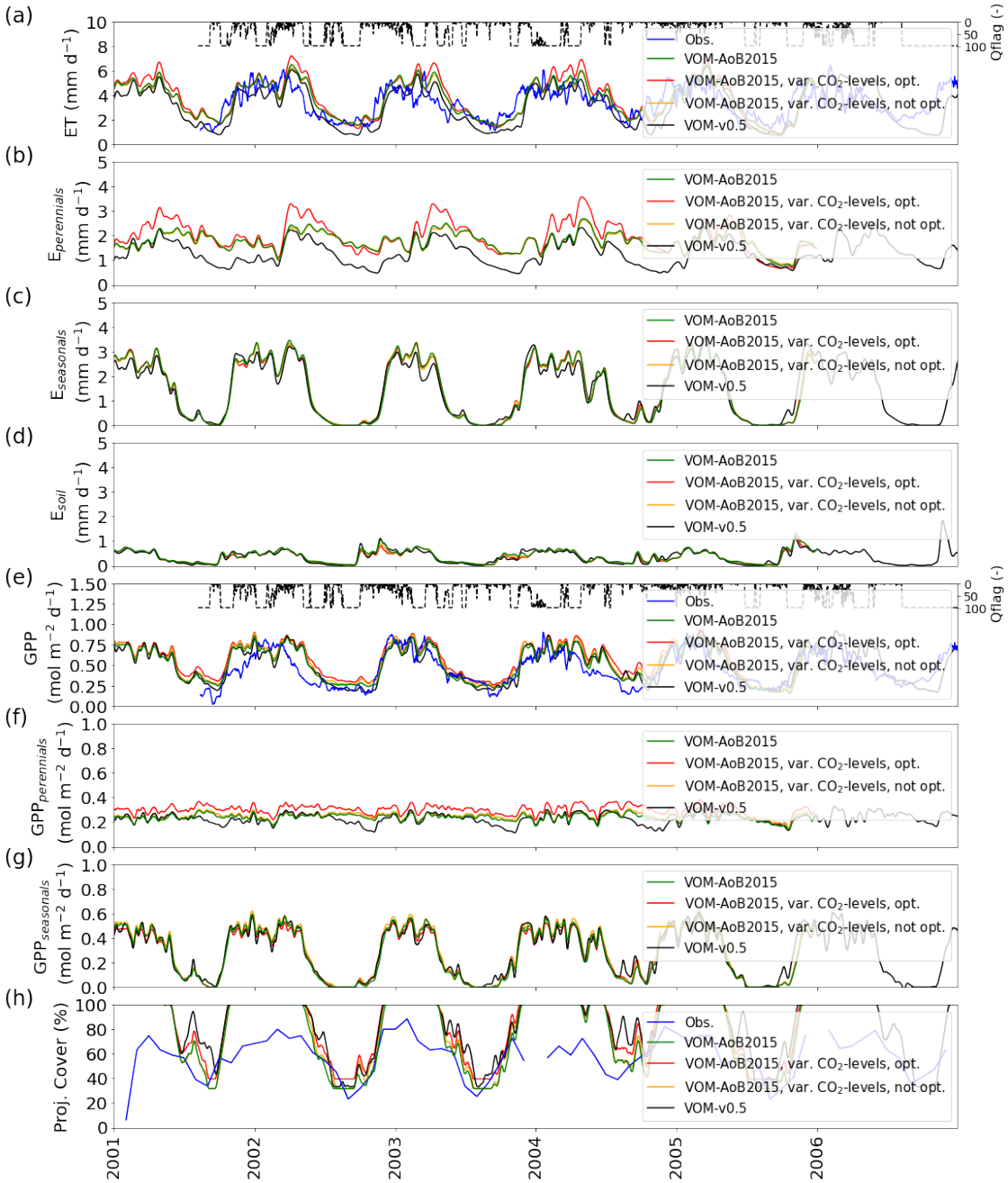

Figure S1.9. *Comparison for Howard Springs from 2001-2006 (subset from 1980-2017) between the results of Schymanski et al. (2015) (VOM-AoB2015, green) where atmospheric CO_2-values were fixed at 317ppm, and a re-optimized reproduction of these results that that uses variable CO_2-levels(VOM-AoB2015, var. CO_2-levels, opt., red), a reproduction of these results without optimization using the parameter from the VOM-AoB2015 (VOM-AoB2015, var. CO_2-levels, opt., not opt., yellow) and the new VOM-v0.5 modelling results (black), for a) ET, b) transpiration perennials (trees), c) transpiration seasonals (grasses), d) soil evaporation, e) GPP, f) GPP perennials (trees), g) GPP seasonals (grasses), all smoothed with a moving average of 7 days, and*

h) projective cover. The daily average quality flags of the fluxtower observations are shown in dashed lines with a value of 100 when a day is completely gap-filled and 1 when it is observed.

Results of total ET are similar between the runs with variable CO_2-levels, and the original results of Schymanski et al. (2015), but the GPP values increase with the new CO_2-values. This is mainly caused by higher GPP-values for the perennial trees. The transpiration remains rather similar between the two different model simulations, with a slight increase for the perennial vegetation and a slight decrease for the seasonal vegetation. The vegetation cover also increases due to the variable CO_2-levels.

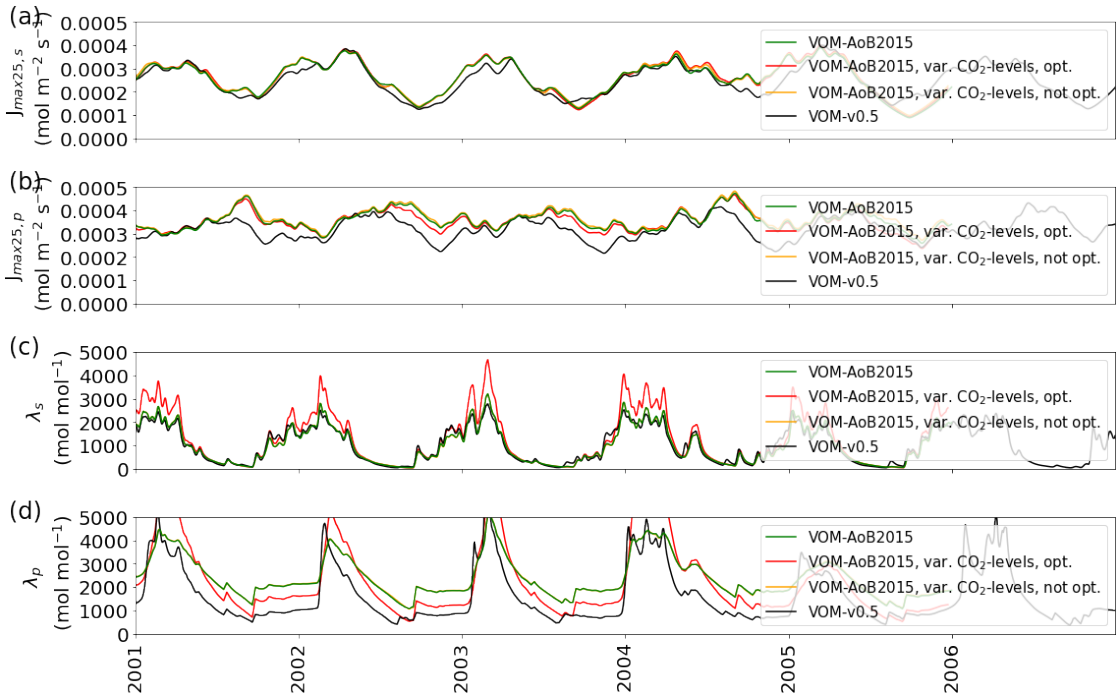

Figure S1.10. *Comparison for Howard Springs from 2001-2006 (subset from 1980-2017) between the results of Schymanski et al. (2015) (VOM-AoB2015, green) where atmospheric CO_2-values were fixed at 317ppm, and a re-optimized reproduction of these results that that uses variable CO_2-levels(VOM-AoB2015, var. CO_2-levels, opt., red), a reproduction of these results without optimization using the parameter from the VOM-AoB2015 (VOM-AoB2015, var. CO_2-levels, not opt., yellow) and the new VOM-v0.5 modelling results (black), for a) the electron transport capacity at 25 ^oC for seasonal grasses ($J_{max25,s}$), b) the electron transport capacity at 25 ^oC for perennials trees ($J_{max25,p}$), d) transpiration seasonals (grasses), d) the daily slope (λ_s) between assimilation and transpiration of the seasonal grasses, e) the daily slope (λ_p) between assimilation and transpiration of the perennials (trees).*

Results are similar between the reproduced runs, and the original results of Schymanski et al. (2015),

but especially the values for λ_p decrease for the new CO_2-values. In contrast, values for λ_s increase during the wet season.

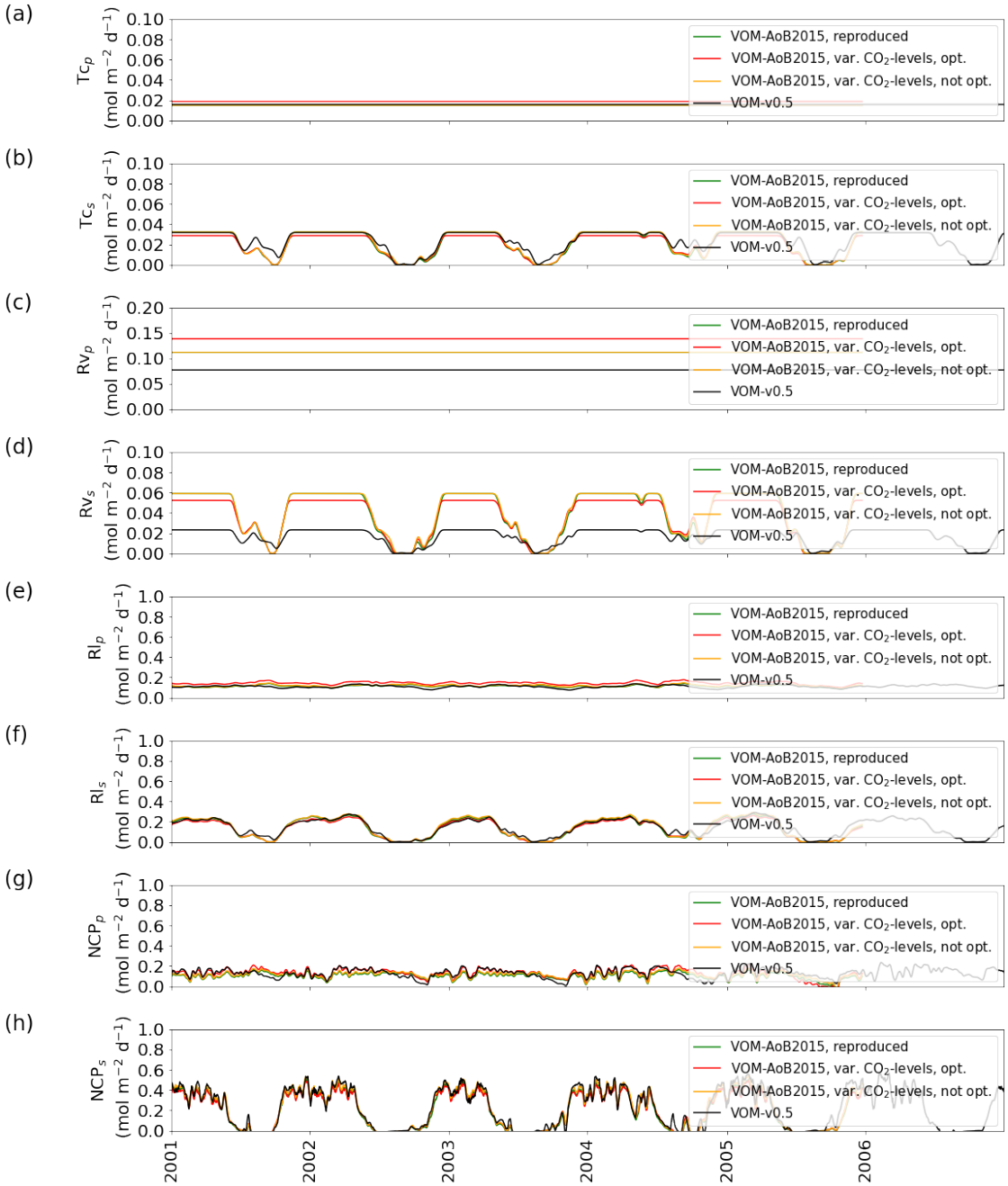

Figure S1.11. *Comparison for Howard Springs from 2001-2006 (subset from 1980-2017) between the reproduced results of Schymanski et al. (2015) (VOM-AoB2015 reproduced, green) where atmospheric CO_2-values were fixed at 317ppm, and a re-optimized reproduction of these results that that uses variable CO_2-levels(VOM-AoB2015, var. CO_2-levels, opt., red), a reproduction of these results without optimization using the parameter from the VOM-AoB2015 (VOM-AoB2015„*

var. CO_2-levels, not opt., yellow) and the new VOM-v0.5 modelling results (black), for a) the foliage turnover costs perennial trees (Tc_p), b) the foliage turnover costs seasonal grasses (Tc_s), c) the water transport costs for perennial trees (Rv_p), d) the water transport costs for seasonal grasses (Rv_s), e) leaf respiration perennial trees (Rl_p), f)leaf respiration seasonal grasses (Rl_s), g) root respiration perennial trees (Rr_p), h) root respiration seasonal grasses (Rr_s), all smoothed with a moving average of 7 days, and h) projective cover. Note that the original results of Schymanski et al. (2015) are not shown, as these variables were not produced as outputs, but only the reproduced values are shown.

The cost for the water transport system for the seasonal vegetation is mainly reduced (Rv_s), but the perennial foliage turnover costs (Tc_p) and leaf respiration (Rl_p) are sligtly increased. Eventually, the NCP for the perennials is higher.

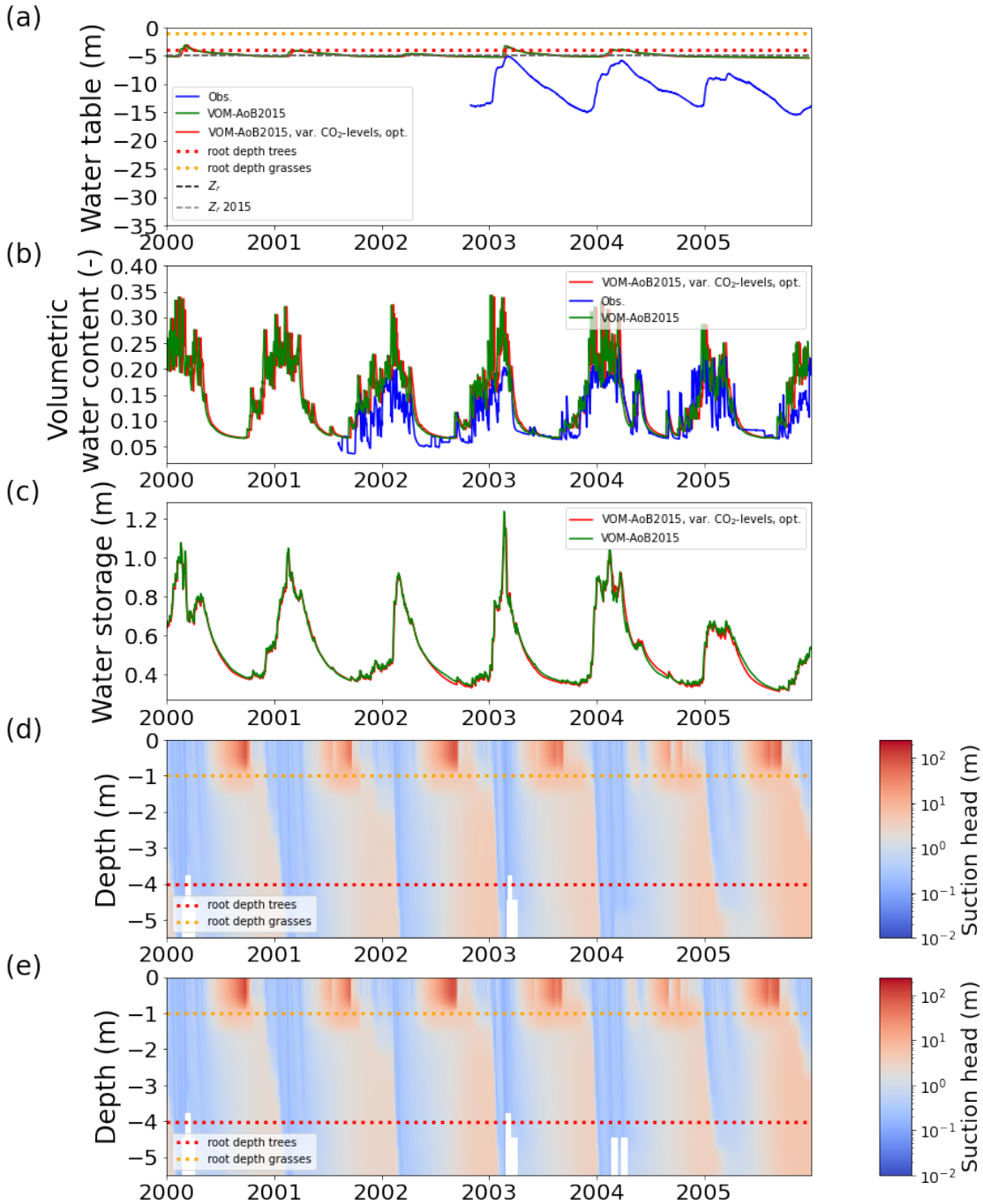

Figure S1.12. *Results for Howard Springs with a) groundwater depths, with dashed lines representing the bedrock depth, dotted lines the rooting depths (trees in red and grasses in orange), the re-optimized, the reproduced results with variable CO_2-levels (VOM-AoB2015, var. CO_2-levels, opt), the results of Schymanski et al. (2015) in green (VOM-AoB2015), and observations of three different boreholes in the vicinity of the study site in blue (Government Northern Territory, Australia, 2018). The soil moisture saturation in the upper soil layer is shown for Howard*

Springs in b) with the reproduced results of Schymanski et al. (2015) in red (VOM-AoB2015, var. CO_2-levels, opt), the results of Schymanski et al. (2015) in green (VOM-AoB2015) and soil moisture measurements at 5 cm depth at the flux tower sites in blue. The total water storage in the root zone is shown in c) for the reproduced results of Schymanski et al. (2015) (VOM-AoB2015, var. CO_2-levels, opt, red) and the results of Schymanski et al. (2015) in green (VOM-AoB2015). The matrix water suction heads are shown in d) for the model runs of the VOM with variable CO_2-levels, whereas e) displays the water suction heads of Schymanski et al. (2015).

The differences here are rather small and are neglible.

Concluding remarks

The new, variable CO_2-levels lead to higher values of GPP for especially the perennial vegetation, but the transpiration stays rather similar (Figures S1.13-1.16). The vegetation cover also showed increased values, but the total evapo-transpiration stays similar. Therefore, the new CO_2-levels will have an affect on the results in comparison with the results of Schymanski et al. (2015), mainly in relation to GPP and vegetation cover.

1.4 Change of soil layer thickness

The soil layer thickness was reduced from 0.5 m to 0.2 m for the new model runs. This should lead to rather similar results, except for numerical differences.

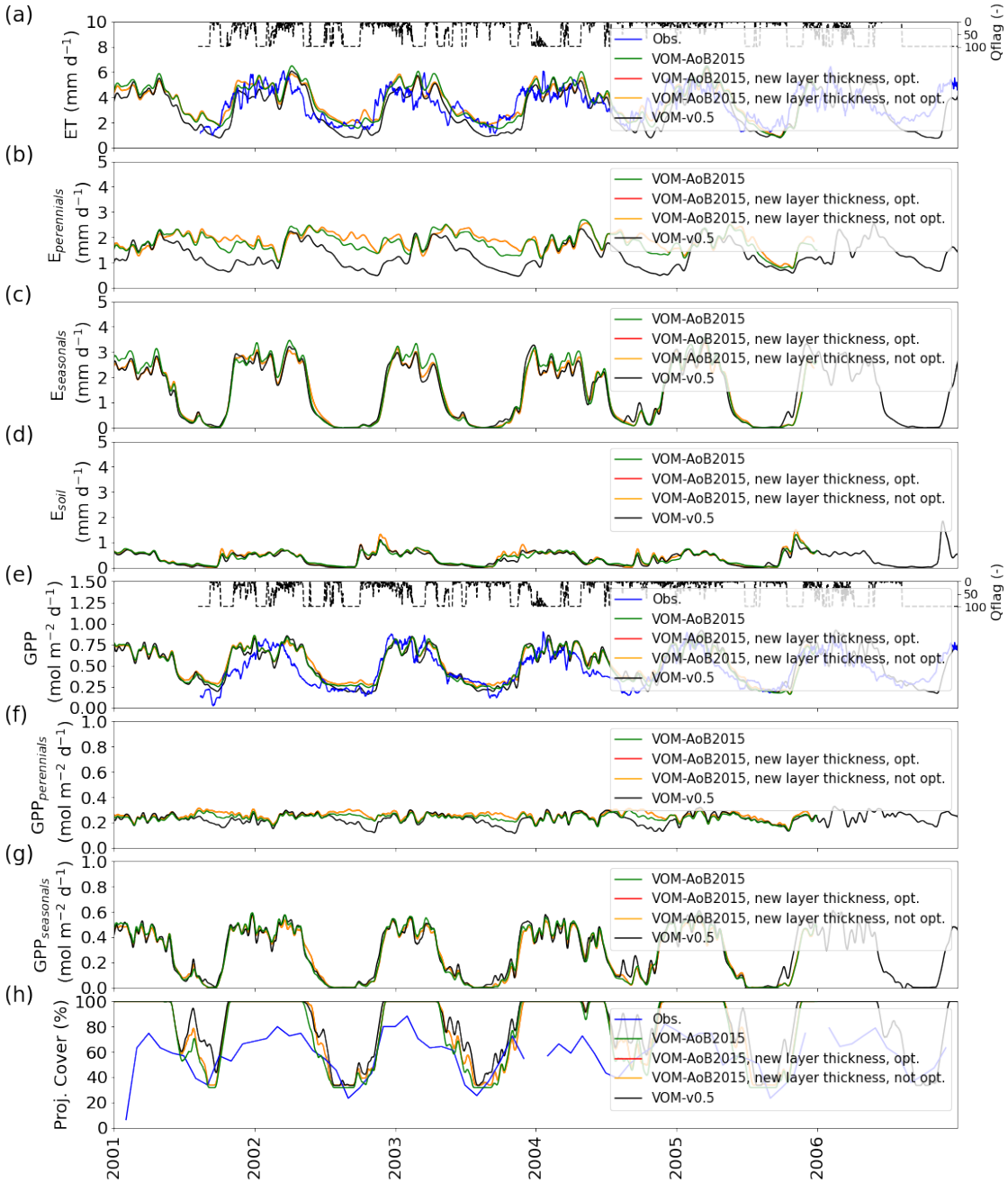

Figure S1.13. *Comparison for Howard Springs from 2001-2006 (subset from 1980-2017) between the results of Schymanski et al. (2015) (VOM-AoB2015, green) where the soil layer thickness was set at 0.5 m, and a re-optimized reproduction of these results that use a soil layer thickness of 0.2 m (VOM-AoB2015, new layer thickness, opt., red), a reproduction of these results without optimization using the parameter from the VOM-AoB2015 (VOM-AoB2015, new layer thickness, not opt., yellow) and the new VOM-v0.5 modelling results (black), for a) ET, b) transpiration perennials (trees), c) transpiration seasonals (grasses), d) soil evaporation, e) GPP, f) GPP perennials (trees), g) GPP seasonals (grasses), all smoothed with a moving average of 7 days, and*

h) projective cover. The daily average quality flags of the fluxtower observations are shown in dashed lines with a value of 100 when a day is completely gap-filled and 1 when it is observed.

There are small differences between the fluxes, but these are generally small. The soil evaporation is slightly higher during the wet season, which leads to small differences in the transpiration for the perennials and seasonals as well. The GPP is slightly lower for the new soil layer thickness.

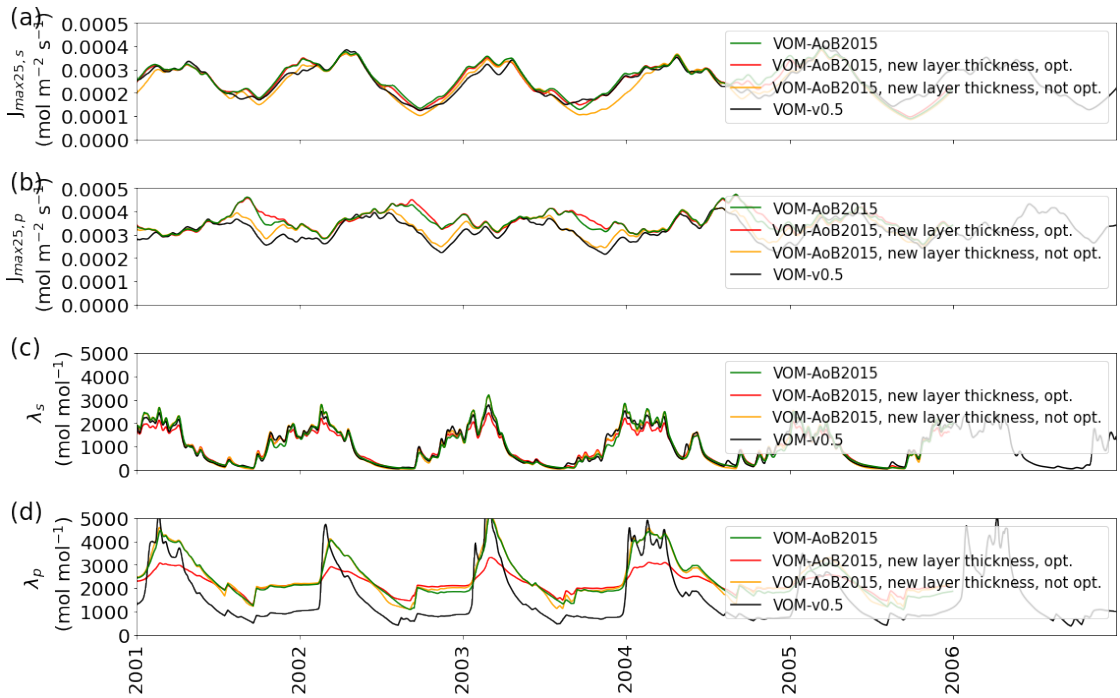

Figure S1.14. *Comparison for Howard Springs from 2001-2006 (subset from 1980-2017) between the results of Schymanski et al. (2015) (VOM-AoB2015, green) where the soil layer thickness was set at 0.5 m, and a re-optimized reproduction of these results that use a soil layer thickness of 0.2 m (VOM-AoB2015, new layer thickness, opt., red), a reproduction of these results without optimization using the parameter from the VOM-AoB2015 (VOM-AoB2015, new layer thickness, not opt., yellow) and the new VOM-v0.5 modelling results (black), for a) the electron transport capacity at 25 ^oC for seasonal grasses ($J_{max25,s}$), b) the electron transport capacity at 25 ^oC for perennials trees ($J_{max25,p}$), d) transpiration seasonals (grasses), d) the daily slope (λ_s) between assimilation and transpiration of the seasonal grasses, e) the daily slope (λ_p) between assimilation and transpiration of the perennials (trees).*

Results are similar between the reproduced runs, and the original results of Schymanski et al. (2015), except for slightly lower values for $J_{max25,s}$ and $J_{max25,p}$. The values for the slope λ_p between assimilation and transpiration of the perennial vegetation is also increased with the new layer thickness in comparison with the original results.

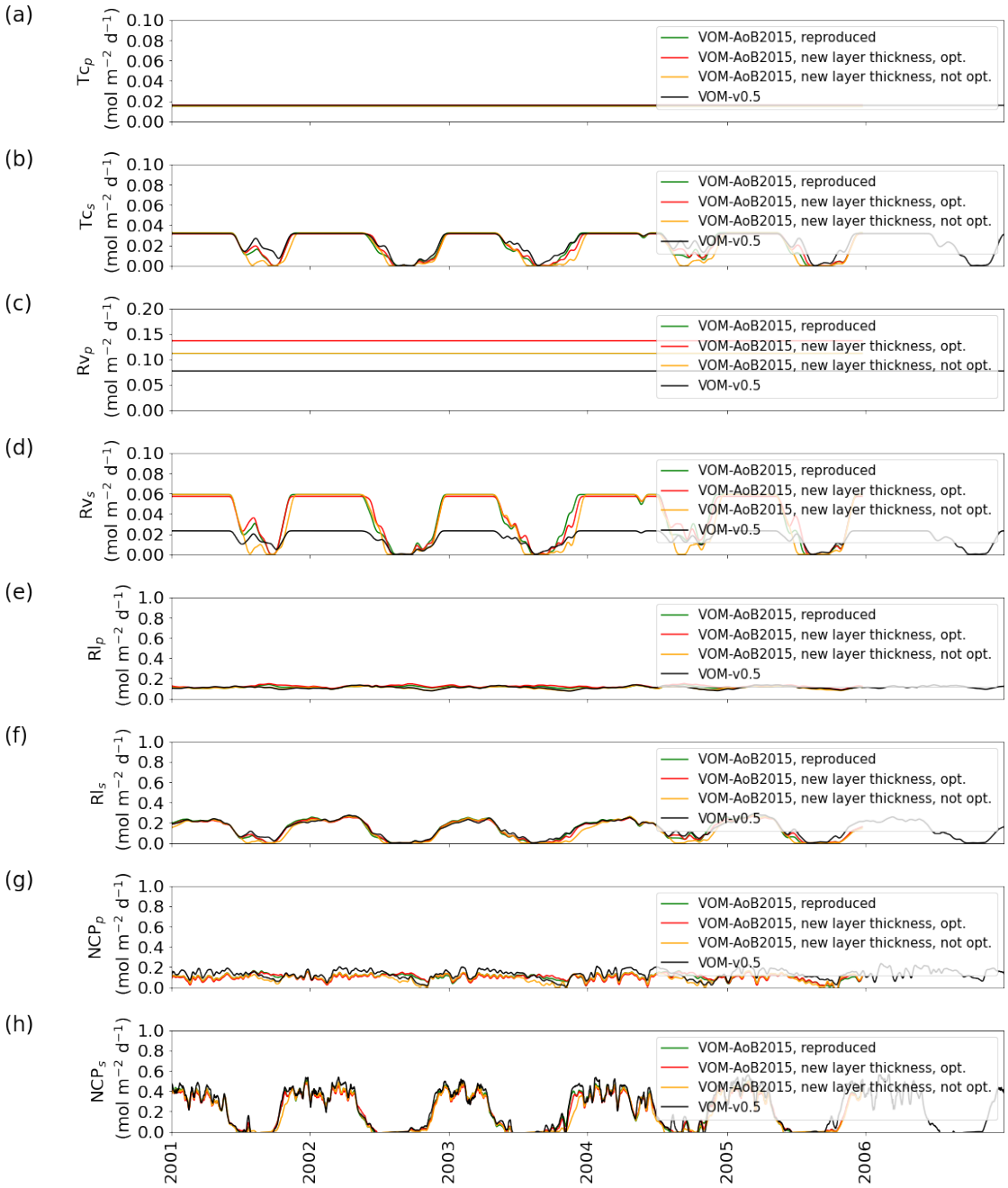

Figure S1.15. *Comparison for Howard Springs from 2001-2006 (subset from 1980-2017) between a reproduction of the results of Schymanski et al. (2015) where atmospheric CO_2-values were fixed at 317ppm (green), where soil layer thickness was set at 0.5 m (green), and a reproduction of these results that use a layer thickness of 0.2 m (red), and the new VOM modelling results (black), for a) the foliage turnover costs perennial trees (Tc_p), b) the foliage turnover costs seasonal grasses (Tc_s), c) the water transport costs for perennial trees (Rv_p), d) the water transport costs for seasonal grasses (Rv_s), e) leaf respiration perennial trees (Rl_p), f)leaf respiration seasonal grasses (Rl_s), g) root respiration perennial trees (Rr_p), h) root respiration seasonal grasses (Rr_s), all smoothed with*

a moving average of 7 days, and h) projective cover. Note that the original results of Schymanski et al. (2015) are not shown, as these variables were not produced as outputs, but only the reproduced values are shown.

The differences between the two model simulations are rather negligible.

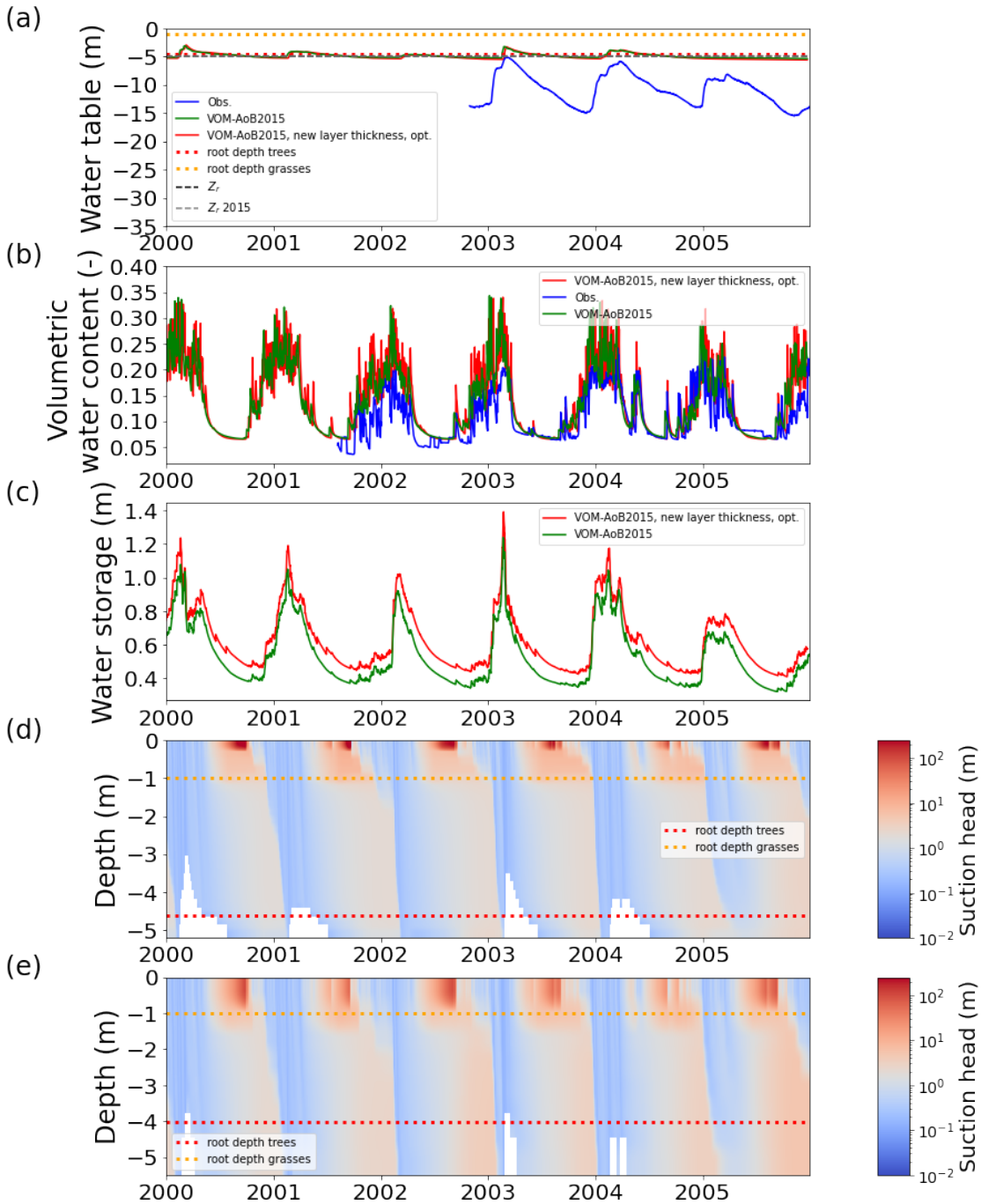

Figure S1.16. *Results for Howard Springs with a) groundwater depths, with dashed lines representing the bedrock depth, dotted lines the rooting depths (trees in red and grasses in orange), the re-optimized, reproduced results with a soil layer thickness of 0.2 m (VOM-AoB2015, new layer thickness, opt), the results of Schymanski et al. (2015) in green (VOM-AoB2015), and observations of three different boreholes in the vicinity of the study site in blue (Government Northern Territory, Australia, 2018). The soil moisture saturation in the upper soil layer is shown for Howard Springs in b) with the reproduced results of Schymanski et al. (2015) in red (VOM-AoB2015, new layer thickness, opt), the results of Schymanski et al. (2015) in green (VOM-AoB2015) and soil moisture measurements at 5 cm depth at the flux tower sites in blue. The total water storage in the root zone is shown in c) for the reproduced results of Schymanski et al. (2015) (VOM-AoB2015, new layer thickness, opt, red) and the results of Schymanski et al. (2015) in green (VOM-AoB2015). The matrix water suction heads are shown in d) for the model runs of the VOM with a new soil layer thickness, whereas e) displays the water suction heads of Schymanski et al. (2015).*

The results between the two model simulations are small, except for the water storage in the upper 5 m that is slightly increased.

Concluding remarks

The new soil layer thickness of 0.2 m does not lead to large differences (Figures S1.17-1.20). The largest influence of the new soil layer thickness is on soil evaporation at the end of the wet season, which also leads to small differences in the other evaporative fluxes.

1.5 Change of atmospheric pressures

The atmospheric pressure was fixed by Schymanski et al. (2015) at 1013.25 hPa, the new runs use variable levels obtained from the SILO meteorological data. This should not lead to large differences.

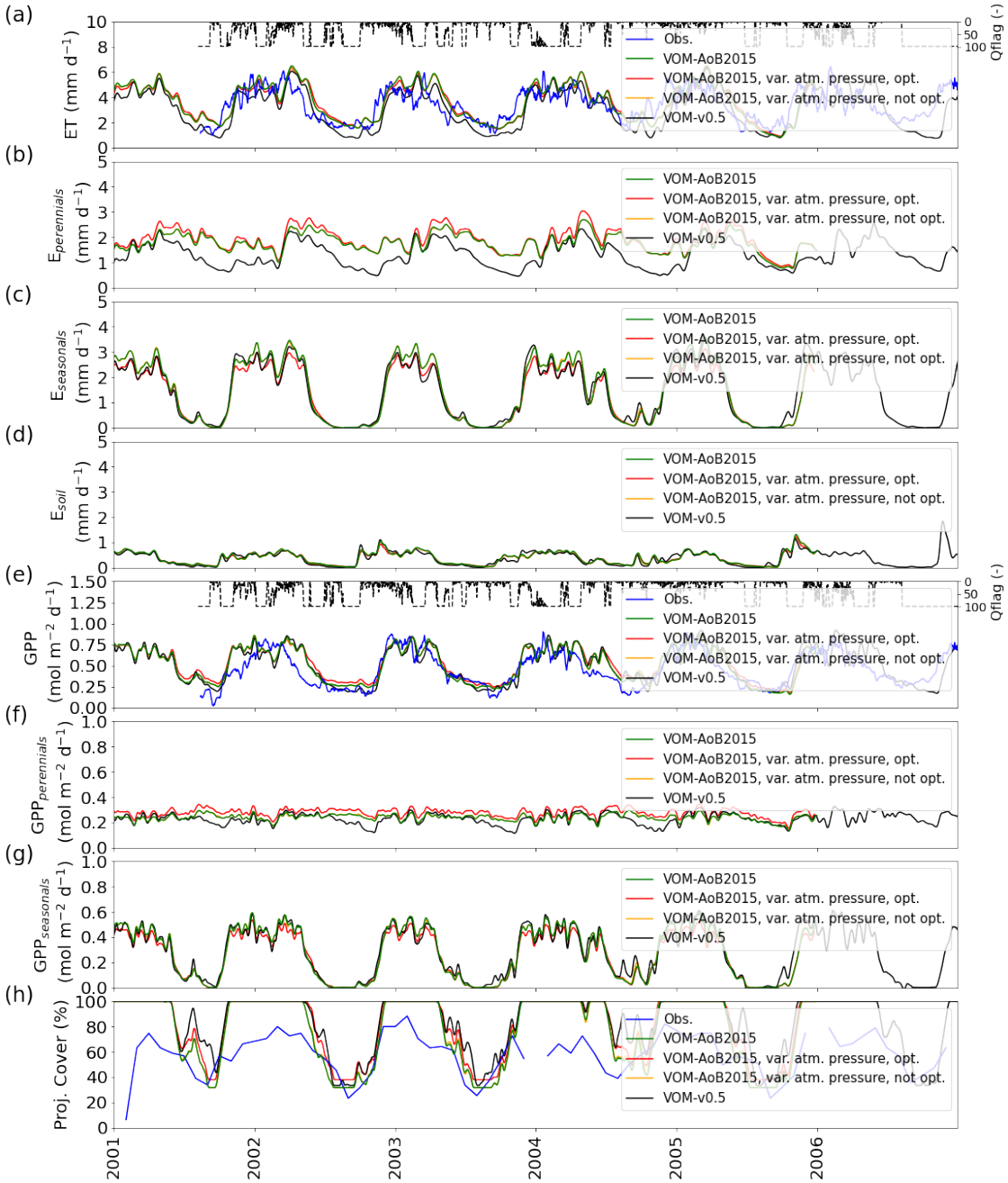

Figure S1.17. *Comparison for Howard Springs from 2001-2006 (subset from 1980-2017) between the results of Schymanski et al. (2015) (VOM-AoB2015, green) where atmosperic pressure was fixed at 1013.25 hPa, and a re-optimized reproduction of these results that use variable levels obtained from the SILO meteorological data (VOM-AoB2015, var. atm. pressure, opt., red), a reproduction of these results without optimization using the parameter from the VOM-AoB2015 (VOM-AoB2015, var. atm. pressure, not opt., yellow) and the new VOM-v0.5 modelling results (black), for a) ET, b) transpiration perennials (trees), c) transpiration seasonals (grasses), d) soil evaporation, e) GPP, f) GPP perennials (trees), g) GPP seasonals (grasses), all smoothed with a*

moving average of 7 days, and h) projective cover. The daily average quality flags of the fluxtower observations are shown in dashed lines with a value of 100 when a day is completely gap-filled and 1 when it is observed.

Results of total GPP and ET are similar between the reproduced runs. The transpiration for the perennials and the seasonals remain also rather similar, but the GPP for the perennials is slightly increased. The projective cover is also slightly higher compared to the original simulations.

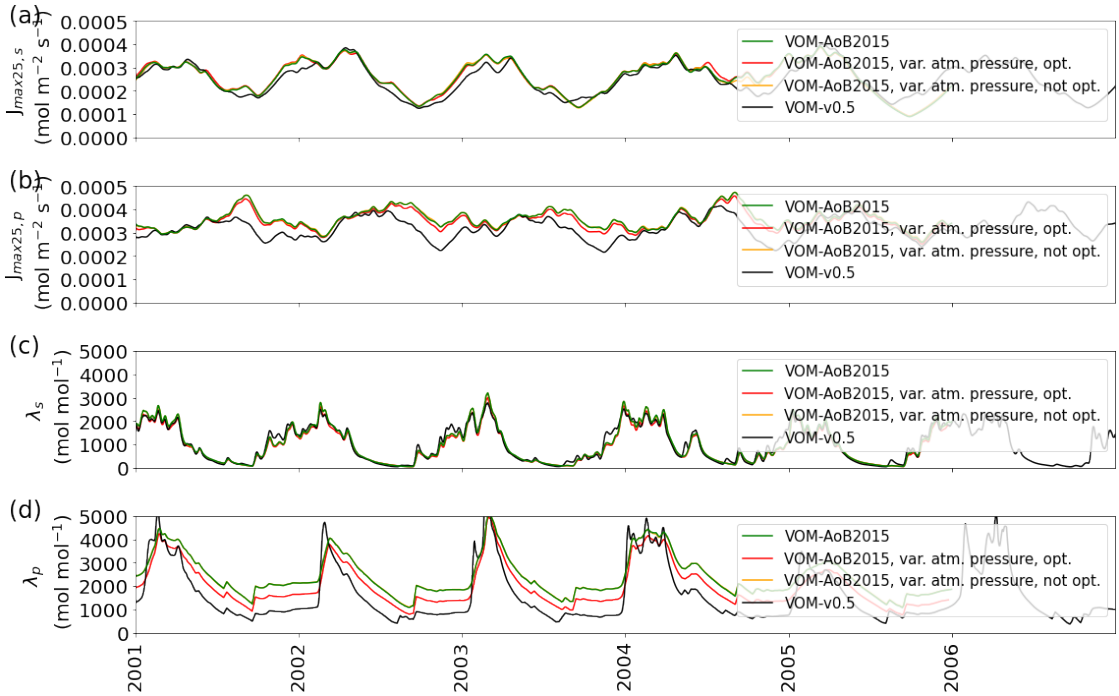

Figure S1.18. *Comparison for Howard Springs from 2001-2006 (subset from 1980-2017) between the results of Schymanski et al. (2015), where atmosperic pressure was fixed at 1013.25 hPa (green) , and a reproduction of these results that use variable levels obtained from the SILO meteorological data (red), and the new VOM modelling results (black), for a) the electron transport capacity at 25 ^oC for seasonal grasses ($J_{max25,s}$), b) the electron transport capacity at 25 ^oC for perennials trees ($J_{max25,p}$), d) transpiration seasonals (grasses), d) the daily slope (λ_s) between assimilation and transpiration of the seasonal grasses, e) the daily slope (λ_p) between assimilation and transpiration of the perennials (trees).*

Results are similar between the reproduced runs, and the original results of Schymanski et al. (2015). The values for the slope λ_p between assimilation and transpiration of the perennial vegetation is slightly reduced, whereas the λ_s is slightly increased.

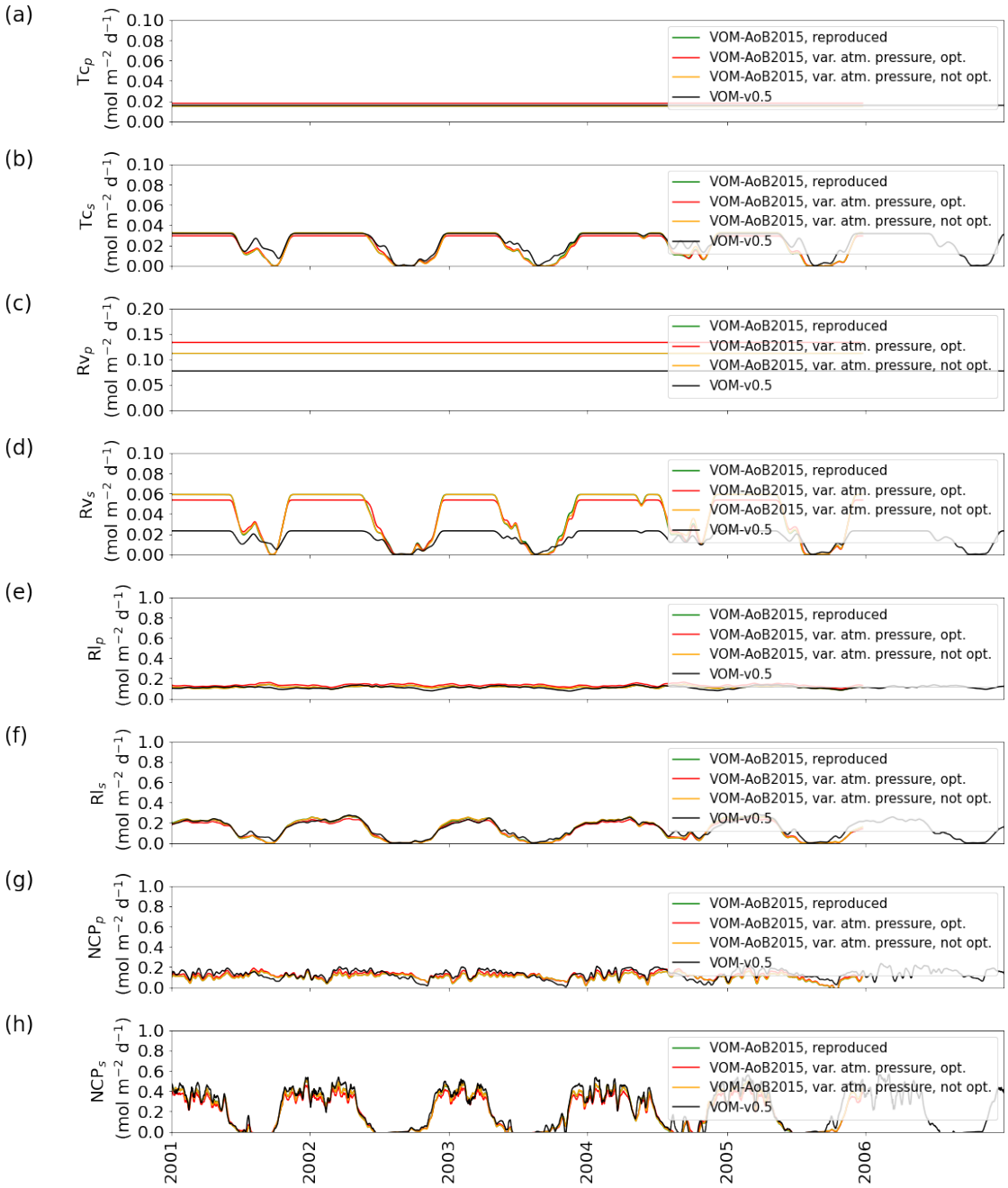

Figure S1.19. *Comparison for Howard Springs from 2001-2006 (subset from 1980-2017) between a reproduction of the results of Schymanski et al. (2015) where atmospheric CO_2-values were fixed at 317ppm (green), where atmosperic pressure was fixed at 1013.25 hPa (green) , and a reproduction of these results that use variable levels obtained from the SILO meteorological data (red), and the new VOM modelling results (black), for a) the foliage turnover costs perennial trees (Tc_p), b) the foliage turnover costs seasonal grasses (Tc_s), c) the water transport costs for perennial trees (Rv_p), d) the water transport costs for seasonal grasses (Rv_s), e) leaf respiration perennial trees (Rl_p), f)leaf respiration seasonal grasses (Rl_s), g) root respiration perennial trees*

(Rr_p), h) root respiration seasonal grasses (Rr_s), all smoothed with a moving average of 7 days, and h) projective cover.

Note that the original results of Schymanski et al. (2015) are not shown, as these variables were not produced as outputs, but only the reproduced values are shown. The values remain rather similar, except for the costs for the water transport system for the seasonal grasses (Rv_s), that are slightly reduced now.

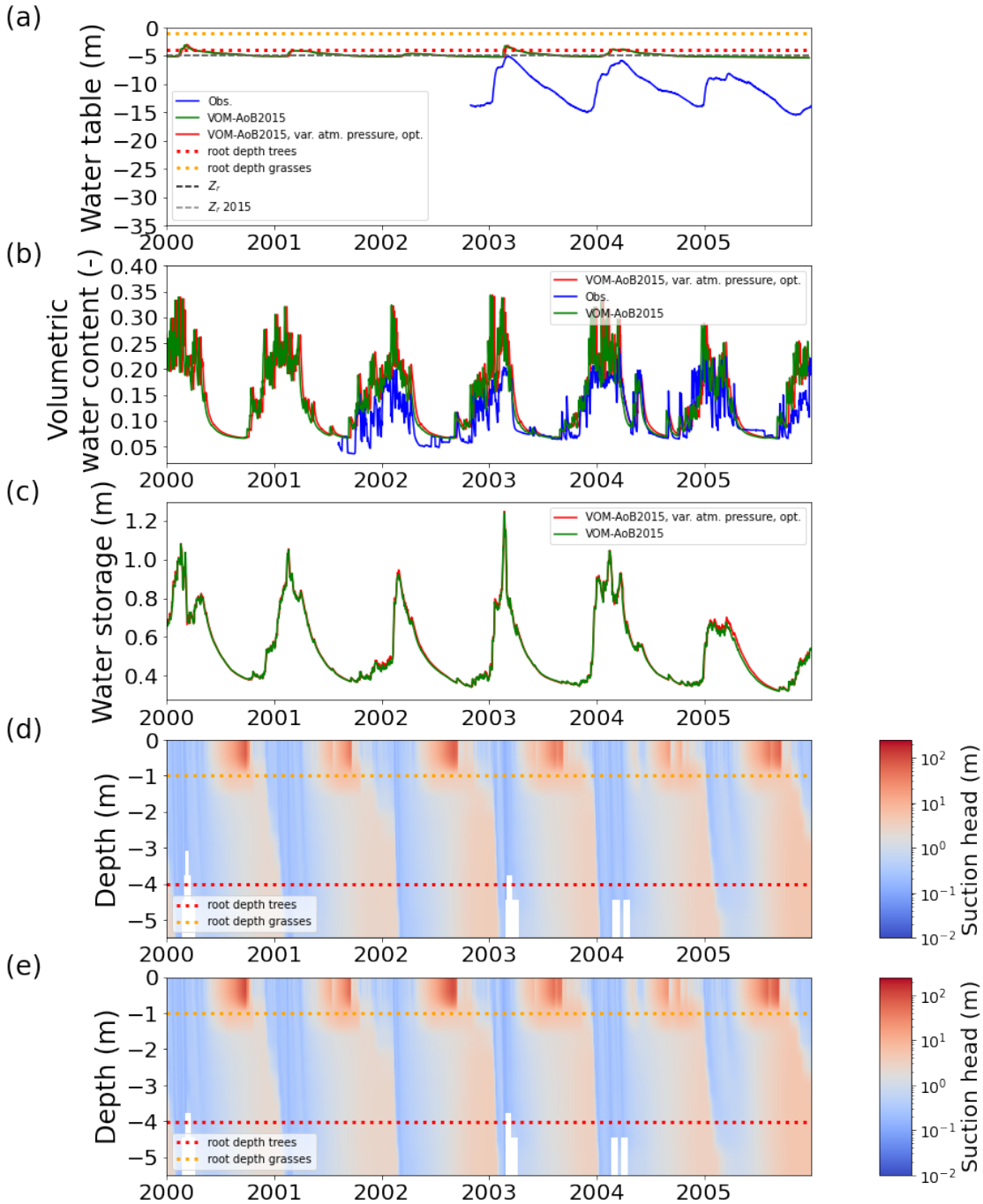

Figure S1.20. *Results for Howard Springs with a) groundwater depths, with dashed lines representing the bedrock depth, dotted lines the rooting depths (trees in red and grasses in orange), the re-optimized, reproduced results with variable atmospheric pressures (VOM-AoB2015, var. atm. pressure, opt., opt), the results of Schymanski et al. (2015) in green (VOM-AoB2015), and observations of three different boreholes in the vicinity of the study site in blue (Government Northern Territory, Australia, 2018). The soil moisture saturation in the upper soil layer is shown for Howard Springs in b) with the reproduced results of Schymanski et al. (2015) in red (VOM-AoB2015, var. atm. pressure, opt.), the results of Schymanski et al. (2015) in green (VOM-AoB2015) and soil moisture measurements at 5 cm depth at the flux tower sites in blue. The total water storage in the root zone is shown in c) for the reproduced results of Schymanski et al. (2015) (VOM-AoB2015, var. atm. pressure, opt., red) and the results of Schymanski et al. (2015) in green (VOM-AoB2015). The matrix water suction heads are shown in d) for the model runs of the VOM with variable atmospheric pressures, whereas e) displays the water suction heads of Schymanski et al. (2015).*

Concluding remarks

The new atmosperhic pressures only led to minor differences in the GPP, with increased values for the perennials, and therefore also in the carbon costs and benefits (Figures S1.21-S1.24). Nevertheless, the effects are small and will not have a strong influence on the results.

1.6 Optimizing rooting depths grasses

The grass rooting depths were fixed at 1.0 m by Schymanski et al. (2015), whereas the new runs optimize the rooting depth of grasses as well.

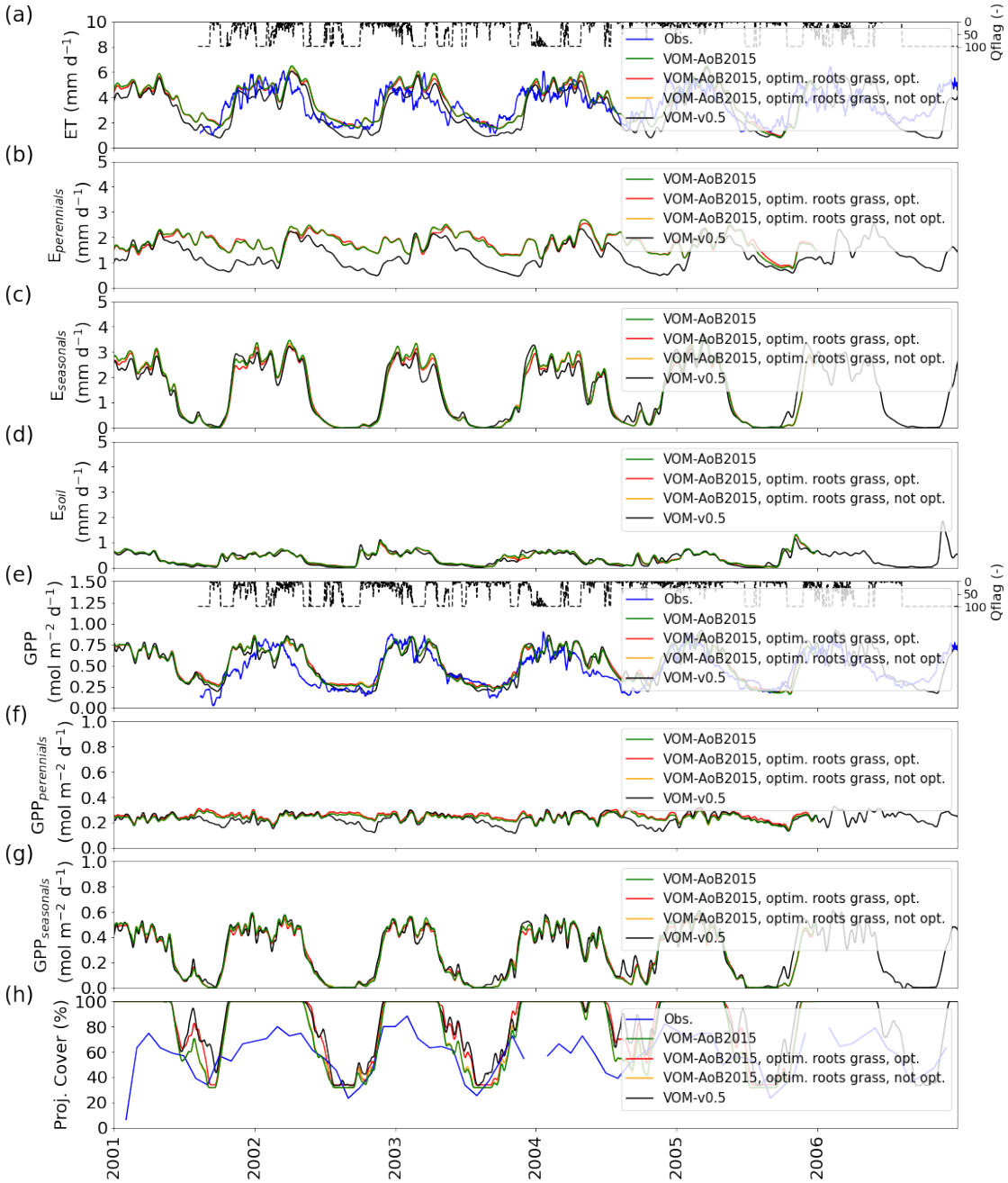

Figure S1.21. *Comparison for Howard Springs from 2001-2006 (subset from 1980-2017) between the results of Schymanski et al. (2015) (VOM-AoB2015, green) grass rooting depths were fixed at 1.0 m, and a re-optimized reproduction of these results that optimize the rooting depth of grasses (VOM-AoB2015, optim. roots grass, opt., red), a reproduction of these results without optimization using the parameter from the VOM-AoB2015 (VOM-AoB2015, optim. roots grass, not opt., yellow) and the new VOM-v0.5 modelling results (black), for a) ET, b) transpiration perennials (trees), c) transpiration seasonals (grasses), d) soil evaporation, e) GPP, f) GPP perennials (trees), g) GPP seasonals (grasses), all smoothed with a moving average of 7 days, and h) projective cover. The*

daily average quality flags of the fluxtower observations are shown in dashed lines with a value of 100 when a day is completely gap-filled and 1 when it is observed.

Total GPP and ET reduced when roots were optimized, whereas the vegetation cover also decreased more strongly after the wet season. The perennial trees transpired less, whereas the transpiration of the seasonal grasses increased. The GPP for the perennials and the seasonals both reduced as well.

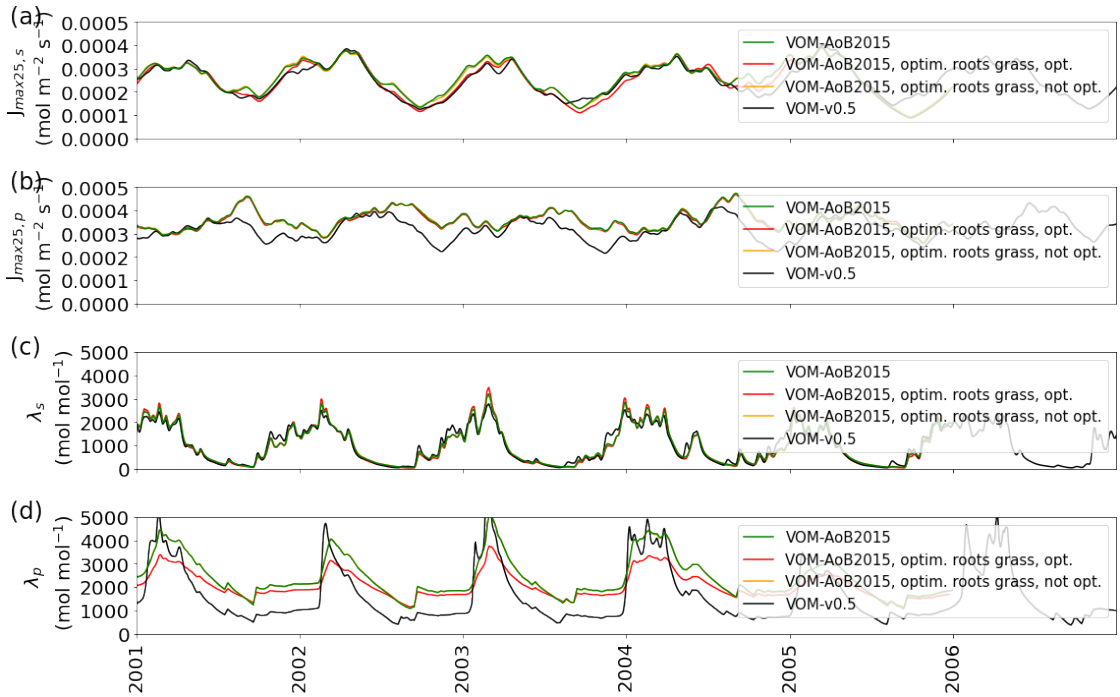

Figure S1.22. *Comparison for Howard Springs from 2001-2006 (subset from 1980-2017) between the results of Schymanski et al. (2015) (VOM-AoB2015, green) grass rooting depths were fixed at 1.0 m, and a re-optimized reproduction of these results that optimize the rooting depth of grasses (VOM-AoB2015, optim. roots grass, opt., red), a reproduction of these results without optimization using the parameter from the VOM-AoB2015 (VOM-AoB2015, optim. roots grass, not opt., yellow) and the new VOM-v0.5 modelling results (black), for a) the electron transport capacity at 25 ^oC for seasonal grasses ($J_{max25,s}$), b) the electron transport capacity at 25 ^oC for perennials trees ($J_{max25,p}$), d) transpiration seasonals (grasses), d) the daily slope (λ_s) between assimilation and transpiration of the seasonal grasses, e) the daily slope (λ_p) between assimilation and transpiration of the perennials (trees).*

The values for the slope λ_p between assimilation and transpiration of the perennial vegetation reduced with the optimized grass roots, just as the electron transport capacities $J_{max25,p}$ and $J_{max25,s}$, in comparison with the original results.

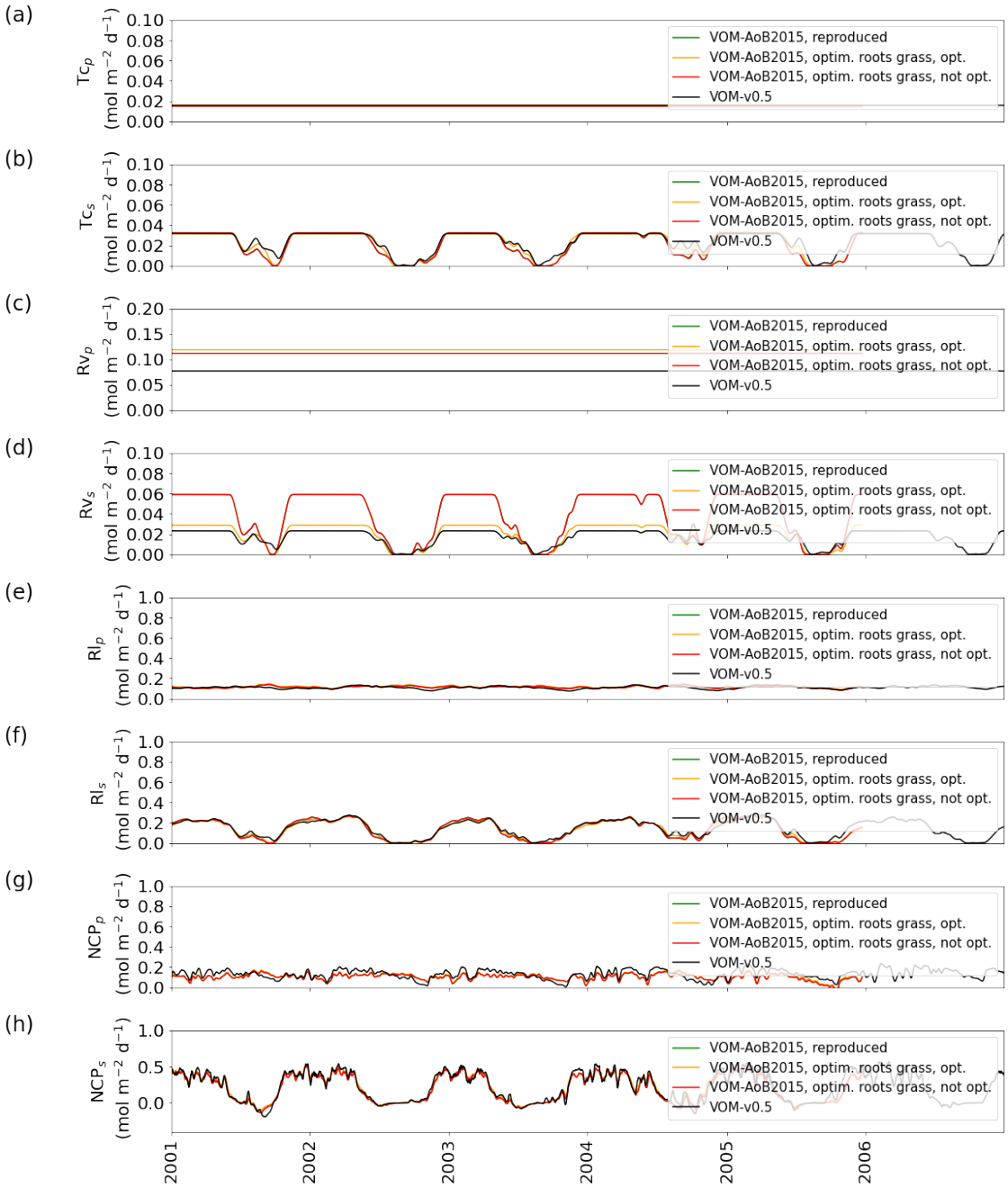

Figure S1.23. *Comparison for Howard Springs from 2001-2006 (subset from 1980-2017) between the reproduced results of Schymanski et al. (2015) (VOM-AoB2015, reproduced, green) grass rooting depths were fixed at 1.0 m, and a re-optimized reproduction of these results that optimize the rooting depth of grasses (VOM-AoB2015, optim. roots grass, opt., red), a reproduction of these results without optimization using the parameter from the VOM-AoB2015 (VOM-AoB2015, optim. roots grass, not opt., yellow) and the new VOM-v0.5 modelling results (black), for a) the foliage turnover costs perennial trees (Tc_p), b) the foliage turnover costs seasonal grasses (Tc_s), c) the water transport costs for perennial trees (Rv_p), d) the water transport costs for seasonal grasses*

(Rv_s), e) leaf respiration perennial trees (Rl_p), f)leaf respiration seasonal grasses (Rl_s), g) root respiration perennial trees (Rr_p), h) root respiration seasonal grasses (Rr_s), all smoothed with a moving average of 7 days, and h) projective cover. Note that the original results of Schymanski et al. (2015) are not shown, as these variables were not produced as outputs, but only the reproduced values are shown.

Most of the costs decrease when grasses are optimized, but most notably the costs for the water transport system.

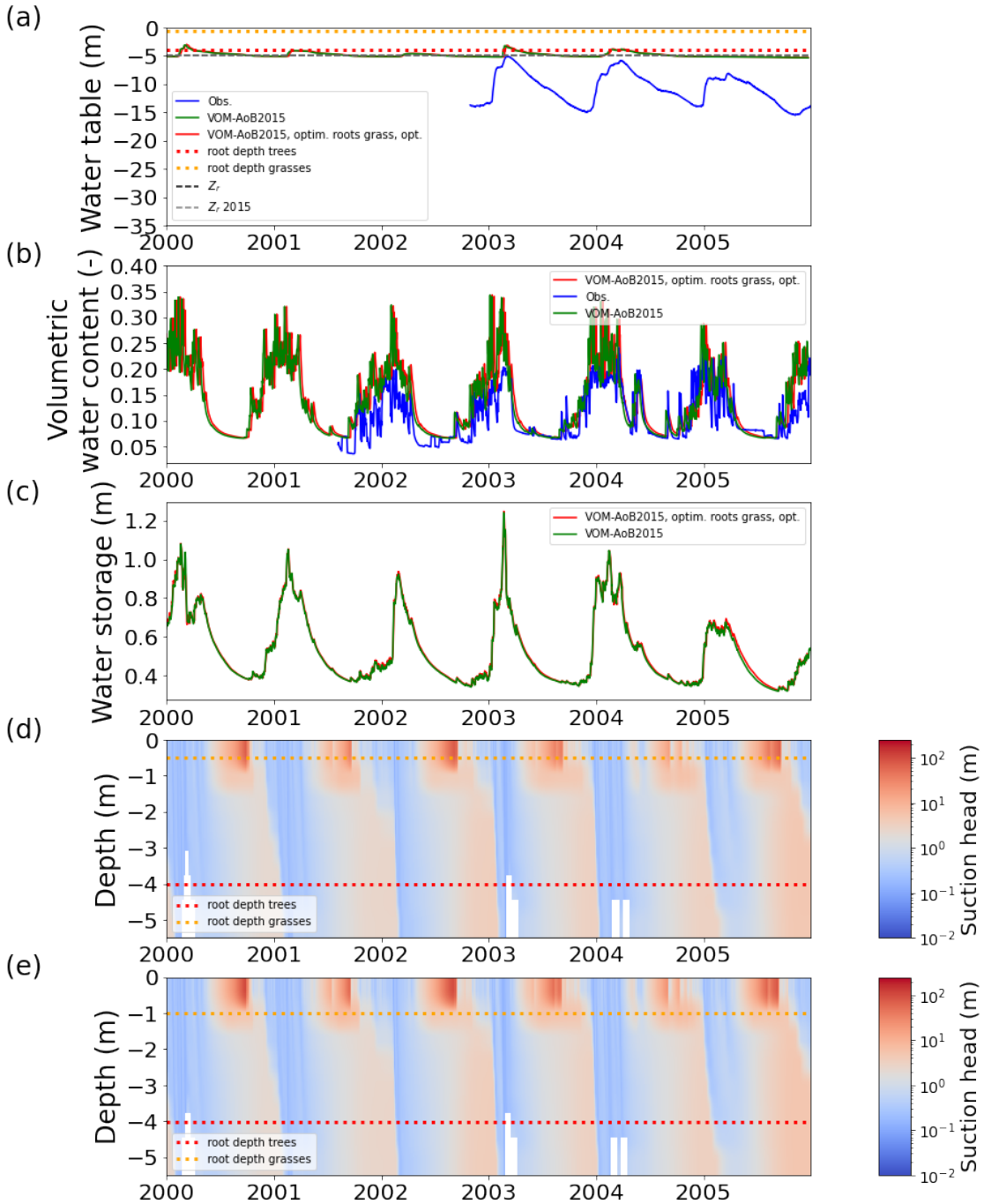

Figure S1.24. *Results for Howard Springs with a) groundwater depths, with dashed lines representing the bedrock depth, dotted lines the rooting depths (trees in red and grasses in orange), the re-optimized, reproduced results with optimized grass roots (VOM-AoB2015, optim. roots grass, opt.), the results of Schymanski et al. (2015) in green (VOM-AoB2015), and observations of three different boreholes in the vicinity of the study site in blue (Government Northern Territory, Australia, 2018). The soil moisture saturation in the upper soil layer is shown for Howard Springs*

in b) with the reproduced results of Schymanski et al. (2015) in red (VOM-AoB2015, optim. roots grass, opt.), the results of Schymanski et al. (2015) in green (VOM-AoB2015) and soil moisture measurements at 5 cm depth at the flux tower sites in blue. The total water storage in the root zone is shown in c) for the reproduced results of Schymanski et al. (2015) (VOM-AoB2015, optim. roots grass, opt., red) and the results of Schymanski et al. (2015) in green (VOM-AoB2015). The matrix water suction heads are shown in d) for the reproduced model runs of the VOM with optimized grass roots, whereas e) displays the water suction heads of Schymanski et al. (2015).

The water storage increases during the dry season, but decreases slightly during the wet season. The matrix potentials are also lower when grass roots are optimized.

Concluding remarks

Adding the grass rooting depths to the optimized vegetation properties leads to strong differences in the results (Figures S1.25-S1.28). Total GPP and ET both reduced when roots were optimized. At the same time, the perennial trees transpired less, whereas the transpiration of the seasonal grasses increased. This is rather surprising, as the rooting depths for both perennials and seasonals decreased, but the daily slope (λ_s) between assimilation and transpiration of the seasonal grasses strongly increased as well, leading to a more efficient CO_2-uptake.

1.7 Updated weatherdata

The meteorological forcing data was updated by a newer version from the Australian SILO. This included variable atmosperic pressure levels.

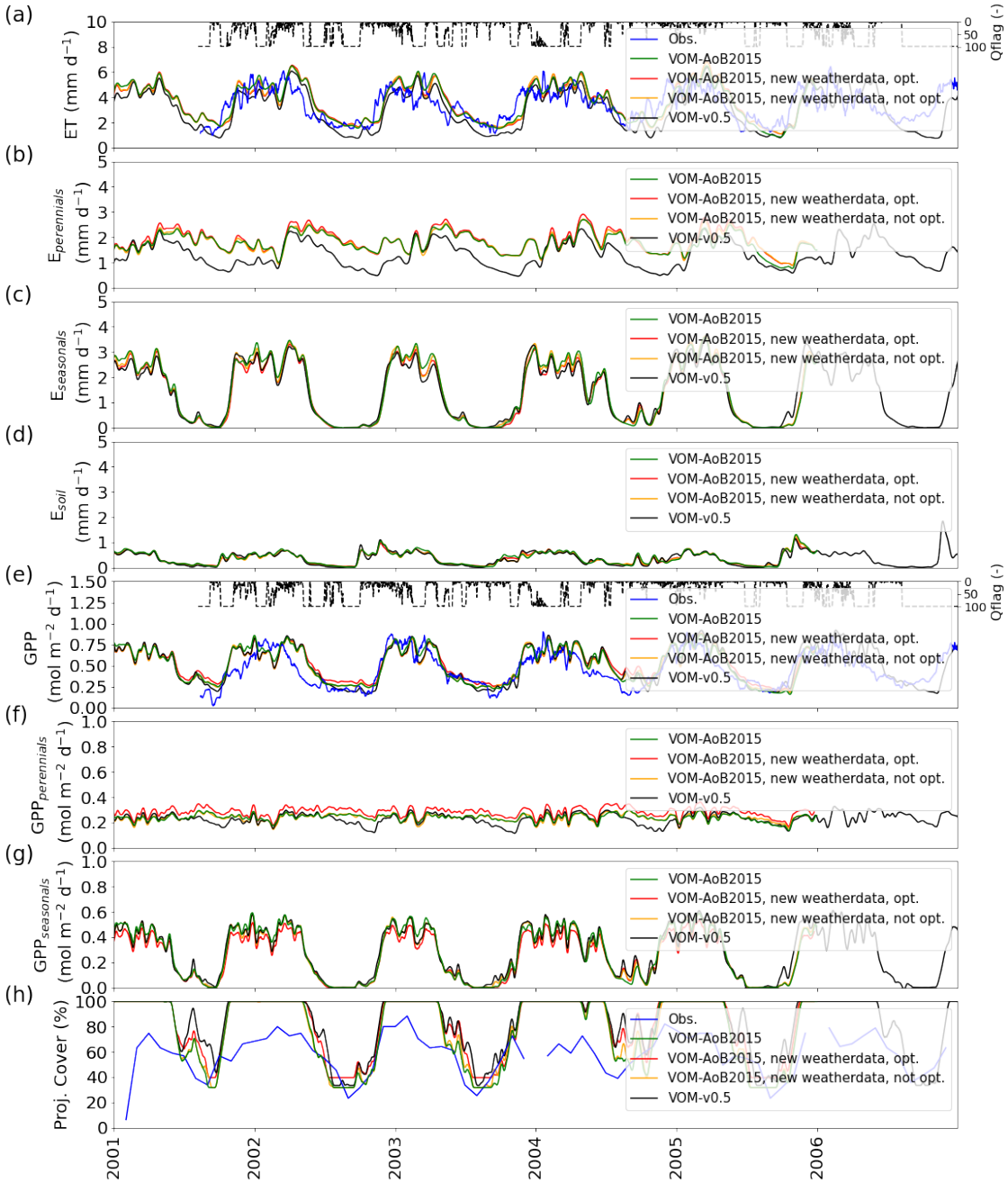

Figure S1.25. *Comparison for Howard Springs from 2001-2006 (subset from 1980-2017) between the results of Schymanski et al. (2015) (VOM-AoB2015, green), and a re-optimized reproduction of these results that use a new version of SILO-datadrill, including variable atmosperic levels (VOM-AoB2015, new weatherdata, opt., red), a reproduction of these results without optimization using the parameter from the VOM-AoB2015 (VOM-AoB2015, new weatherdata, not opt., yellow) and the new VOM-v0.5 modelling results (black), for a) ET, b) transpiration perennials (trees), c) transpiration seasonals (grasses), d) soil evaporation, e) GPP, f) GPP perennials (trees), g) GPP seasonals (grasses), all smoothed with a moving average of 7 days, and h) projective cover. The*

daily average quality flags of the fluxtower observations are shown in dashed lines with a value of 100 when a day is completely gap-filled and 1 when it is observed.

The new weatherdata hardly leads to any differences, except for slightly reduced values of the transpiration of the seasonal vegetation. Minor differences in the vegetation cover can be found as well.

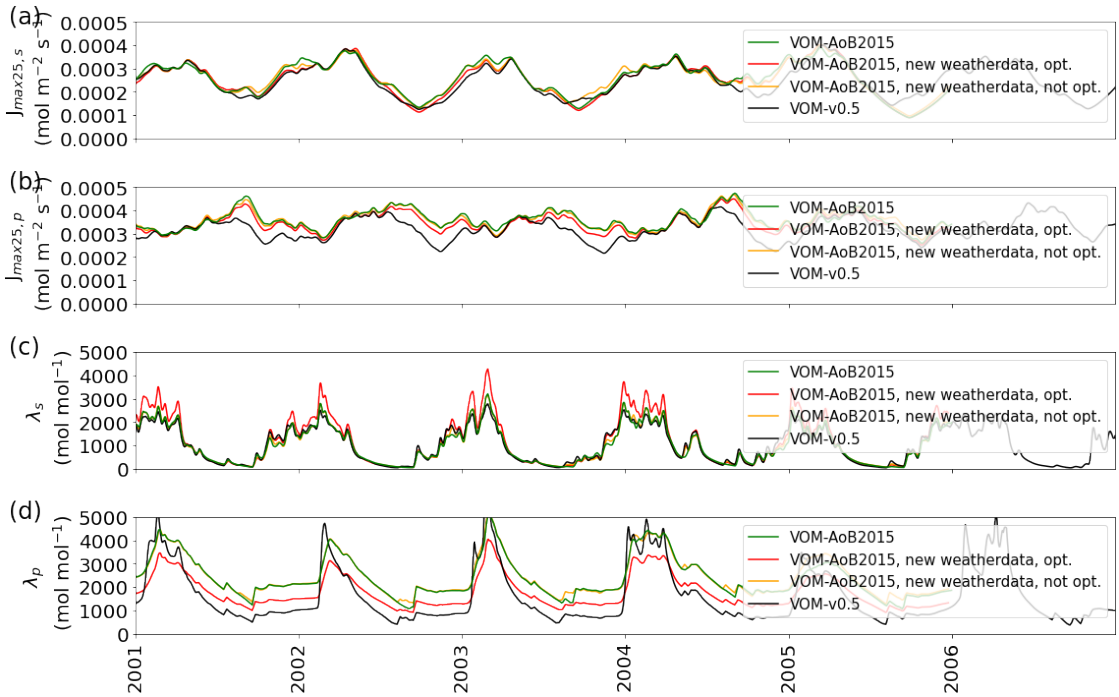

Figure S1.26. *Comparison for Howard Springs from 2001-2006 (subset from 1980-2017) between the results of Schymanski et al. (2015) (VOM-AoB2015, green), and a re-optimized reproduction of these results that use a new version of SILO-datadrill, including variable atmosperic levels (VOM-AoB2015, new weatherdata, opt., red), a reproduction of these results without optimization using the parameter from the VOM-AoB2015 (VOM-AoB2015, new weatherdata, not opt., yellow) and the new VOM-v0.5 modelling results (black), for a) the electron transport capacity at 25 ^oC for seasonal grasses ($J_{max25,s}$), b) the electron transport capacity at 25 ^oC for perennials trees ($J_{max25,p}$), d) transpiration seasonals (grasses), d) the daily slope (λ_s) between assimilation and transpiration of the seasonal grasses, e) the daily slope (λ_p) between assimilation and transpiration of the perennials (trees).*

The values for the slope λ_p between assimilation and transpiration of the perennial vegetation is slighty reduced with the new weatherdata, in comparison with the original results, but the results remain rather similar again.

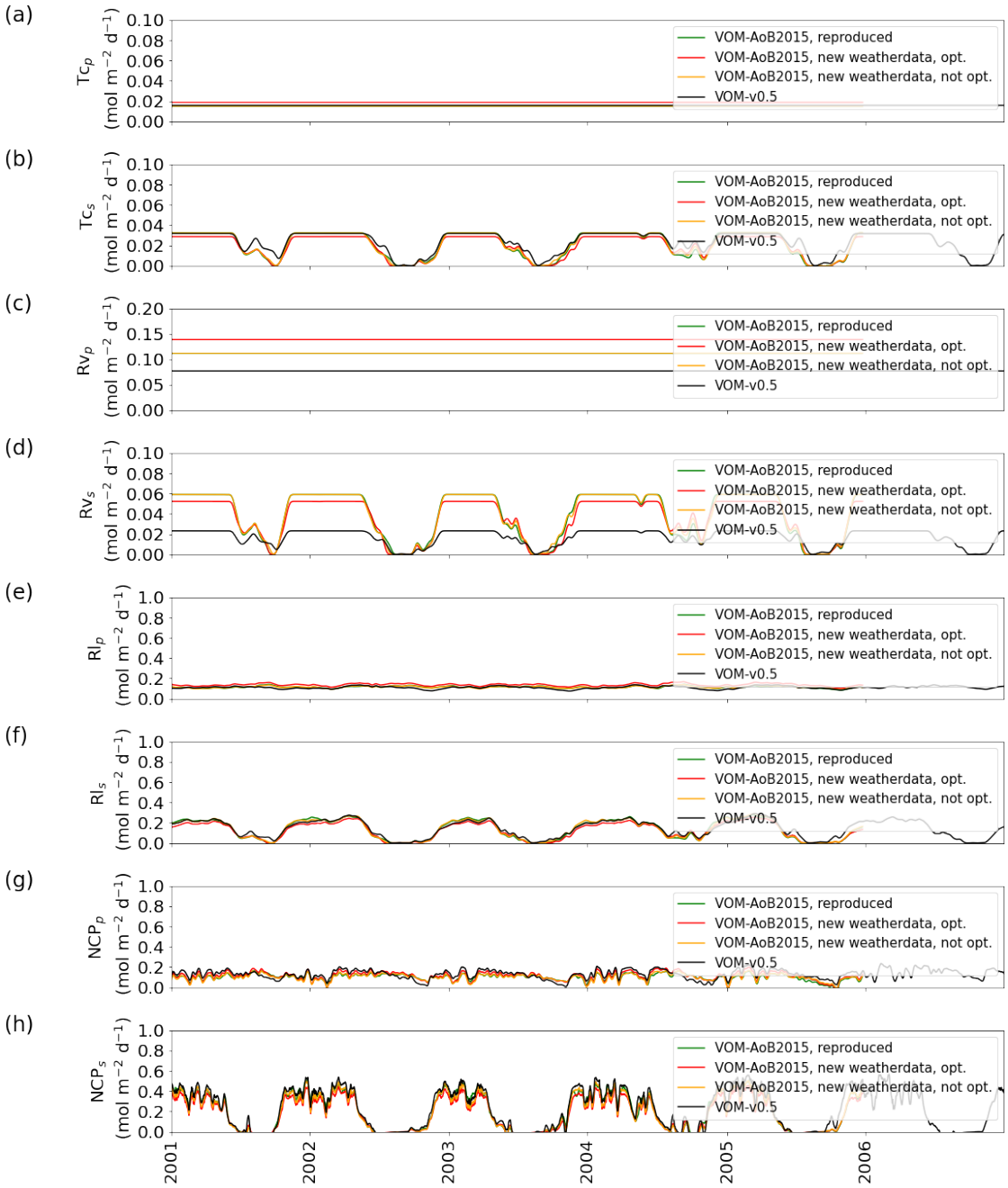

Figure S1.27. *Comparison for Howard Springs from 2001-2006 (subset from 1980-2017) between the reproduced results of Schymanski et al. (2015) (VOM-AoB2015, reproduced, green), and a re-optimized reproduction of these results that use a new version of SILO-datadrill, including variable atmosperic levels (VOM-AoB2015, new weatherdata, opt., red), a reproduction of these results without optimization using the parameter from the VOM-AoB2015 (VOM-AoB2015, new weatherdata, not opt., yellow) and the new VOM-v0.5 modelling results (black), for a) the foliage turnover costs perennial trees (Tc_p), b) the foliage turnover costs seasonal grasses (Tc_s), c) the water transport costs for perennial trees (Rv_p), d) the water transport costs for seasonal grasses*

(Rv_s), e) leaf respiration perennial trees (Rl_p), f)leaf respiration seasonal grasses (Rl_s), g) root respiration perennial trees (Rr_p), h) root respiration seasonal grasses (Rr_s), all smoothed with a moving average of 7 days, and h) projective cover. Note that the original results of Schymanski et al. (2015) are not shown, as these variables were not produced as outputs, but only the reproduced values are shown.

The results remain rather similar between the runs with the new weatherdata and the reproduced results of Schymanski et al. (2015).

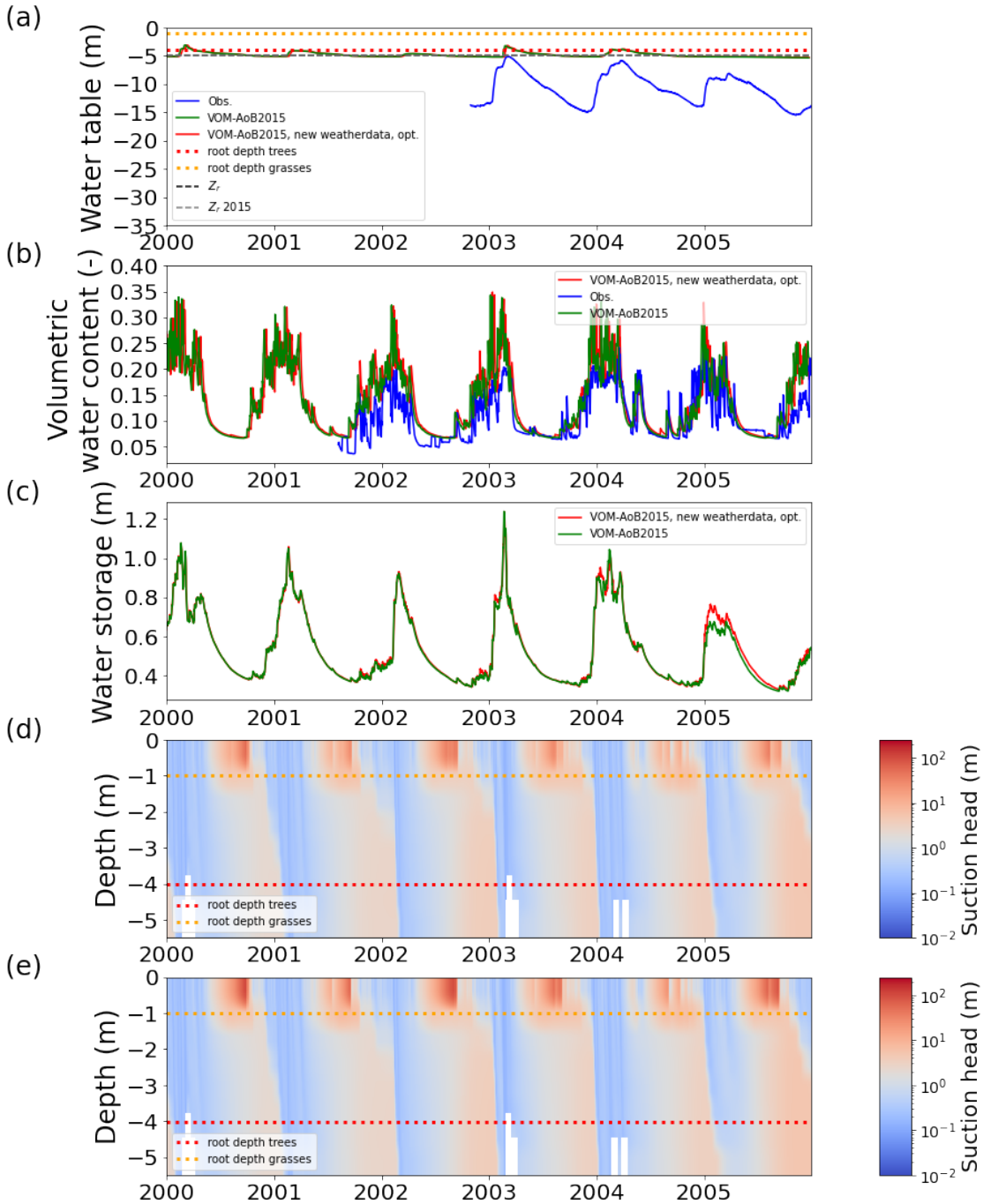

Figure S1.28. *Results for Howard Springs with a) groundwater depths, with dashed lines representing the bedrock depth, dotted lines the rooting depths (trees in red and grasses in orange), the re-optimized, reproduced results that use a new version of SILO-datadrill, including variable atmosperic levels (VOM-AoB2015, new weatherdata, opt.), the results of Schymanski et al. (2015) in green (VOM-AoB2015), and observations of three different boreholes in the vicinity of the study site in blue (Government Northern Territory, Australia, 2018). The soil moisture saturation in*

the upper soil layer is shown for Howard Springs in b) with the reproduced results of Schymanski et al. (2015) in red (VOM-AoB2015, new weatherdata, opt.), the results of Schymanski et al. (2015) in green (VOM-AoB2015) and soil moisture measurements at 5 cm depth at the flux tower sites in blue. The total water storage in the root zone is shown in c) for the reproduced results of Schymanski et al. (2015) (VOM-AoB2015, new weatherdata, opt., red) and the results of Schymanski et al. (2015) in green (VOM-AoB2015). The matrix water suction heads are shown in d) for the model runs of the VOM with updated weatherdata, whereas e) displays the water suction heads of Schymanski et al. (2015).

Concluding remarks

The new weather data only had a minor effect on the results (Figures S1.29-1.32), and will therefore not have a big effect on the new modelling results.

1.8 Updated and extended meteorological data

The model runs of Schymanski et al. (2015) were run from 1976 until 2005, whereas the new runs start from 1980 until 2017, as the new version of the meteorological data from the Australian SILO Data Drill (Jeffrey et al., 2001) includes more recent years. This should not lead to large differences in the results.

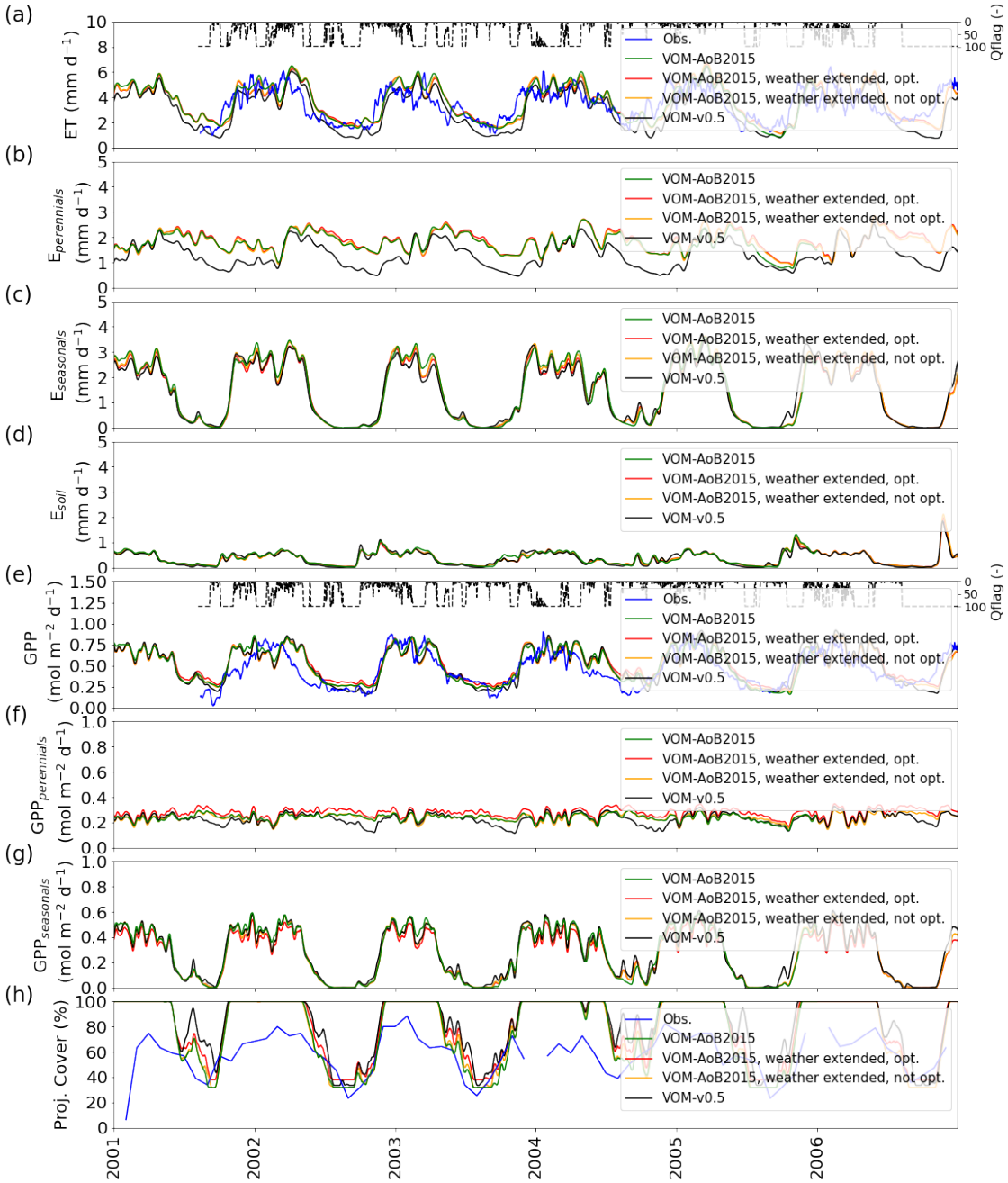

Figure S1.29. *Comparison for Howard Springs from 2001-2006 (subset from 1980-2017) between the results of Schymanski et al. (2015) (VOM-AoB2015, green) where the model period was set from 1976 until 2005, and a re-optimized reproduction of these results that use updated and extended meteorological data (VOM-AoB2015, new model period, opt., red), a reproduction of these results without optimization using the parameter from the VOM-AoB2015 (VOM-AoB2015,, new model period, not opt., yellow) and the new VOM-v0.5 modelling results (black), for a) ET, b) transpiration perennials (trees), c) transpiration seasonals (grasses), d) soil evaporation, e) GPP, f) GPP perennials (trees), g) GPP seasonals (grasses), all smoothed with a moving average of 7*

days, and h) projective cover. The daily average quality flags of the fluxtower observations are shown in dashed lines with a value of 100 when a day is completely gap-filled and 1 when it is observed.

Results of total GPP and ET are similar between the reproduced runs and the original results of Schymanski et al. (2015). The GPP and transpiration for the perennials are slightly increased for the new modelling period, just as the vegetative cover.

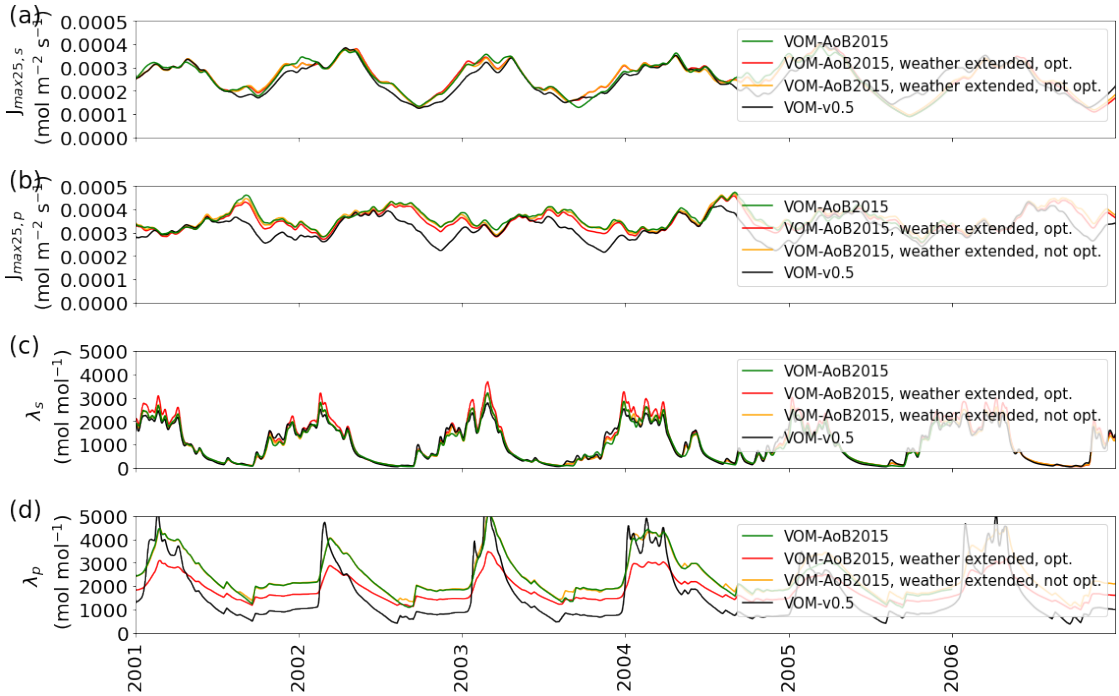

Figure S1.30. *Comparison for Howard Springs from 2001-2006 (subset from 1980-2017) between the results of Schymanski et al. (2015) (VOM-AoB2015, green) where the model period was set from 1976 until 2005, and a re-optimized reproduction of these results that updated and extended meteorological data (VOM-AoB2015, new model period, opt., red), a reproduction of these results without optimization using the parameters from the VOM-AoB2015 (VOM-AoB2015, new model period, not opt., yellow) and the new VOM-v0.5 modelling results (black), for a) the electron transport capacity at 25 ^oC for seasonal grasses ($J_{max25,s}$), b) the electron transport capacity at 25 ^oC for perennials trees ($J_{max25,p}$), d) transpiration seasonals (grasses), d) the daily slope (λ_s) between assimilation and transpiration of the seasonal grasses, e) the daily slope (λ_p) between assimilation and transpiration of the perennials (trees).*

Results are similar between the reproduced runs, and the original results of Schymanski et al. (2015), except for lower values for λ_p and $J_{max25,p}$.

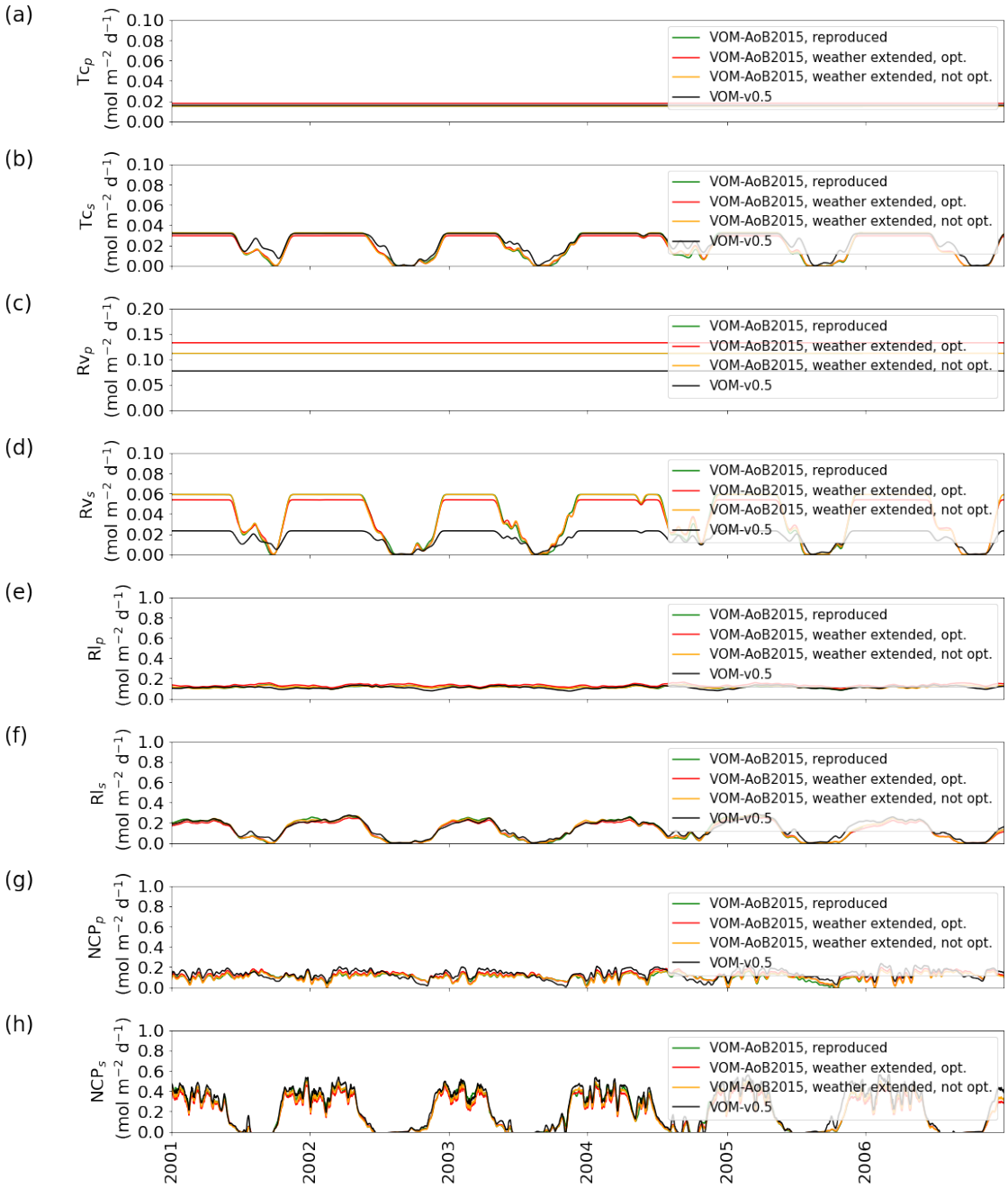

Figure S1.31. *Comparison for Howard Springs from 2001-2006 (subset from 1980-2017) between the reprpoduced results of Schymanski et al. (2015) (VOM-AoB2015, reproduced, green) where the model period was set from 1976 until 2005, and a re-optimized reproduction of these results that use updated and extended meteorological data(VOM-AoB2015, new model period, opt., red), a reproduction of these results without optimization using the parameters from the VOM-AoB2015 (VOM-AoB2015, new model period, not opt., yellow) and the new VOM-v0.5 modelling results (black), for a) the foliage turnover costs perennial trees (Tc_p), b) the foliage turnover costs seasonal grasses (Tc_s), c) the water transport costs for perennial trees (Rv_p), d) the water transport costs for*

seasonal grasses (Rv_s), e) leaf respiration perennial trees (Rl_p), f)leaf respiration seasonal grasses (Rl_s), g) root respiration perennial trees (Rr_p), h) root respiration seasonal grasses (Rr_s), all smoothed with a moving average of 7 days, and h) projective cover. Note that the original results of Schymanski et al. (2015) are not shown, as these variables were not produced as outputs, but only the reproduced values are shown. The results remain similar, except for lower values of the water transport costs for seasonal grasses (Rv_s).

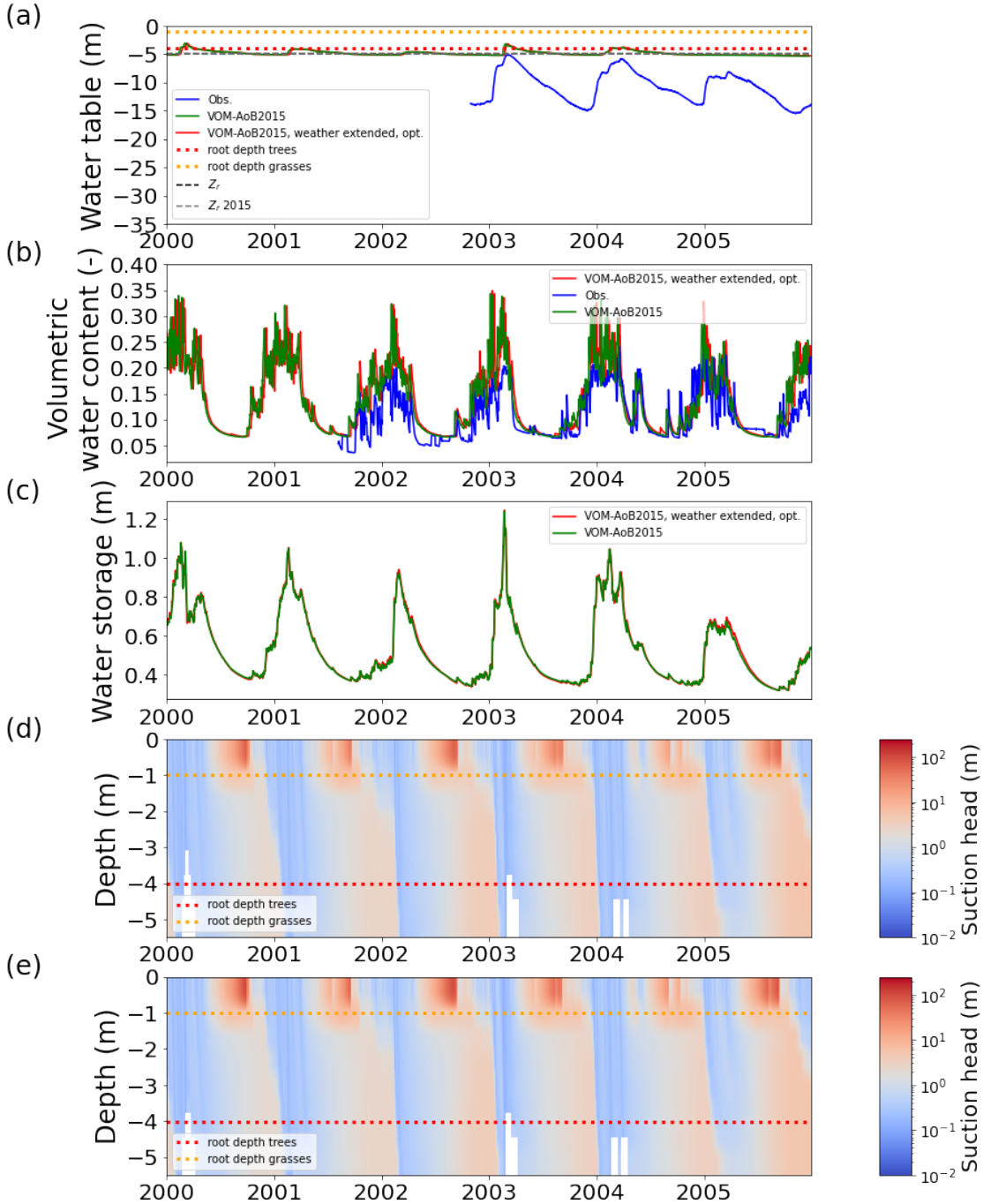

Figure S1.32. *Results for Howard Springs with a) groundwater depths, with dashed lines representing the bedrock depth, dotted lines the rooting depths (trees in red and grasses in orange), the re-optimized, reproduced results that use updated and extended meteorological data in red (VOM-AoB2015, new model period, opt), the results of Schymanski et al. (2015) in green (VOM-AoB2015), and observations of three different boreholes in the vicinity of the study site in blue (Government Northern Territory, Australia, 2018). The soil moisture saturation in the upper soil layer is shown for Howard Springs in b) with the reproduced results of Schymanski et al. (2015) in red (VOM-AoB2015, new model period, opt), the results of Schymanski et al. (2015) in green (VOM-AoB2015) and soil moisture measurements at 5 cm depth at the flux tower sites in blue. The total water storage in the root zone is shown in c) for the reproduced results of Schymanski et al. (2015) (VOM-AoB2015, new model period, opt, red) and the results of Schymanski et al. (2015) in green (VOM-AoB2015). The matrix water suction heads are shown in d) for the model runs of the VOM with updated and extended meteorological data, whereas e) displays the water suction heads of Schymanski et al. (2015).*

The differences between the model runs with the model period and the original results of Schymanski et al. (2015) remain small.

Concluding remarks

The changed modelling period (from 1976-2005 to 1980-2017) did not show strong differences in ET and GPP, but also other variables, such as carbon costs and electron transport capacities, remained similar as the the original results of Schymanski et al. (2015) (Figures S1.9-S1.12). Therefore, we can conclude that the new modelling period will not have a strong influence on the new results.

1.9 New hydrology

The hydrological parameters were changed in order to have freely draining conditions. The soil parameters are kept the same as for Schymanski et al (2015).

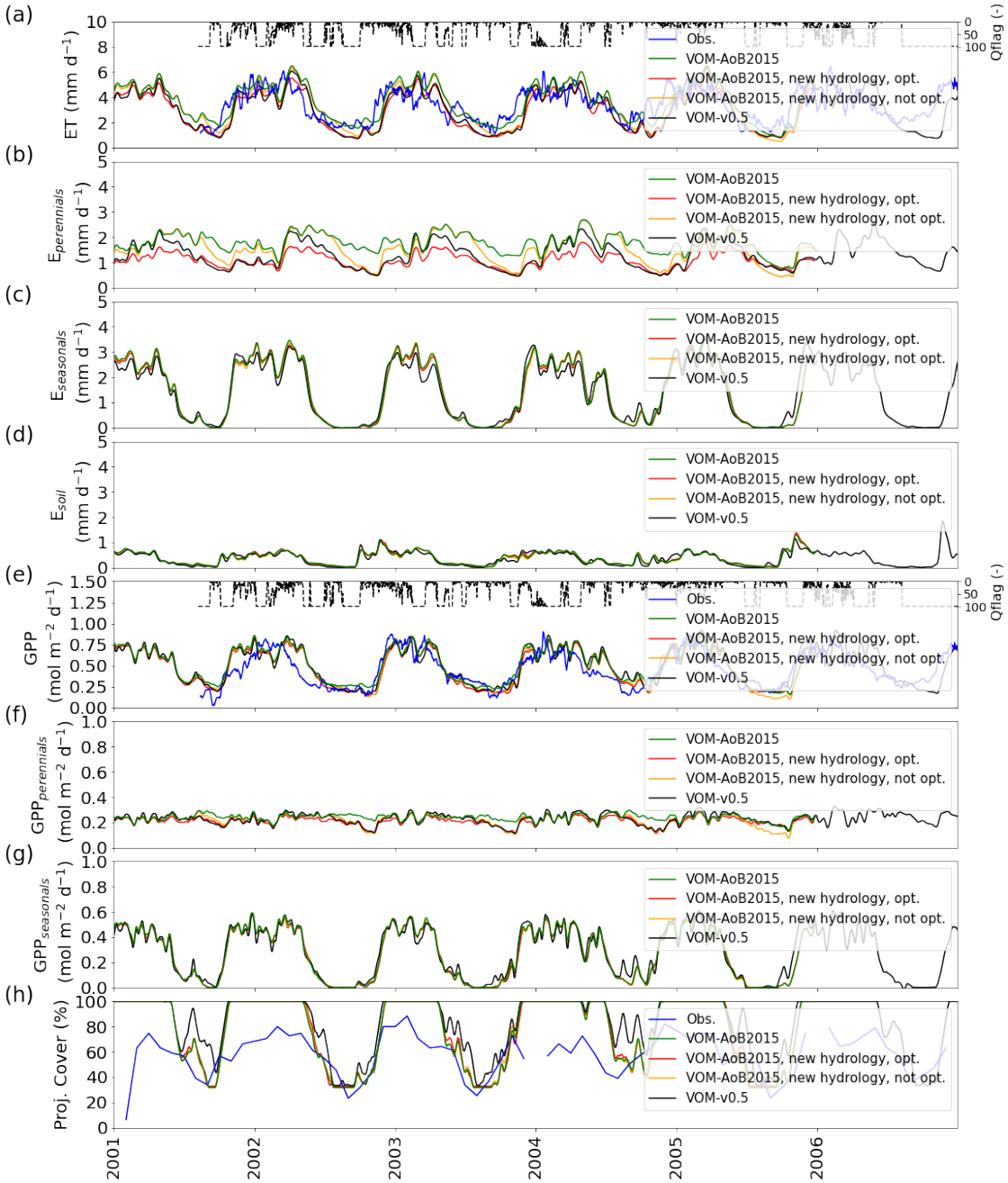

Figure S1.33. *Comparison for Howard Springs from 2001-2006 (subset from 1980-2017) between the results of Schymanski et al. (2015) (VOM-AoB2015, green), and a re-optimized reproduction of these results that use free draining hydrological parameters(VOM-AoB2015, new hydrology, opt., red), a reproduction of these results without optimization using the parameter from the VOM-AoB2015 (VOM-AoB2015, new hydrology, not opt., yellow) and the new VOM-v0.5 modelling results (black), for a) ET, b) transpiration perennials (trees), c) transpiration seasonals (grasses), d) soil evaporation, e) GPP, f) GPP perennials (trees), g) GPP seasonals (grasses), all smoothed with a moving average of 7 days, and h) projective cover. The daily average quality flags of the*

fluxtower observations are shown in dashed lines with a value of 100 when a day is completely gap-filled and 1 when it is observed.

The new hydrological parameterization leads to a strong decrease in the transpiration of the perennial vegetation, just as reduced values for the GPP of the perennial vegetation.

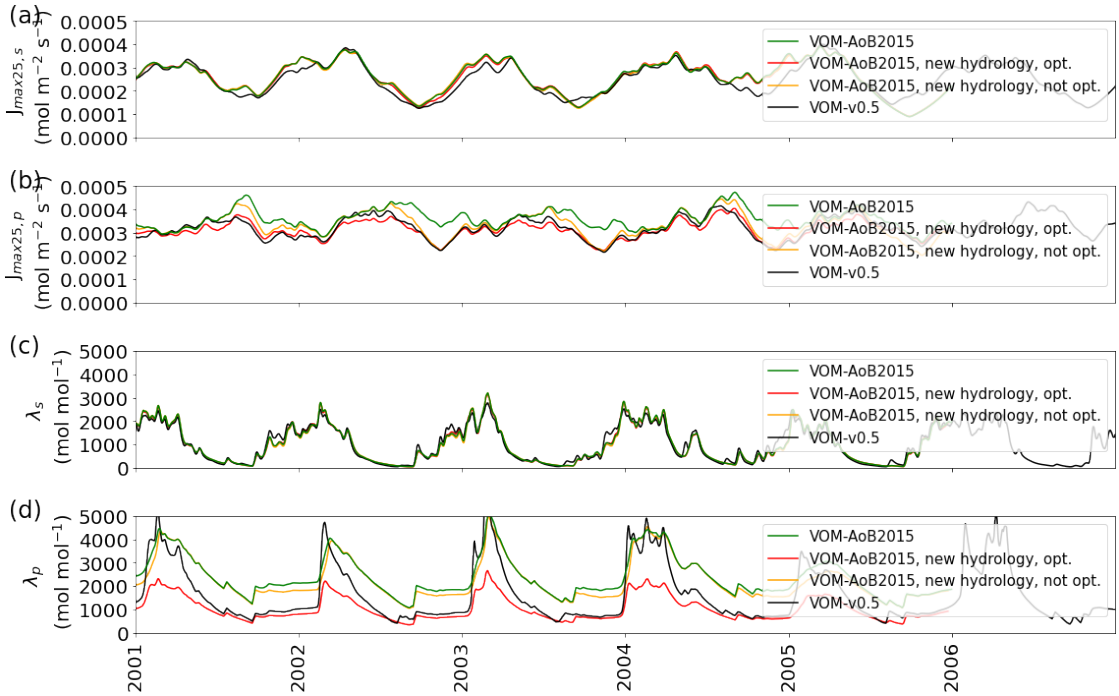

Figure S1.34. *Comparison for Howard Springs from 2001-2006 (subset from 1980-2017) between the results of Schymanski et al. (2015) (VOM-AoB2015, green), and a re-optimized reproduction of these results that use free draining hydrological parameters(VOM-AoB2015, new hydrology, opt., red), a reproduction of these results without optimization using the parameter from the VOM-AoB2015 (VOM-AoB2015, new hydrology, not opt., yellow) and the new VOM-v0.5 modelling results (black), for a) the electron transport capacity at 25 ^oC for seasonal grasses ($J_{max25,s}$), b) the electron transport capacity at 25 ^oC for perennials trees ($J_{max25,p}$), d) transpiration seasonals (grasses), d) the daily slope (λ_s) between assimilation and transpiration of the seasonal grasses, e) the daily slope (λ_p) between assimilation and transpiration of the perennials (trees).*

The values for the slope λ_p between assimilation and transpiration of the perennial vegetation are reduced with the new hydrological parameterization, just as the electron transport capacity $J_{max25,p}$, in comparison with the original results.

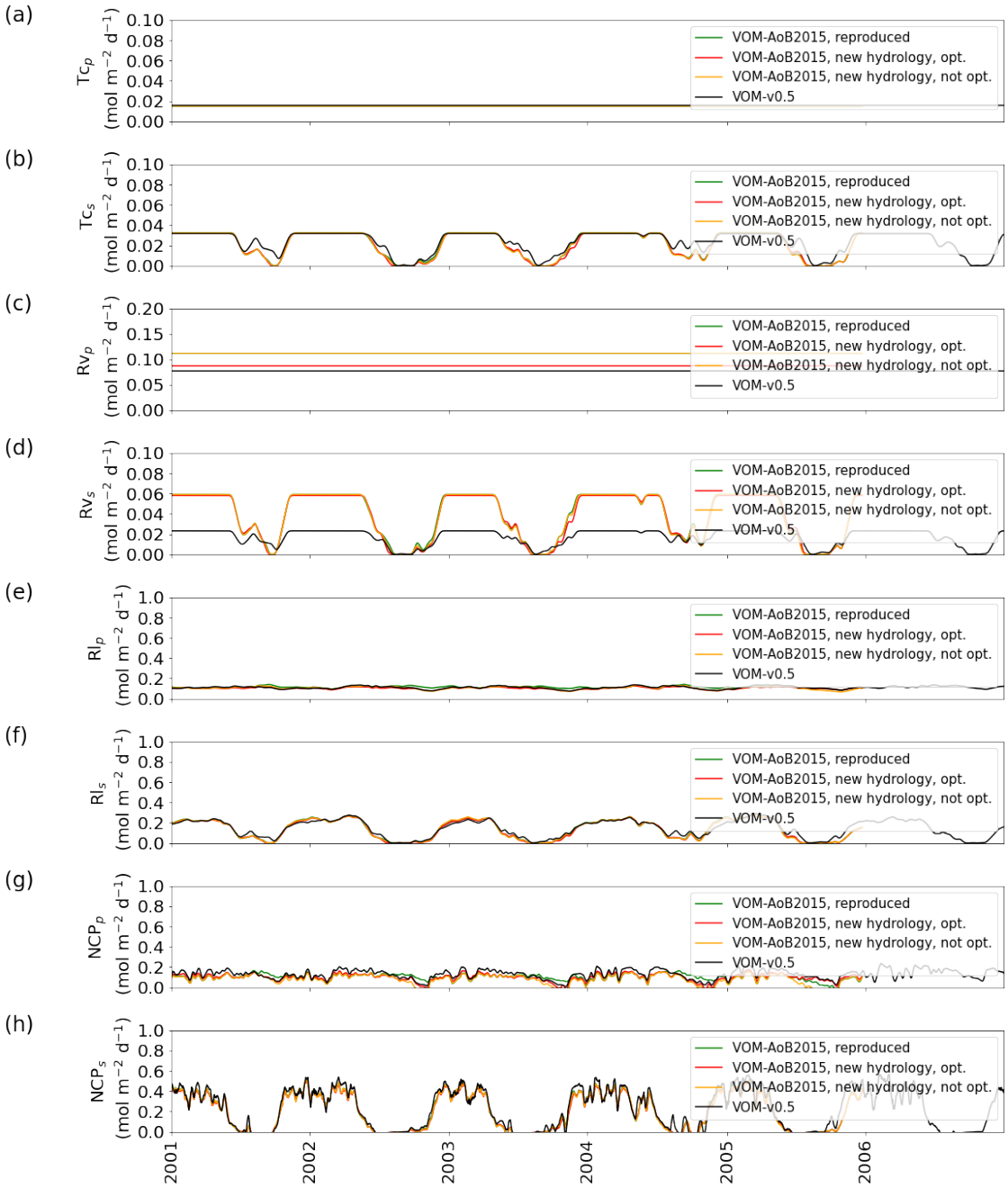

Figure S1.35. *Comparison for Howard Springs from 2001-2006 (subset from 1980-2017) between the reproduced results of Schymanski et al. (2015) (VOM-AoB2015, reproduced, green), and a re-optimized reproduction of these results that use free draining hydrological parameters(VOM-AoB2015, new hydrology, opt., red), a reproduction of these results without optimization using the parameter from the VOM-AoB2015 (VOM-AoB2015, new hydrology, not opt., yellow) and the new VOM-v0.5 modelling results (black), for a) the foliage turnover costs perennial trees (Tc_p), b) the foliage turnover costs seasonal grasses (Tc_s), c) the water transport costs for perennial trees (Rv_p), d) the water transport costs for seasonal grasses (Rv_s), e) leaf respiration perennial trees*

(Rl_p), f)leaf respiration seasonal grasses (Rl_s), g) root respiration perennial trees (Rr_p), h) root respiration seasonal grasses (Rr_s), all smoothed with a moving average of 7 days, and h) projective cover. Note that the original results of Schymanski et al. (2015) are not shown, as these variables were not produced as outputs, but only the reproduced values are shown.

The results in terms of carbon costs remain rather similar between the runs with the new hydrology and the reproduced results of Schymanski et al. (2015).

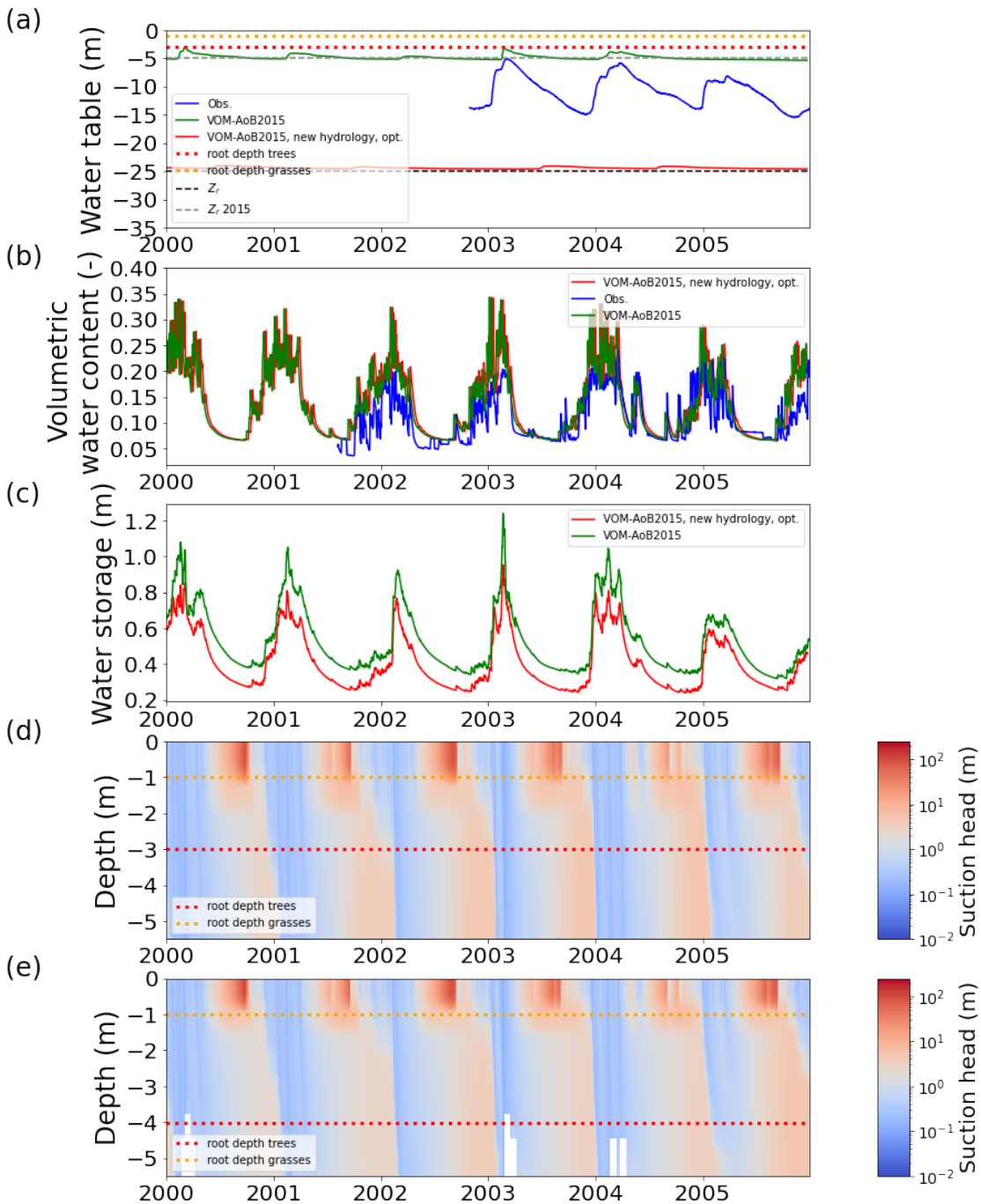

Figure S1.36. *Results for Howard Springs with a) groundwater depths, with dashed lines representing the bedrock depth, dotted lines the rooting depths (trees in red and grasses in orange), the re-optimized, reproduced results that use free draining hydrological parameters (VOM-AoB2015, new hydrology, opt.), the results of Schymanski et al. (2015) in green (VOM-AoB2015), and observations of three different boreholes in the vicinity of the study site in blue (Government Northern Territory, Australia, 2018). The soil moisture saturation in the upper soil layer is shown for Howard Springs in b) with the reproduced results of Schymanski et al. (2015) in red (VOM-AoB2015, new hydrology, opt.), the results of Schymanski et al. (2015) in green (VOM-AoB2015) and soil moisture measurements at 5 cm depth at the flux tower sites in blue. The total water storage in the root zone is shown in c) for the reproduced results of Schymanski et al. (2015) (VOM-AoB2015, new hydrology, opt., red) and the results of Schymanski et al. (2015) in green (VOM-AoB2015). The matrix water suction heads are shown in d) for the model runs of the VOM with free draining hydrological parameters, whereas e) displays the water suction heads of Schymanski et al. (2015).*

The groundwater tables are much deeper with new hydrological parameterization. However, storage in the upper 5 meters increases, just as matrix potentials around 5 meters depth.

Concluding remarks

The new hydrological parameterization affected especially the evapo-transpiration, that were lower in total, but especially for the perennial trees (Figures S1.33-S1.36). The GPP of the seasonal grasses remained rather similar, but the GPP for the perennial trees reduced as well. This relates to the deeper groundwater tables, and a quicker drainage of water.

1.10 New soil parameters

The soil column was now changed to a soil profile of sandy clay loam, with especially a lower saturated hydraulic conductivity, and sandy loam in the top 0.5m.

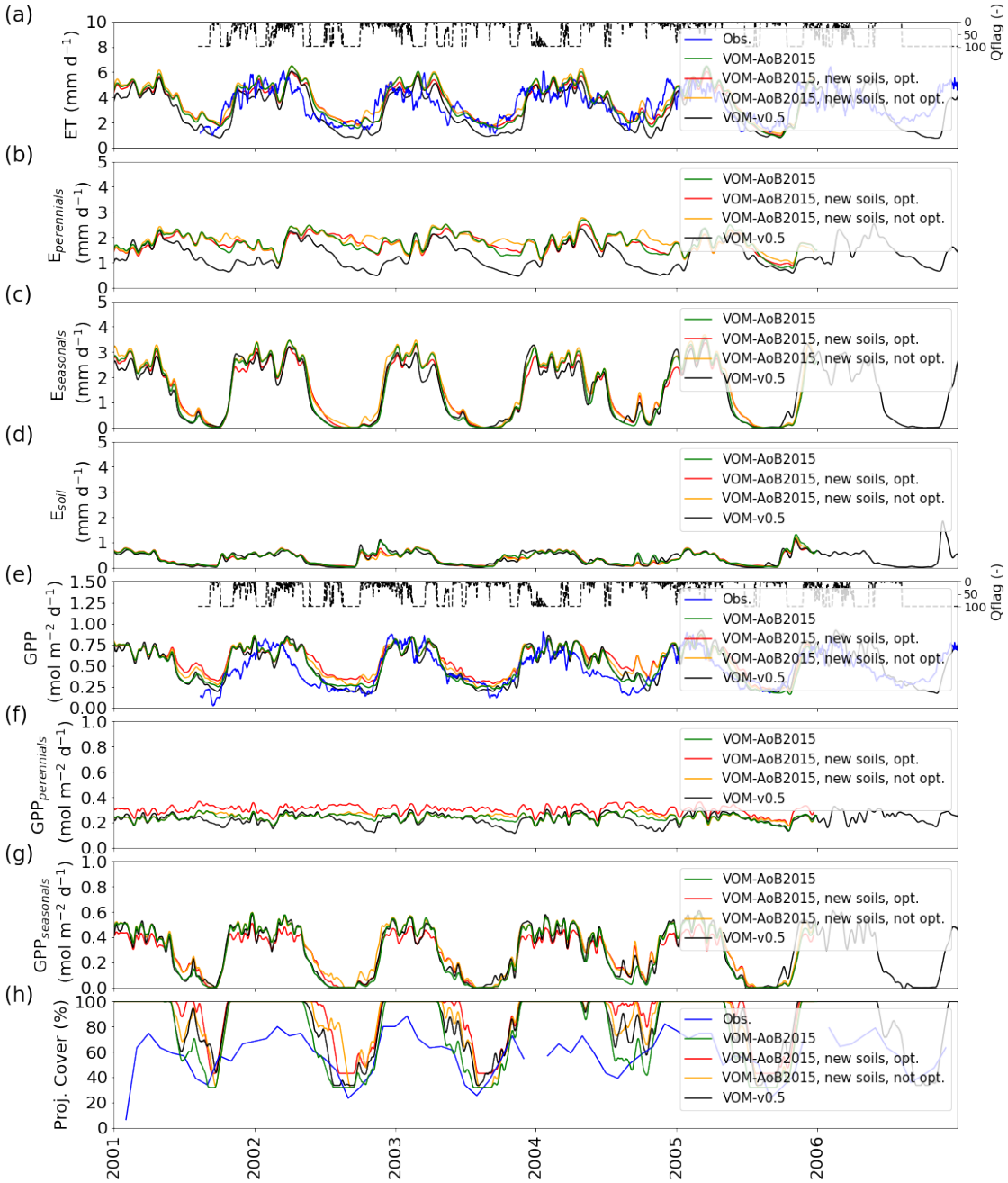

Figure S1.37. *Comparison for Howard Springs from 2001-2006 (subset from 1980-2017) between the results of Schymanski et al. (2015) (VOM-AoB2015, green), and a re-optimized reproduction of these results that use different, homogeneous soil parameters (VOM-AoB2015, new soils, opt., red), a reproduction of these results without optimization using the parameter from the VOM-AoB2015 (VOM-AoB2015, new soils, not opt., yellow) and the new VOM-v0.5 modelling results (black), for a) ET, b) transpiration perennials (trees), c) transpiration seasonals (grasses), d) soil evaporation, e) GPP, f) GPP perennials (trees), g) GPP seasonals (grasses), all smoothed with a moving average of 7 days, and h) projective cover. The daily average quality flags of the fluxtower observations*

are shown in dashed lines with a value of 100 when a day is completely gap-filled and 1 when it is observed.

The new soil parameterization leads to a decrease in perennial and seasonal transpiration, but an increase in soil evaporation. The GPP values for the perennial vegetation remains similar, but the GPP for the seasonal vegetation decreases and shows a delayed signal.

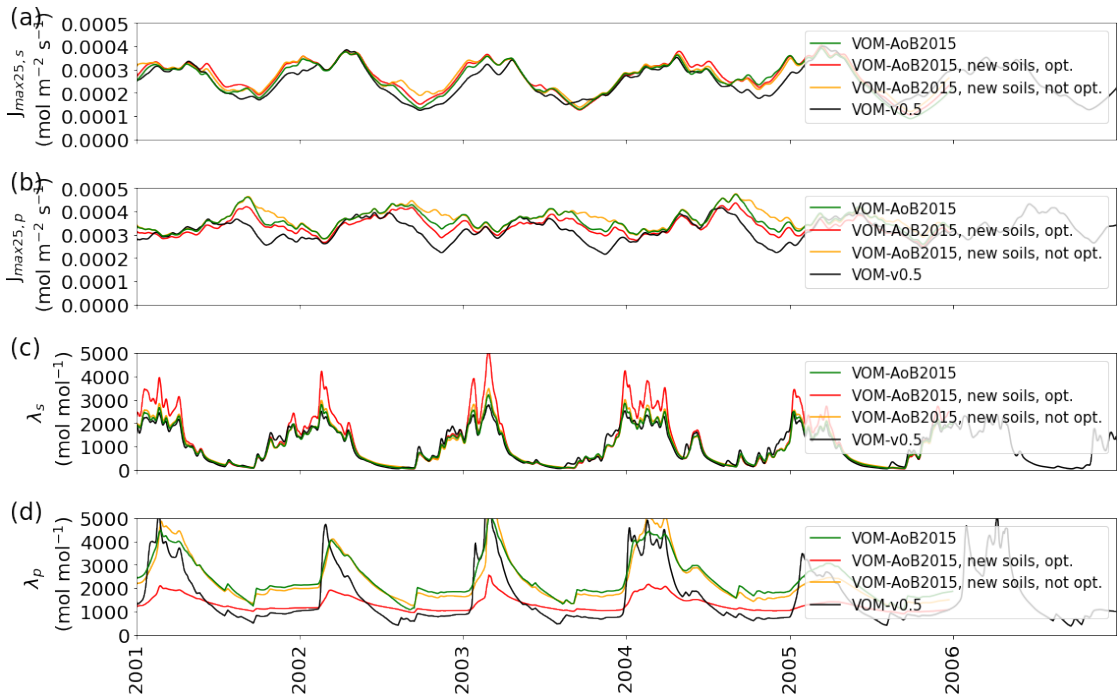

Figure S1.38. *Comparison for Howard Springs from 2001-2006 (subset from 1980-2017) between the results of Schymanski et al. (2015) (VOM-AoB2015, green), and a re-optimized reproduction of these results that use different, homogeneous soil parameters (VOM-AoB2015, new soils, opt., red), a reproduction of these results without optimization using the parameter from the VOM-AoB2015 (VOM-AoB2015, new soils, not opt., yellow) and the new VOM-v0.5 modelling results (black), for a) the electron transport capacity at 25 ^oC for seasonal grasses ($J_{max25,s}$), b) the electron transport capacity at 25 ^oC for perennials trees ($J_{max25,p}$), d) transpiration seasonals (grasses), d) the daily slope (λ_s) between assimilation and transpiration of the seasonal grasses, e) the daily slope (λ_p) between assimilation and transpiration of the perennials (trees).*

The values for the slope λ_p between assimilation and transpiration of the perennial vegetation are reduced with the new soil parameterization, whereas the slope increases during the wet season for the seasonal vegetation. The electron transport capacities for both seasonal and perennial vegetation decrease after changing the soil parameterization.

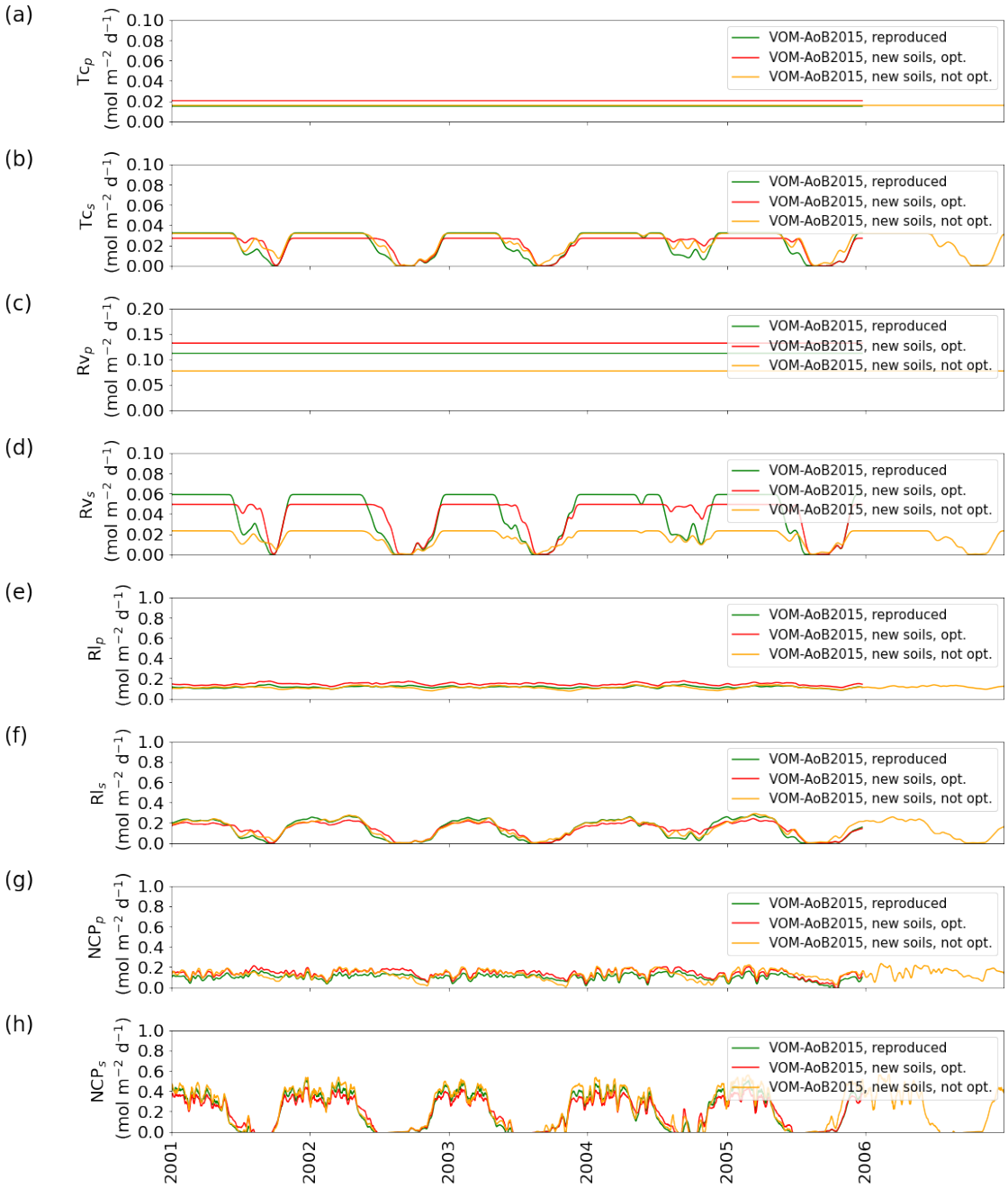

Figure S1.39. *Comparison for Howard Springs from 2001-2006 (subset from 1980-2017) between the reproduced results of Schymanski et al. (2015) (VOM-AoB2015, green), and a re-optimized reproduction of these results that use different, homogeneous soil parameters (VOM-AoB2015, new soils, opt., red), a reproduction of these results without optimization using the parameter from the VOM-AoB2015 (VOM-AoB2015, new soils, not opt., yellow) and the new VOM-v0.5 modelling results (black), for a) the foliage turnover costs perennial trees (Tc_p), b) the foliage turnover costs seasonal grasses (Tc_s), c) the water transport costs for perennial trees (Rv_p), d) the water transport costs for seasonal grasses (Rv_s), e) leaf respiration perennial trees (Rl_p), f)leaf respiration seasonal*

grasses (Rl_s), g) root respiration perennial trees (Rr_p), h) root respiration seasonal grasses (Rr_s), all smoothed with a moving average of 7 days, and h) projective cover. Note that the original results of Schymanski et al. (2015) are not shown, as these variables were not produced as outputs, but only the reproduced values are shown.

The results in terms of carbon costs are slightly different for the grasses for the water transport system (Rv_s) and the foliage turnover costs (Tc_s).

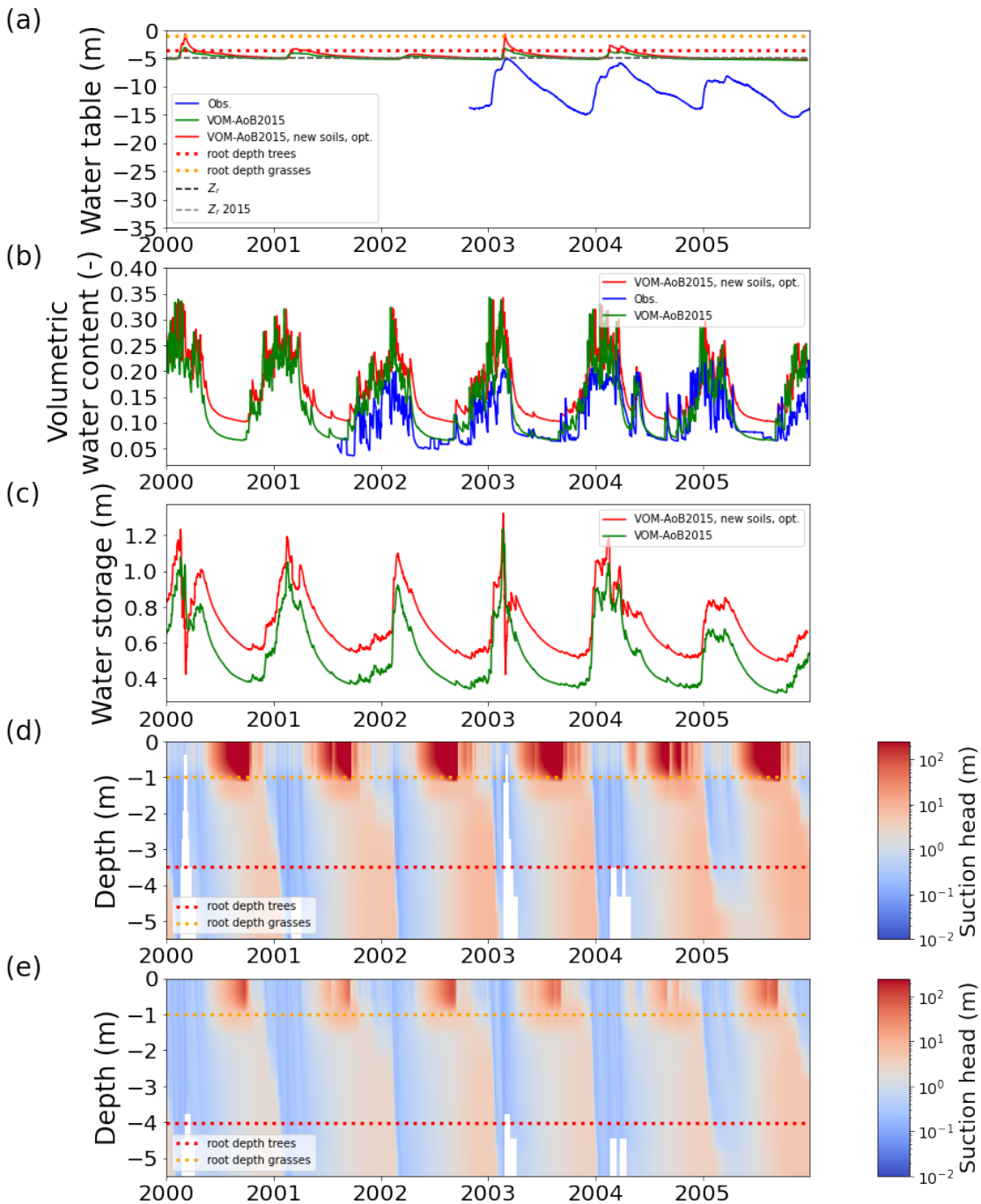

Figure S1.40. *Results for Howard Springs with a) groundwater depths, with dashed lines representing the bedrock depth, dotted lines the rooting depths (trees in red and grasses in orange), the re-optimized, reproduced results that use different, homogeneous soil parameters (VOM-AoB2015, new soils, opt.), the results of Schymanski et al. (2015) in green (VOM-AoB2015), and observations of three different boreholes in the vicinity of the study site in blue (Government Northern Territory, Australia, 2018). The soil moisture saturation in the upper soil layer is shown for Howard Springs in b) with the reproduced results of Schymanski et al. (2015) in red (VOM-AoB2015, new soils, opt.), the results of Schymanski et al. (2015) in green (VOM-AoB2015) and soil moisture measurements at 5 cm depth at the flux tower sites in blue. The total water storage in the root zone is shown in c) for the reproduced results of Schymanski et al. (2015) (VOM-AoB2015, new soils, opt., red) and the results of Schymanski et al. (2015) in green (VOM-AoB2015). The matrix water suction heads are shown in d) for the model runs of the VOM with new soil parameters, whereas e) displays the water suction heads of Schymanski et al. (2015).*

The volumetric water content and the water storage increased with the new soil parameterization, als matrix potentials showed increased values in the upper layers.

Concluding remarks

The new soil parameterization led to higher soil evaporation and lower transpiration, as well as lower GPP values for the seasonal grasses (Figures S1.37-1.40). More water stays in the soil due to a higher resistance to flow, making more moisture available for soil evaporation, which can also be noted from the volumtric water content and the matrix potentials.

1.11 New Ksat

The saturated hydraulic conductivity was changed to a much smaller value (similar as for sandy clay loam), in order to assess the sensitivity to just this soil parameter.

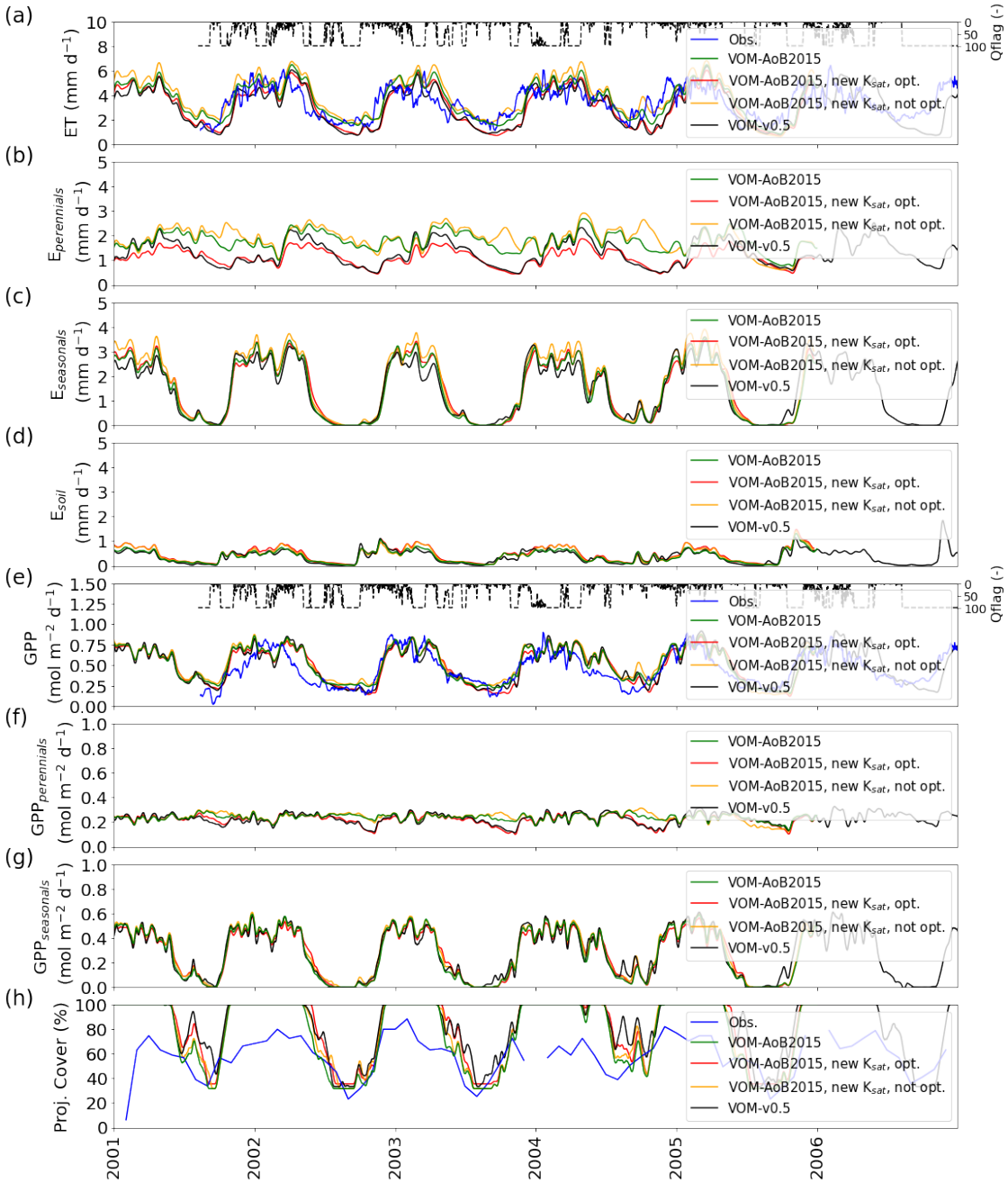

Figure S1.41. *Comparison for Howard Springs from 2001-2006 (subset from 1980-2017) between the results of Schymanski et al. (2015) (VOM-AoB2015, green), and a re-optimized reproduction of these results that use the same homogeneous soil parameters except for a decreases saturated hydraulic conductivity (VOM-AoB2015, new K_{sat}, opt., red), a reproduction of these results without optimization using the parameters from the VOM-AoB2015 (VOM-AoB2015, new K_{sat}, not opt., yellow) and the new VOM-v0.5 modelling results (black), for a) ET, b) transpiration perennials (trees), c) transpiration seasonals (grasses), d) soil evaporation, e) GPP, f) GPP perennials (trees), g) GPP seasonals (grasses), all smoothed with a moving average of 7 days, and*

h) projective cover. The daily average quality flags of the fluxtower observations are shown in dashed lines with a value of 100 when a day is completely gap-filled and 1 when it is observed.

The new soil saturated hydraulic conductivity leads to a decrease in especially the transpiration of the perennials, but also the seasonals. The GPP values for the perennial vegetation reduces as well, whereas the projective cover increases.

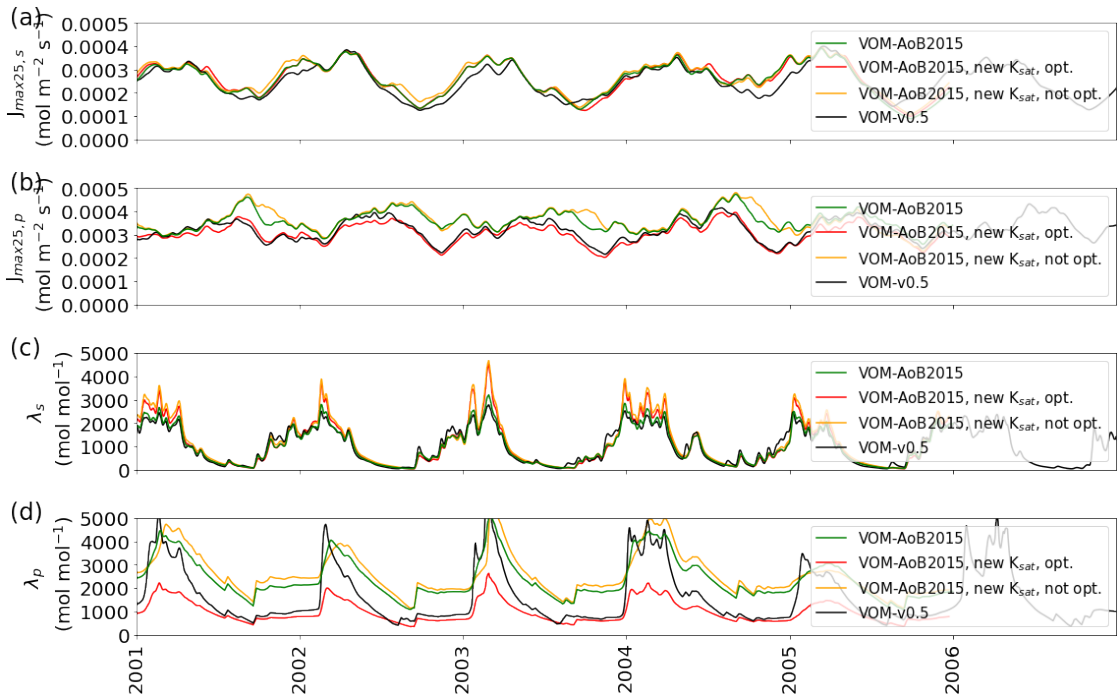

Figure S1.42. *Comparison for Howard Springs from 2001-2006 (subset from 1980-2017) between the results of Schymanski et al. (2015) (VOM-AoB2015, green), and a re-optimized reproduction of these results that use the same homogeneous soil parameters except for a decreases saturated hydraulic conductivity (VOM-AoB2015, new K_{sat}, opt., red), a reproduction of these results without optimization using the parameters from the VOM-AoB2015 (VOM-AoB2015, new K_{sat}, not opt., yellow) and the new VOM-v0.5 modelling results (black), for a) the electron transport capacity at 25 ^oC for seasonal grasses ($J_{max25,s}$), b) the electron transport capacity at 25 ^oC for perennials trees ($J_{max25,p}$), d) transpiration seasonals (grasses), d) the daily slope (λ_s) between assimilation and transpiration of the seasonal grasses, e) the daily slope (λ_p) between assimilation and transpiration of the perennials (trees).*

The values for the slope λ_p between assimilation and transpiration of the perennial vegetation are reduced with the new hydraulic conductivity, whereas the slope λ_s stays similar for the seasonal vegetation. The electron transport capacities for perennial vegetation decreases as well after changing the hydraulic conductivity.

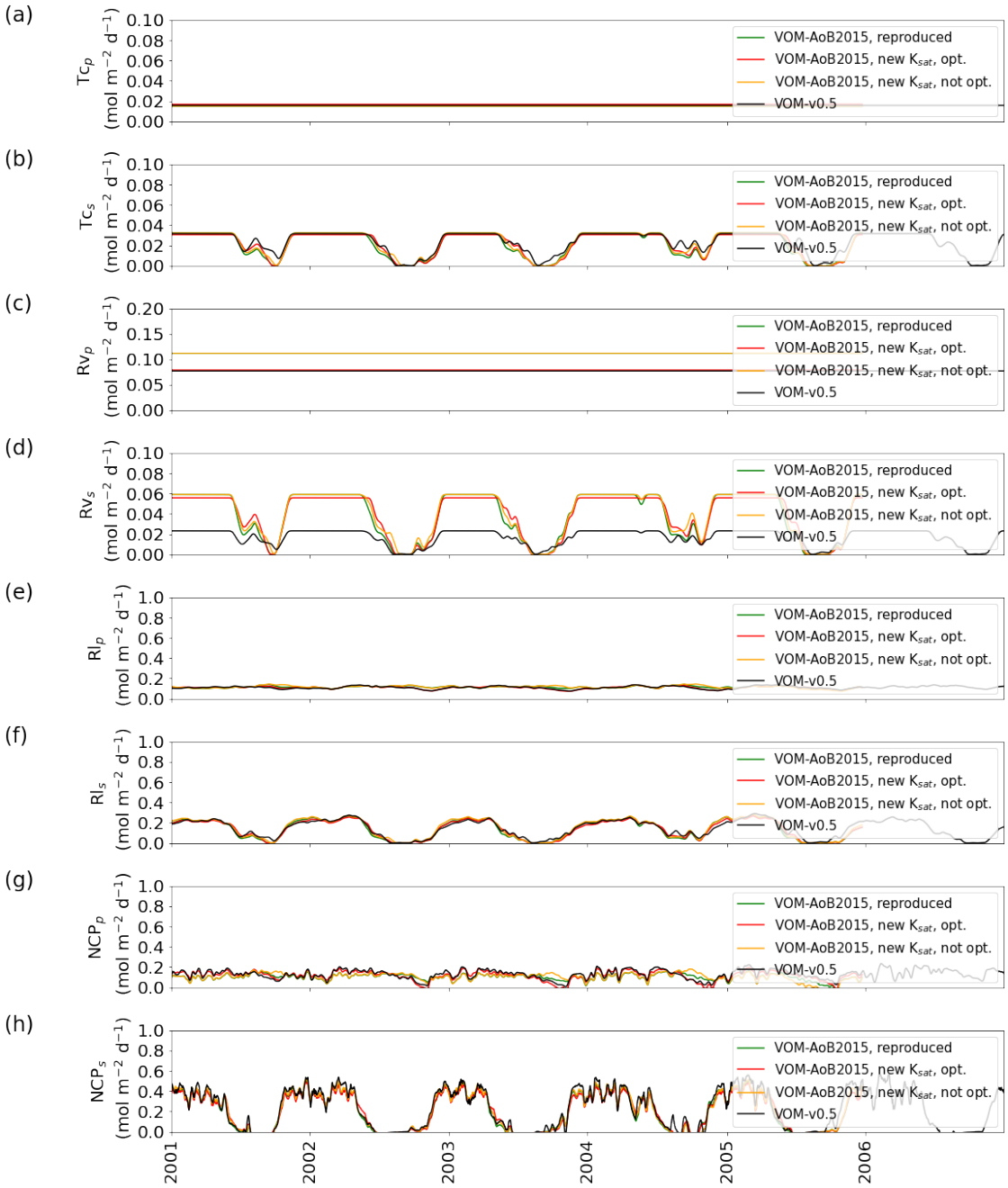

Figure S1.43. *Comparison for Howard Springs from 2001-2006 (subset from 1980-2017) between the reproduced results of Schymanski et al. (2015) (VOM-AoB2015, green), and a re-optimized reproduction of these results that use the same homogeneous soil parameters except for a decreases saturated hydraulic conductivity (VOM-AoB2015, new K_{sat}, opt., red), a reproduction of these results without optimization using the parameters from the VOM-AoB2015 (VOM-AoB2015, new K_{sat}, not opt., yellow) and the new VOM-v0.5 modelling results (black), for a) the foliage turnover costs perennial trees (Tc_p), b) the foliage turnover costs seasonal grasses (Tc_s), c) the water transport costs for perennial trees (Rv_p), d) the water transport costs for seasonal grasses*

(Rv_s), e) leaf respiration perennial trees (Rl_p), f)leaf respiration seasonal grasses (Rl_s), g) root respiration perennial trees (Rr_p), h) root respiration seasonal grasses (Rr_s), all smoothed with a moving average of 7 days, and h) projective cover.Note that the original results of Schymanski et al. (2015) are not shown, as these variables were not produced as outputs, but only the reproduced values are shown.

The results in terms of carbon costs remain rather similar, except for small changes in the costs for the seasonal vegetation.

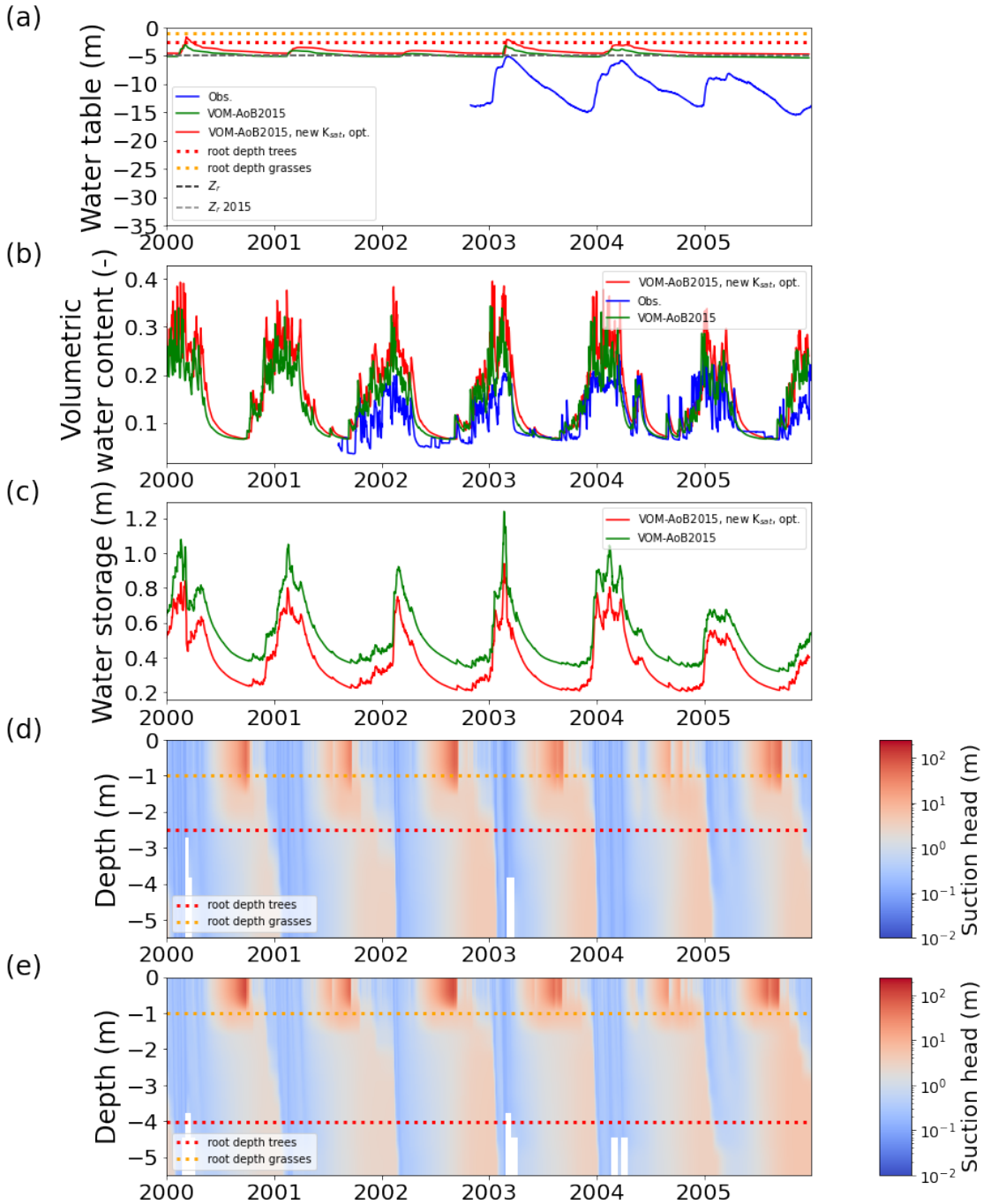

Figure S1.44. *Results for Howard Springs with a) groundwater depths, with dashed lines representing the bedrock depth, dotted lines the rooting depths (trees in red and grasses in orange), the re-optimized, reproduced results that use the same homogeneous soil parameters except for a decreases saturated hydraulic conductivity (VOM-AoB2015, new K_{sat}, opt.), the results of Schymanski et al. (2015) in green (VOM-AoB2015), and observations of three different boreholes in the vicinity of the study site in blue (Government Northern Territory, Australia, 2018). The*

soil moisture saturation in the upper soil layer is shown for Howard Springs in b) with the reproduced results of Schymanski et al. (2015) in red (VOM-AoB2015, new K_{sat}, opt.), the results of Schymanski et al. (2015) in green (VOM-AoB2015) and soil moisture measurements at 5 cm depth at the flux tower sites in blue. The total water storage in the root zone is shown in c) for the reproduced results of Schymanski et al. (2015) (VOM-AoB2015, new K_{sat}, opt., red) and the results of Schymanski et al. (2015) in green (VOM-AoB2015). The matrix water suction heads are shown in d) for the model runs of the VOM with a new saturated hydraulic conductivity, whereas e) displays the water suction heads of Schymanski et al. (2015).

The groundwater, volumetric water content and water storage slightly increased due to the lower saturated conductivity. The differences in matrix potentials are however minor.

Concluding remarks

A lower saturated conductivity mainly affects the perennial trees, that have lower values of GPP and transpiration (Figures S1.41-S1.44), but also the seasonal grasses show reduced values for the transpiration. This relates to the deeper roots of the perennial trees, and the different hydraulic conductivity makes it harder to maintain a higher root water uptake.

1.12 New soil profile and hydrology

A new soil profile was added in contrast to the homogeneous soil profile used by Schymanski et al. (2015). At the same time, hydrology was now set to be freely draining.

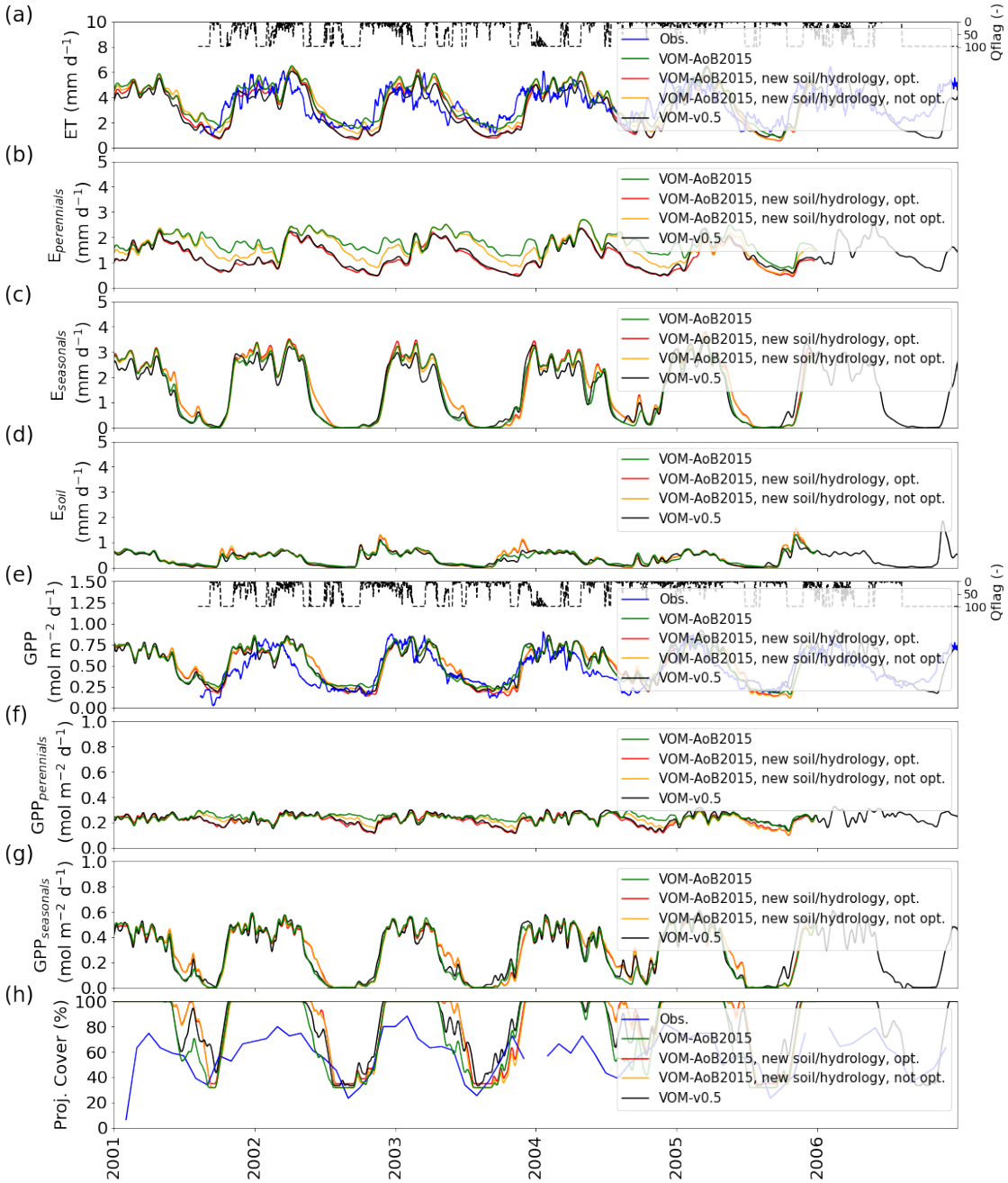

Figure S1.45. *Comparison for Howard Springs from 2001-2006 (subset from 1980-2017) between the results of Schymanski et al. (2015) (VOM-AoB2015, green), and a re-optimized reproduction of these results that use a new soil and hydrological parameterization (VOM-AoB2015, new soil/hydrology, opt., red), a reproduction of these results without optimization using the parameters from the VOM-AoB2015 (VOM-AoB2015, new soil/hydrology, not opt., yellow) and the new VOM-v0.5 modelling results (black), for a) ET, b) transpiration perennials (trees), c) transpiration seasonals (grasses), d) soil evaporation, e) GPP, f) GPP perennials (trees), g) GPP seasonals (grasses), all smoothed with a moving average of 7 days, and h) projective cover. The daily average*

quality flags of the fluxtower observations are shown in dashed lines with a value of 100 when a day is completely gap-filled and 1 when it is observed.

It can be noted that especially the transpiration of the perennial vegetation decreases, but also the GPP of the perennial vegetation. The projective cover also increases for the new set-up.

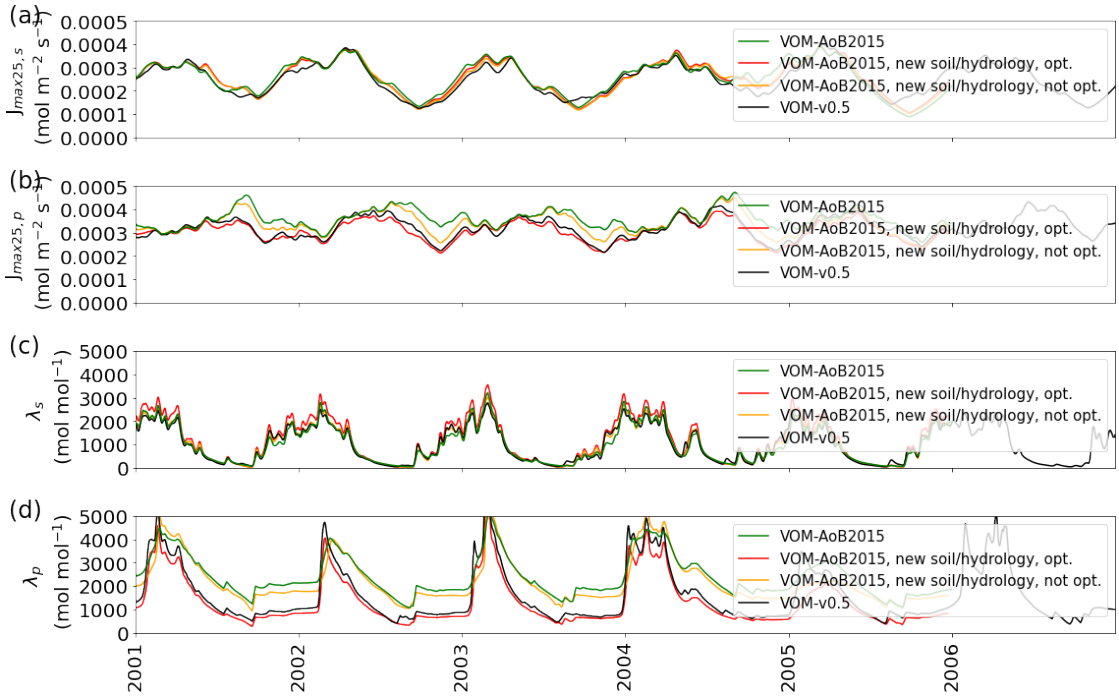

Figure S1.46. *Comparison for Howard Springs from 2001-2006 (subset from 1980-2017) between the results of Schymanski et al. (2015) (VOM-AoB2015, green), and a re-optimized reproduction of these results that use a new soil and hydrological parameterization (VOM-AoB2015, new soil/hydrology, opt., red), a reproduction of these results without optimization using the parameters from the VOM-AoB2015 (VOM-AoB2015, new soil/hydrology, not opt., yellow) and the new VOM-v0.5 modelling results (black), for a) the electron transport capacity at 25 ^oC for seasonal grasses ($J_{max25,s}$), b) the electron transport capacity at 25 ^oC for perennials trees ($J_{max25,p}$), d) transpiration seasonals (grasses), d) the daily slope (λ_s) between assimilation and transpiration of the seasonal grasses, e) the daily slope (λ_p) between assimilation and transpiration of the perennials (trees).*

The values for the slope λ_p between assimilation and transpiration of the perennial vegetation are reduced with the new soil parameterization, whereas the slope λ_s stays similar for the seasonal vegetation. The electron transport capacities for both seasonal and perennial vegetation decreases after changing the soil and hydrological parameterization.

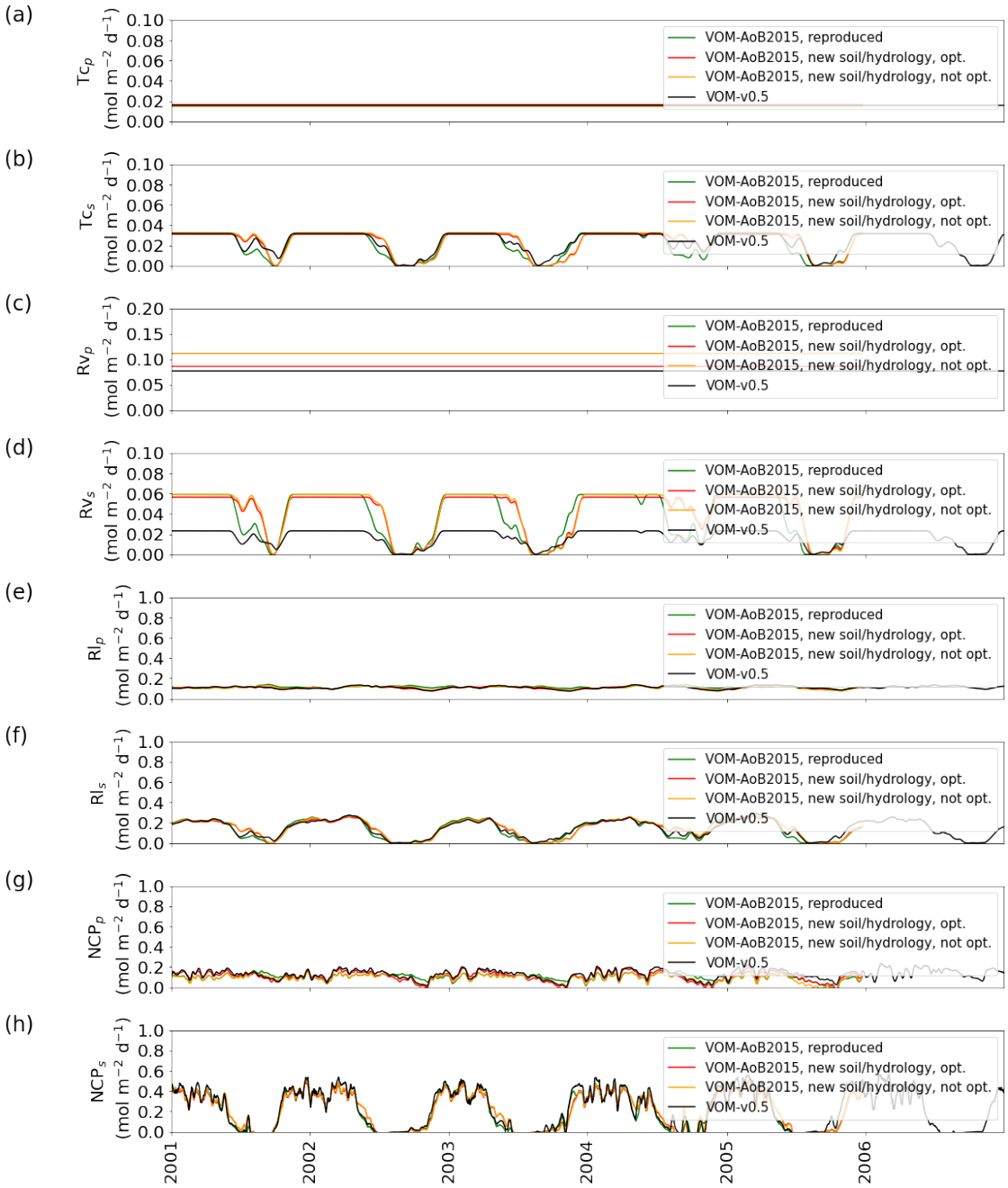

Figure S1.47. *Comparison for Howard Springs from 2001-2006 (subset from 1980-2017) between the reproduced results of Schymanski et al. (2015) (VOM-AoB2015, reproduced, green), and a re-optimized reproduction of these results that use a new soil and hydrological parameterization (VOM-AoB2015, new soil/hydrology, opt., red), a reproduction of these results without optimization using the parameters from the VOM-AoB2015 (VOM-AoB2015, new soil/hydrology, not opt., yellow) and the new VOM-v0.5 modelling results (black), for a) the foliage turnover costs perennial trees (Tc_p), b) the foliage turnover costs seasonal grasses (Tc_s), c) the water transport costs for perennial trees (Rv_p), d) the water transport costs for seasonal grasses (Rv_s), e) leaf respiration*

perennial trees (Rl_p), f)leaf respiration seasonal grasses (Rl_s), g) root respiration perennial trees (Rr_p), h) root respiration seasonal grasses (Rr_s), all smoothed with a moving average of 7 days, and h) projective cover. Note that the original results of Schymanski et al. (2015) are not shown, as these variables were not produced as outputs, but only the reproduced values are shown.

The results in terms of carbon costs are slightly different for the grasses for the water system (Rv_s) and the foliage turnover costs (Tc_s).

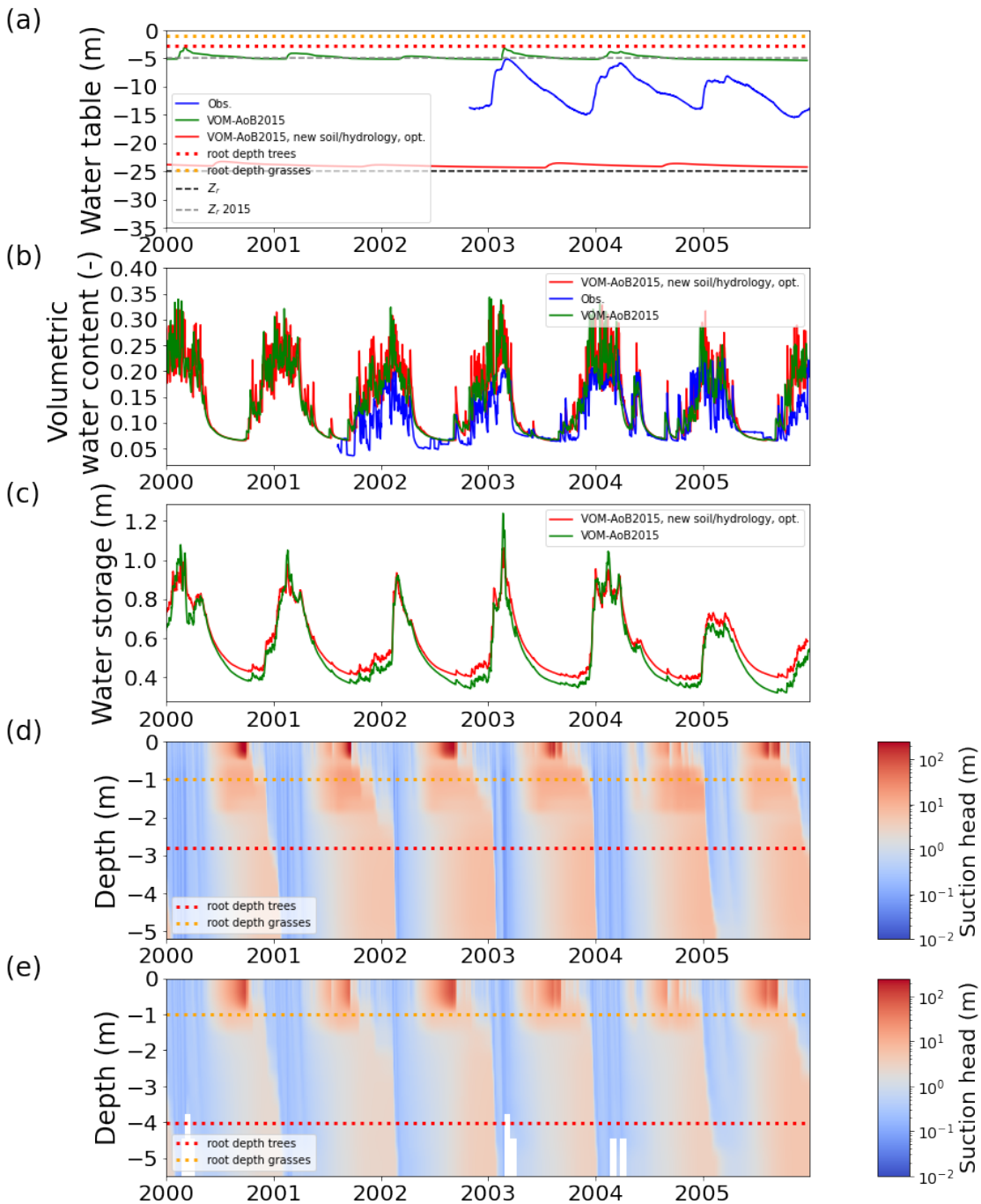

Figure S1.48. *Results for Howard Springs with a) groundwater depths, with dashed lines representing the bedrock depth, dotted lines the rooting depths (trees in red and grasses in orange), the re-optimized, reproduced results that use a new soil and hydrological parameterization (VOM-AoB2015, new soil/hydrology, opt.), the results of Schymanski et al. (2015) in green (VOM-AoB2015), and observations of three different boreholes in the vicinity of the study site in blue (Government Northern Territory, Australia, 2018). The soil moisture saturation in the upper soil layer is shown for Howard Springs in b) with the reproduced results of Schymanski et al. (2015) in red (VOM-AoB2015, new K_{sat}, opt.), the results of Schymanski et al. (2015) in green (VOM-AoB2015) and soil moisture measurements at 5 cm depth at the flux tower sites in blue. The total water storage in the root zone is shown in c) for the reproduced results of Schymanski et al. (2015) (VOM-AoB2015, new soil/hydrology, red) and the results of Schymanski et al. (2015) in green (VOM-AoB2015). The matrix water suction heads are shown in d) for the model runs of the VOM with a new soil and hydrological parameterization, whereas e) displays the water suction heads of Schymanski et al. (2015).*

The groundwater table is deeper for the new hydrological and soil parameterization. The water storage in the upper 5 meters increases as well as the matrix potentials.

Concluding remarks

Changing the soil and hydrological parameterization leads to a decrease in GPP and transpiration for especially the perennial trees (Figures S1.45-S1.48), whereas the values for the grasses remain rather similar. The groudwater tables are much deeper, but water storage and matrix potentials increase.

2 Comparative analysis

The effects of the changes are compared here. The starting points are therefore still the parameters and settings used by Schymanski et al. (2015). From there, one change is included at a time, to see the specific influence of each change.

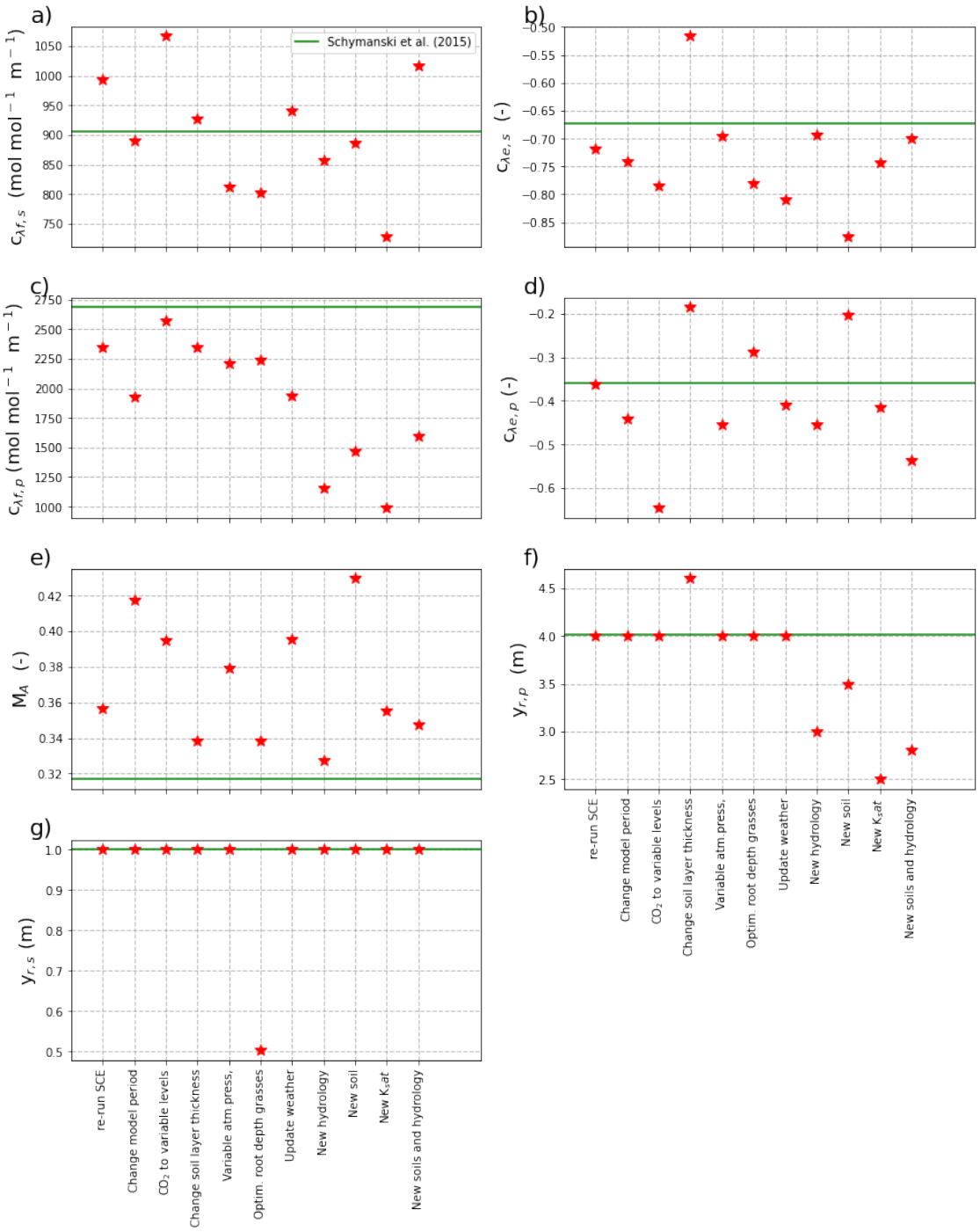

Figure S1.49. *Optimal vegetation parameters for the different incremental changes compared to Schymanski et al.(2015) (green line), for a) and b) the two parameters $c_{\lambda f,s}$ and $c_{\lambda e,s}$ effecting the water use for perennial vegetation, c) and d) the two parameters $c_{\lambda f,p}$ and $c_{\lambda e,p}$ effecting the water use for seasonal vegetation, e) vegetation cover of the perennial vegetation $M_{A,p}$, f) the rooting depth for the perennial vegetation $y_{r,p}$ and g) the rooting depth for the seasonal vegetation $y_{r,s}$.*

The vegetation cover M_A is especially sensitive to the new variable CO_2-levels, that are generally higher for the most recent years. The water use strategy parameters $c_{\lambda f,s}$, $c_{\lambda e,s}$, $c_{\lambda f,p}$ and $c_{\lambda e,p}$ show also the highest sensitivity for changes in hydrology, but also to the new soil parameters.

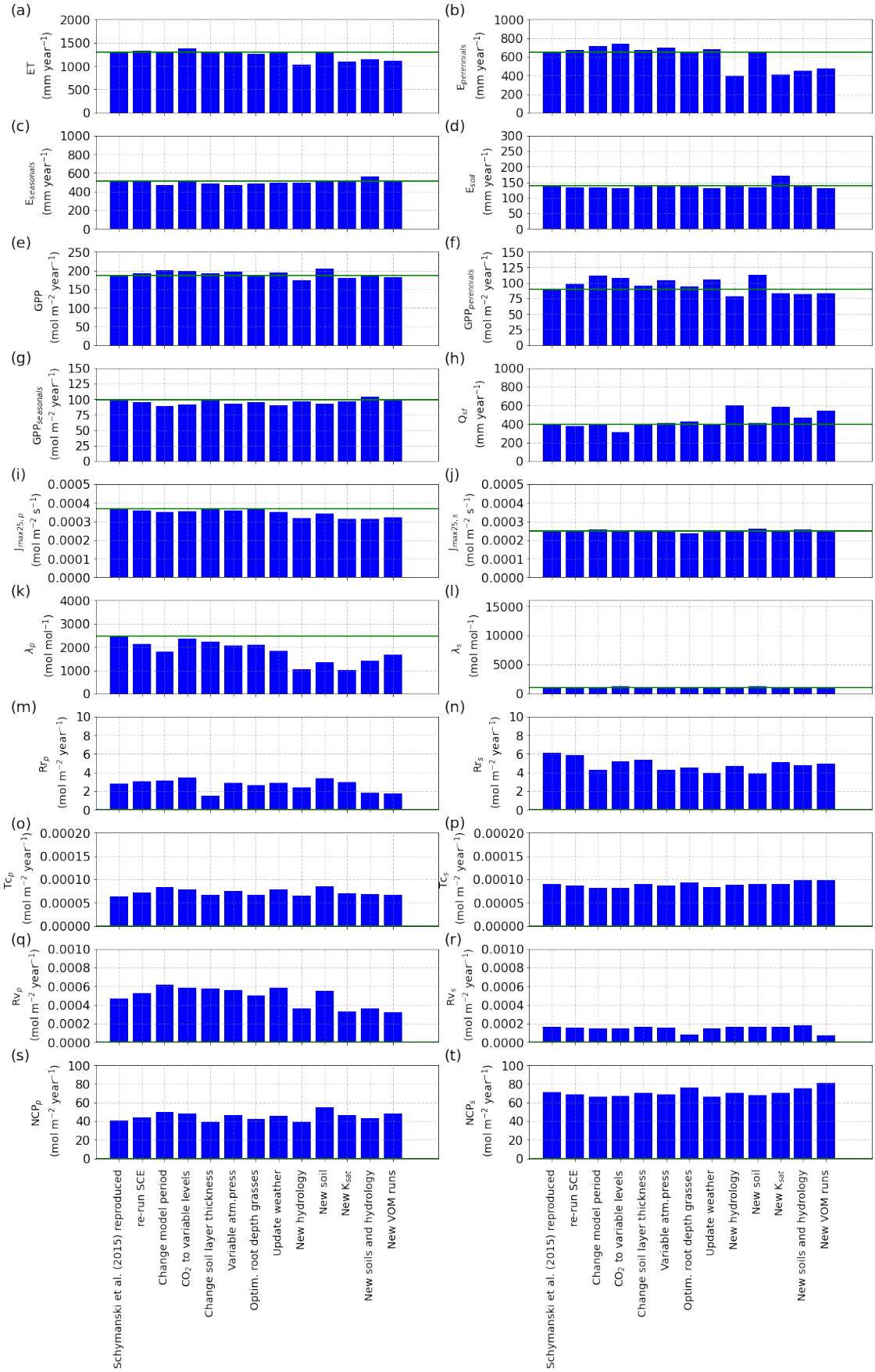
(a)
ET
(mm year^{-1})
(b)
$E_{perennials}$
(mm year^{-1})
(c)
$E_{seasonals}$
(mm year^{-1})
(d)
E_{soil}
(mm year^{-1})
(e)
GPP
(mol m^{-2} year^{-1})
(f)
$GPP_{perennials}$
(mol m^{-2} year^{-1})
(g)
$GPP_{seasonals}$
(mol m^{-2} year^{-1})
(h)
Q_{sf}
(mm year^{-1})
(i)
$J_{max25,p}$
(mol m^{-2} s^{-1})
(j)
$J_{max25,s}$
(mol m^{-2} s^{-1})
(k)
λ_p
(mol mol^{-1})
(l)
λ_s
(mol mol^{-1})
(m)
Rr_p
(mol m^{-2} year^{-1})
(n)
Rr_s
(mol m^{-2} year^{-1})
(o)
Tc_p
(mol m^{-2} year^{-1})
(p)
Tc_s
(mol m^{-2} year^{-1})
(q)
Rv_p
(mol m^{-2} year^{-1})
(r)
Rv_s
(mol m^{-2} year^{-1})
(s)
NCP_p
(mol m^{-2} year^{-1})
(t)
NCP_s
(mol m^{-2} year^{-1})
Schymanski et al. (2015) reproduced
re-run SCE
Change model period
CO_2 to variable levels
Change soil layer thickness
Variable atm.press
Optim. root depth grasses
Update weather
New hydrology
New soil
New K_{sat}
New soils and hydrology
New VOM runs

Figure S1.50. *Annual values for the different (incremental) changes in comparison with Schymanski et al. (2015) (green line), with a) mean annual ET, b) mean annual transpiration perennials (trees), c) mean annual transpiration seasonals (grasses), d) mean annual soil evaporation, e) mean annual GPP, f) mean annual GPP perennials (trees), g) mean annual GPP seasonals (grasses), h) mean annual seepage face flow (Q_sf), i) the mean electron transport capacity at 25 ^oC for seasonal grasses ($J_{max25,s}$), j) the mean electron transport capacity at 25 ^oC for perennials trees ($J_{max25,p}$), k) the mean daily slope (λ_s) between assimilation and transpiration of the seasonal grasses, l) the mean daily slope (λ_p) between assimilation and transpiration of the perennials (trees), m) the mean annual root respiration perennial trees (Rr_p), n) the mean annual root respiration seasonal grasses (Rr_s), o) the mean annual foliage turnover costs perennial trees (Tc_p), p) the mean annual foliage turnover costs seasonal grasses (Tc_s), q) the mean annual water transport costs for perennial trees (Rv_p), r) the mean annual water transport costs for seasonal grasses (Rv_s), s) mean annual net carbon profit for perennial trees (NCP_p), t) mean annual net carbon profit for seasonal grasses (NCP_s).*

GPP and ET are mainly reduced after changes in the soil and hydrology parameterizations. In contrast, using variable CO_2-levels leads to increased values of GPP. It can also be noted that especially λ_s and the soil evaporation increase due to changes in the soil parameterizations.

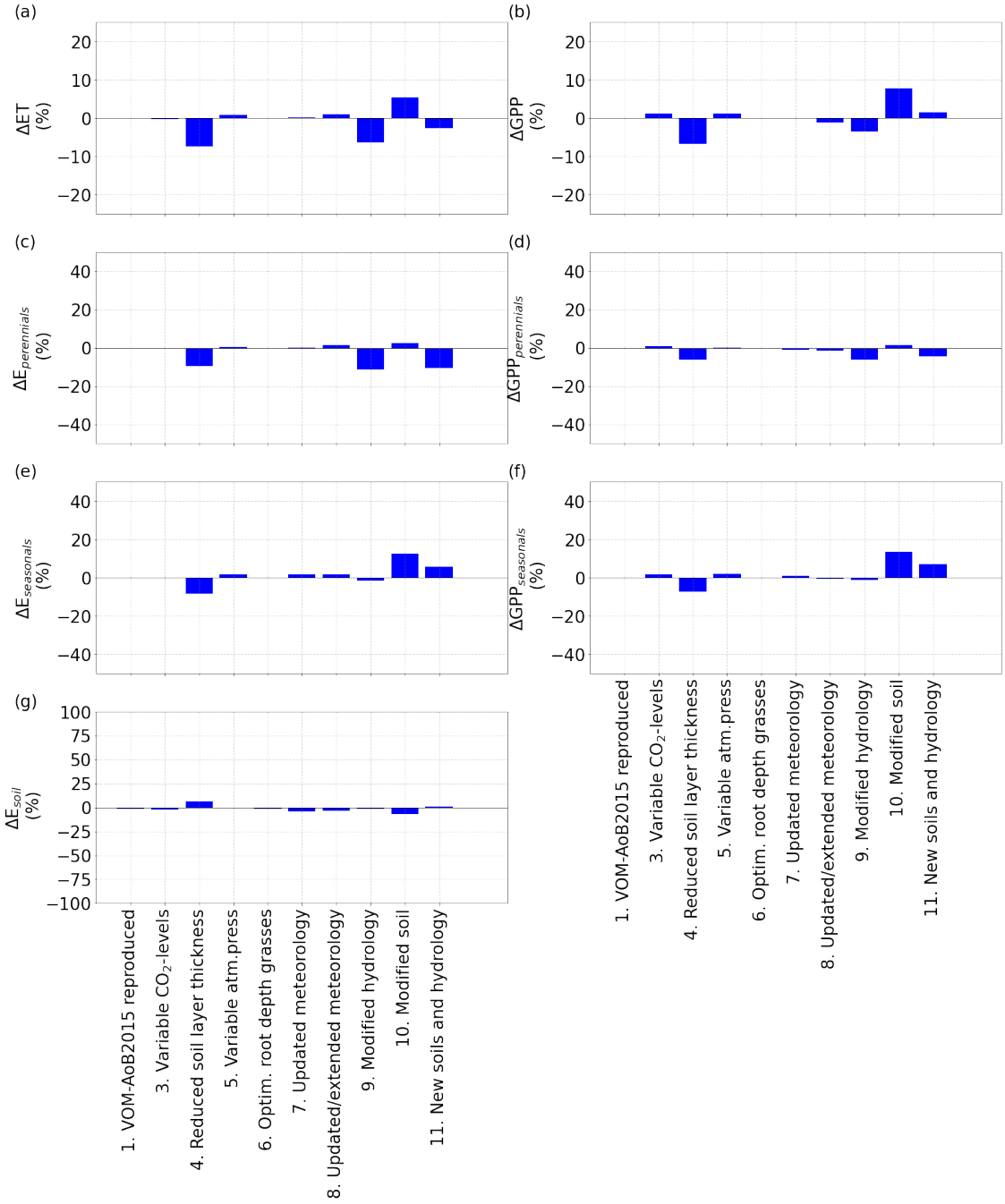

Figure S1.51. *Relative changes in mean annual values of the fluxes for the different (incremental) changes, without re-optimizing (i.e. with the vegetation parameters of the VOM-AoB2015), in comparison with the VOM-AoB2015, for for a) ET, b) GPP, c) transpiration perennials (trees), d) GPP perennials (trees), e) transpiration seasonals (grasses), f) GPP seasonals (grasses), g) soil evaporation.*

3 Resulting differences

Eventually, all implemented changes lead to differences in model results, that are assesed here.

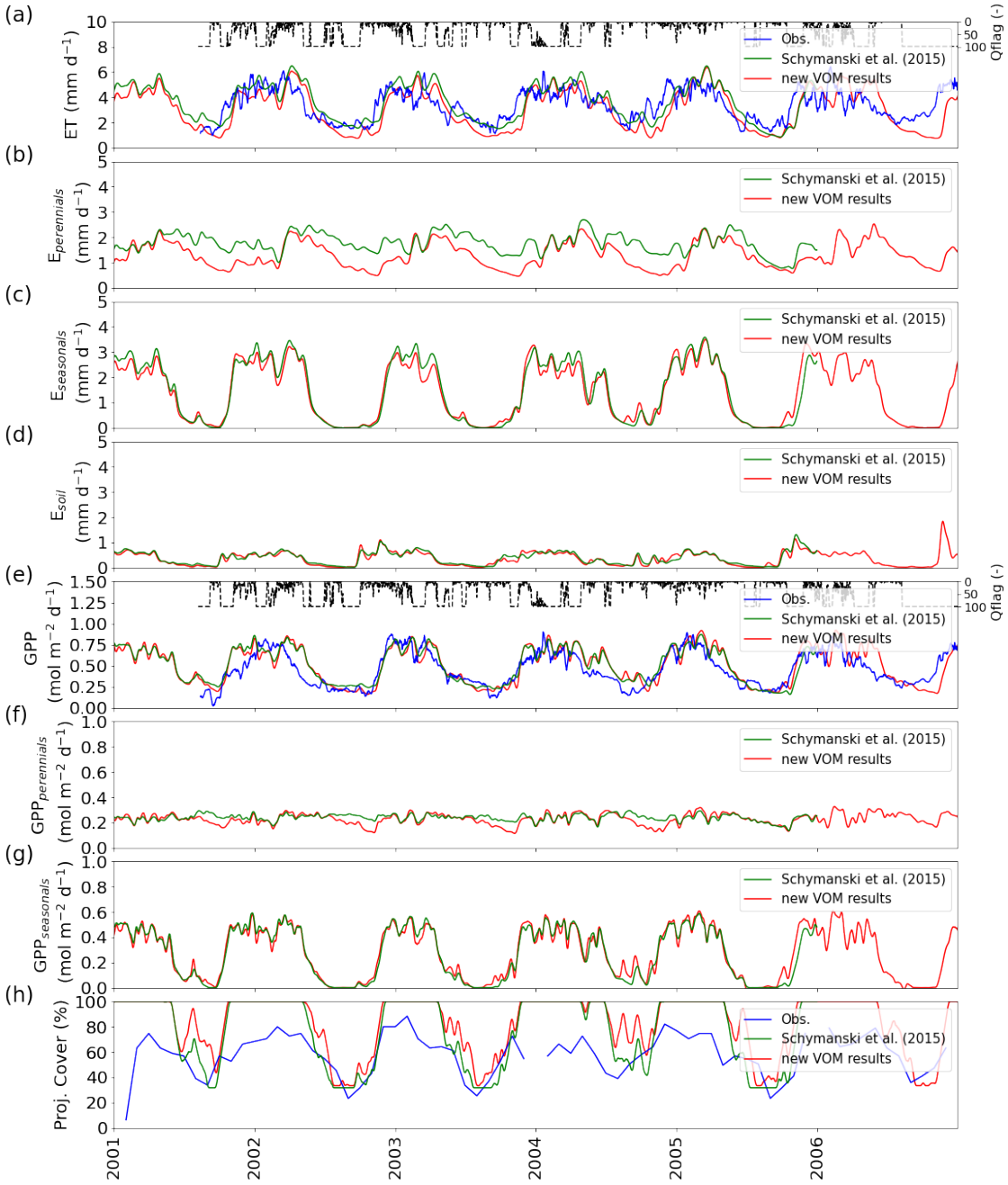

Figure S1.52. *Comparison for Howard Springs from 2001-2006 (subset from 1980-2017) between the results of Schymanski et al. (2015) (green) and the new results that implemented all changes (red), for a) ET, b) transpiration perennials (trees), c) transpiration seasonals (grasses), d) soil evaporation, e) GPP, f) GPP perennials (trees), g) GPP seasonals (grasses), all smoothed with a*

moving average of 7 days, and h) projective cover. The daily average quality flags of the fluxtower observations are shown in dashed lines with a value of 100 when a day is completely gap-filled and 1 when it is observed.

These smoothed results are similar between the reproduced runs, and the original results of Schymanski et al. (2015), but there is a small a shift in time due to leap years, that were not accounted for by Schymanski et al. (2015).

Figure S1.53. *Comparison for Howard Springs from 2001-2006 (subset from 1980-2017) between the results of Schymanski et al. (2015) (green) and the new results that implemented all changes (red), for a) the electron transport capacity at 25 ^oC for seasonal grasses ($J_{max25,s}$), b) the electron transport capacity at 25 ^oC for perennials trees ($J_{max25,p}$), d) transpiration seasonals (grasses), d) the daily slope (λ_s) between assimilation and transpiration of the seasonal grasses, e) the daily slope (λ_p) between assimilation and transpiration of the perennials (trees).*

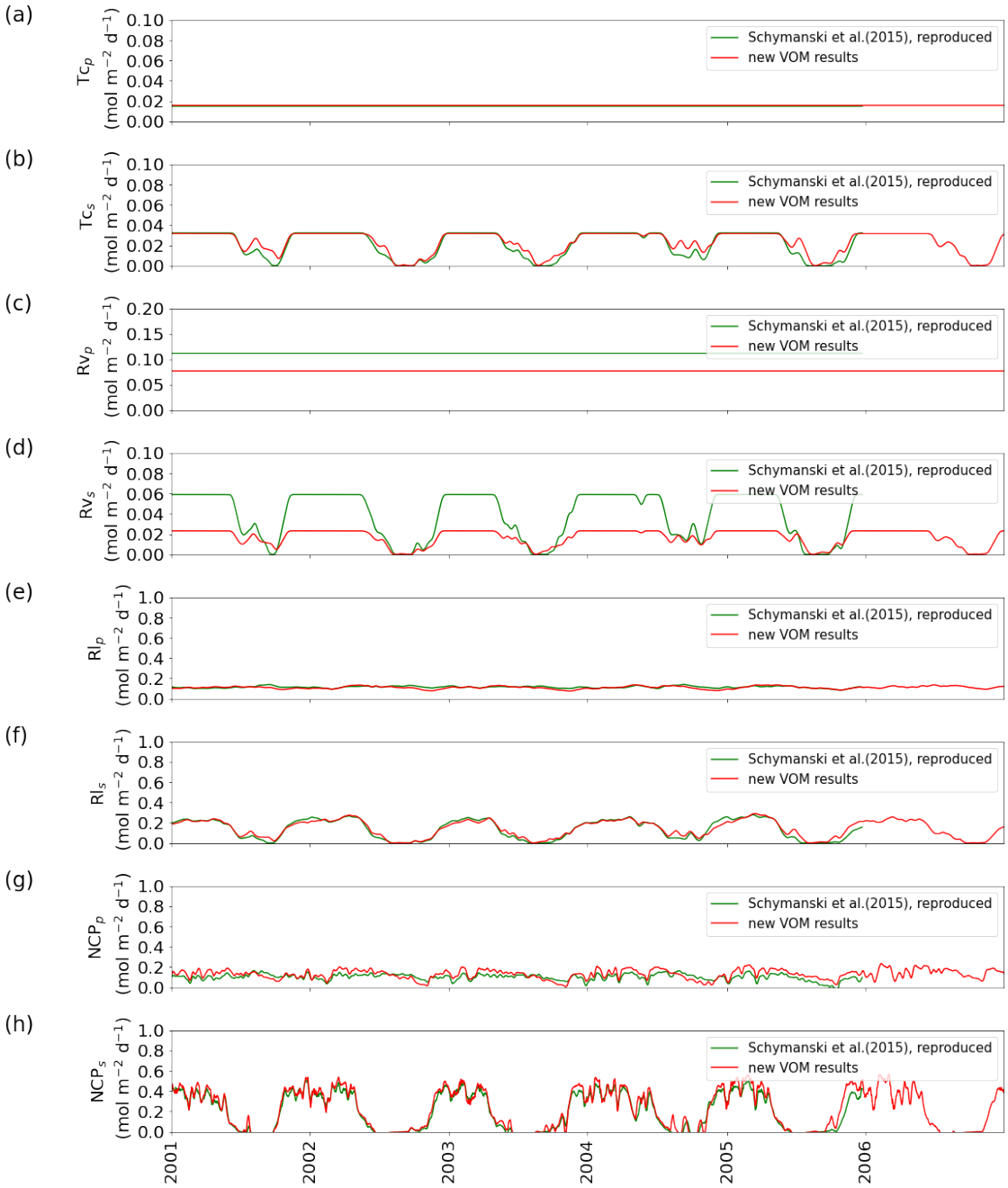

Figure S1.54. *Comparison for Howard Springs from 2001-2006 (subset from 1980-2017) between a reproduction of the results of Schymanski et al. (2015) (green) based on the best run of the SCE-algorithm from Schymanski et al. (2015), and the new VOM modelling results that implemented all changes (red), for a) the foliage turnover costs perennial trees (Tc_p), b) the foliage turnover costs seasonal grasses (Tc_s), c) the water transport costs for perennial trees (Rv_p), d) the water transport costs for seasonal grasses (Rv_s), e) leaf respiration perennial trees (Rl_p), f)leaf respiration seasonal grasses (Rl_s), g) root respiration perennial trees (Rr_p), h) root respiration seasonal grasses (Rr_s), all smoothed with a moving average of 7 days, and h) projective cover. Note that the original results*

of Schymanski et al. (2015) are not shown, as these variables were not produced as outputs, but only the reproduced values are shown.

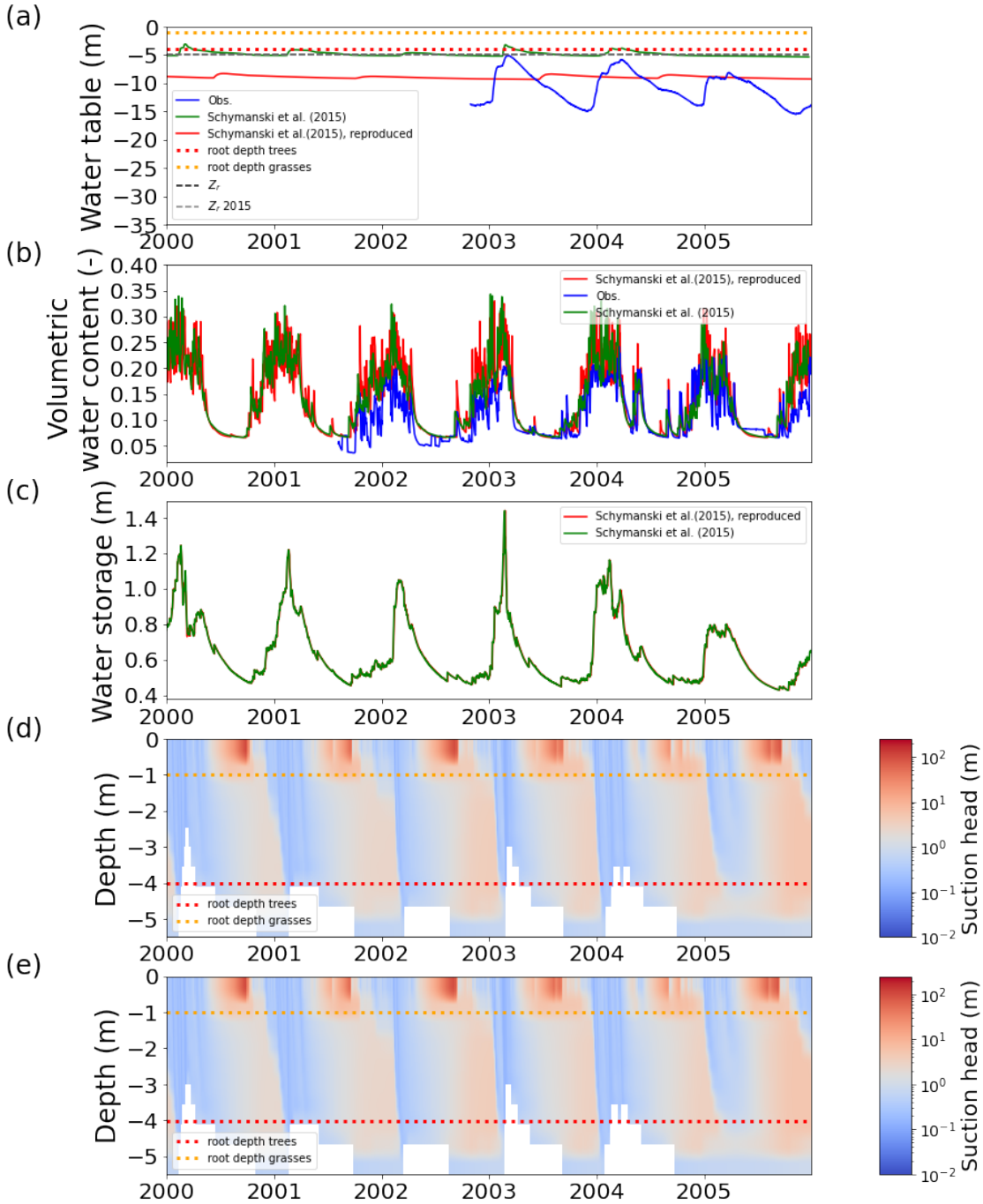

Figure S1.55. *Results for Howard Springs with a) groundwater depths, with dashed lines representing the bedrock depth, dotted lines the rooting depths (trees in red and grasses in orange), the ne VOM results in red, the results of Schymanski et al. (2015) in green, and observations of three different boreholes in the vicinity of the study site in blue (Government Northern Territory,*

Australia, 2018). The soil moisture saturation in the upper soil layer is shown for Howard Springs in b) with the new VOM results in red, the results of Schymanski et al. (2015) in green and soil moisture measurements at 5 cm depth at the flux tower sites in blue. The total water storage in the upper 5 m is shown in c) for the new VOM results (red) and the results of Schymanski et al. (2015) in green. The matrix water potentials are shown in d) for the current model runs of the VOM, whereas e) displays the matrix water potentials of Schymanski et al. (2015).

4 Influence of water use parameters

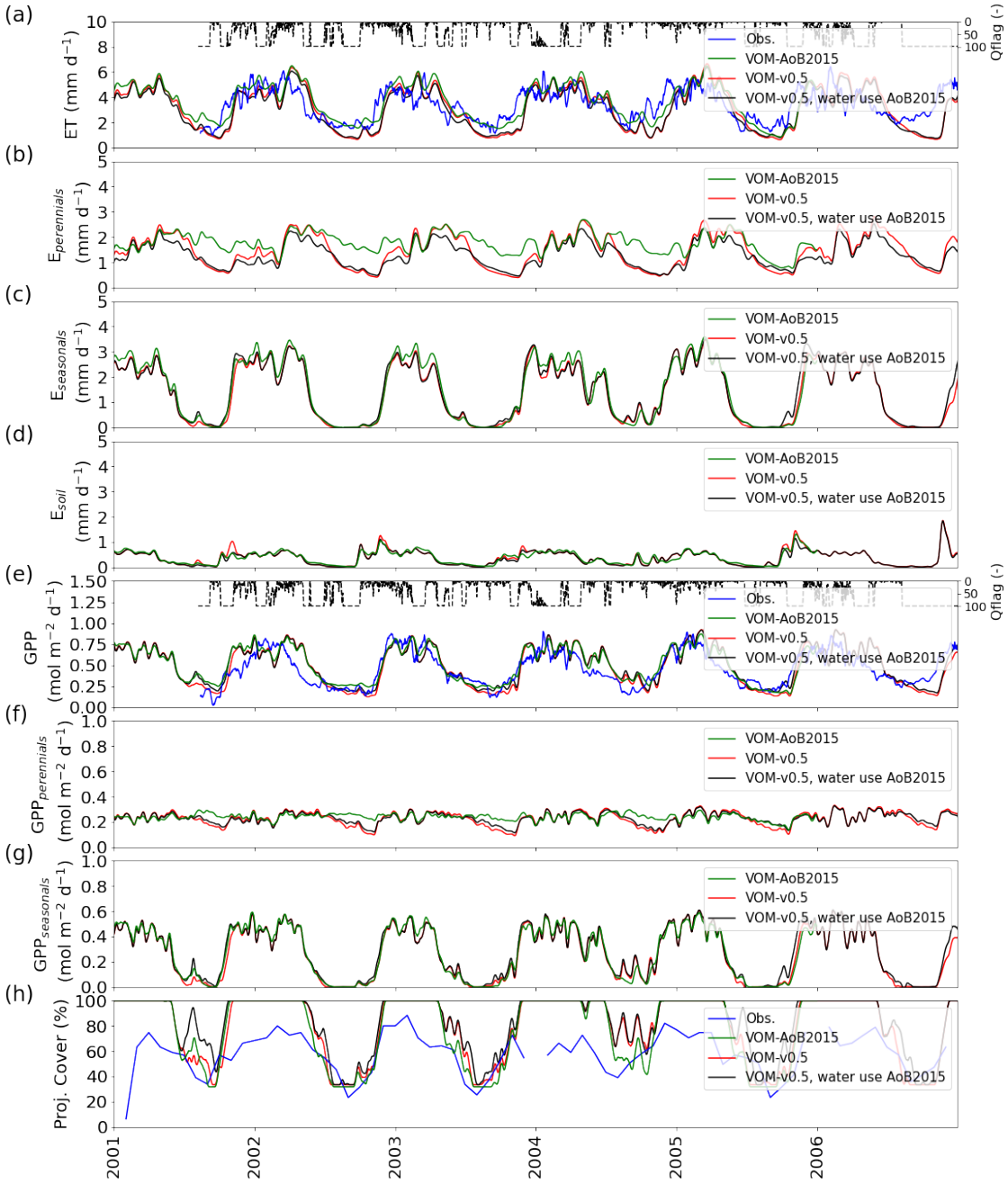

Figure S1.56. *Comparison for Howard Springs from 2001-2006 (subset from 1980-2017) between the results of Schymanski et al. (2015) (green) and the new results that implemented all changes (VOM-v0.5, red) and the VOM-v0.5 with the water use parameters of Schymanski et al. (2015), for a) ET, b) transpiration perennials (trees), c) transpiration seasonals (grasses), d) soil evaporation, e) GPP, f) GPP perennials (trees), g) GPP seasonals (grasses), all smoothed with a moving average of 7 days, and h) projective cover. The daily average quality flags of the fluxtower observations are shown in dashed lines with a value of 100 when a day is completely gap-filled and 1 when it is observed.*

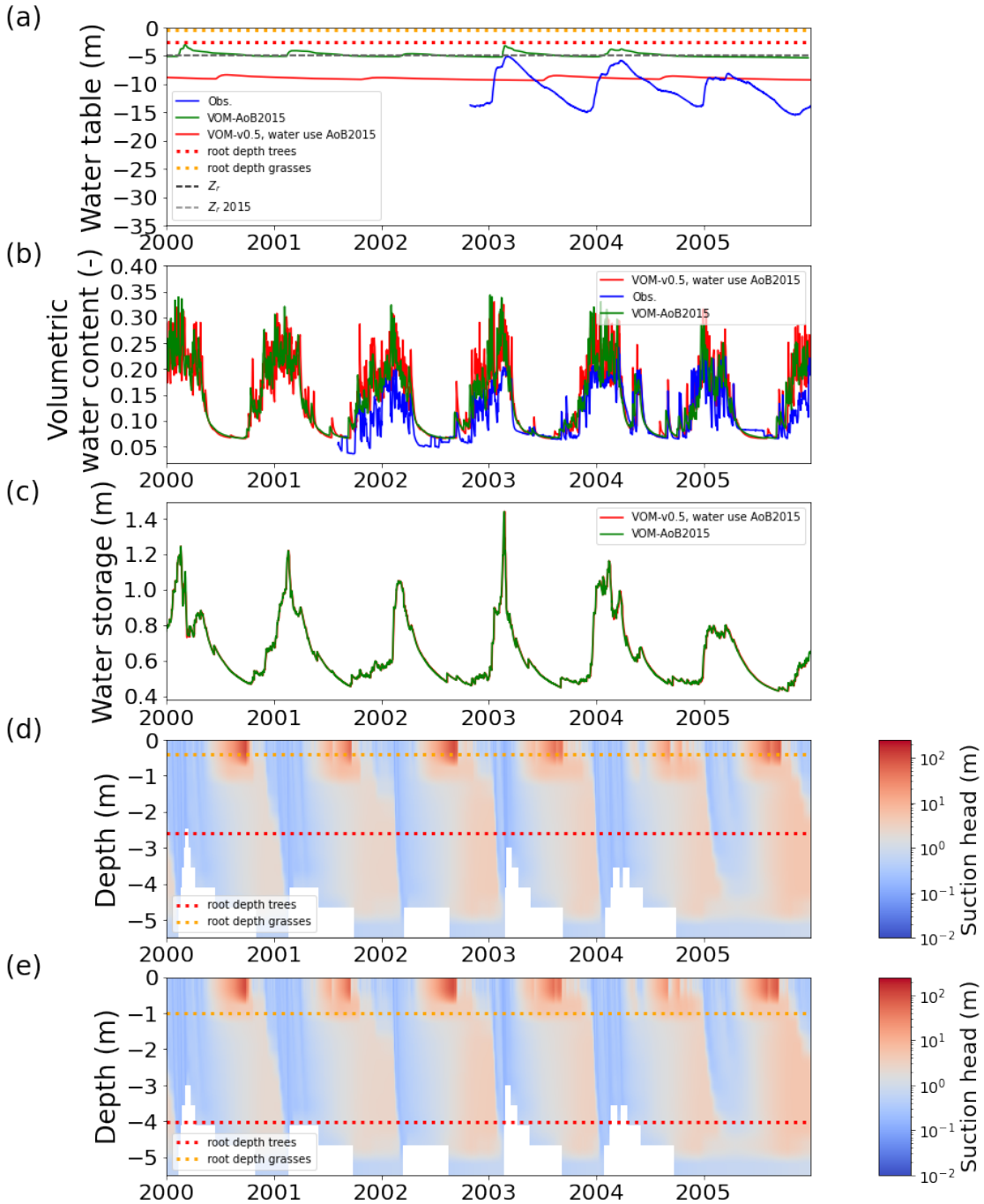

Figure S1.57. *Results for Howard Springs with a) groundwater depths, with dashed lines representing the bedrock depth, dotted lines the rooting depths (trees in red and grasses in orange), the results of Schymanski et al. (2015) (green) and the new results that implemented all changes (VOM-v0.5, red) and the VOM-v0.5 with the water use parameters of Schymanski et al. (2015), and observations of three different boreholes in the vicinity of the study site in blue (Government Northern Territory, Australia, 2018). The soil moisture saturation in the upper soil layer is shown*

for Howard Springs in b) with the new VOM results in red, the results of Schymanski et al. (2015) in green and soil moisture measurements at 5 cm depth at the flux tower sites in blue. The total water storage in the upper 5 m is shown in c) for the new VOM results (red) and the results of Schymanski et al. (2015) in green. The matrix water potentials are shown in d) for the current model runs of the VOM, whereas e) displays the matrix water potentials of the VOM-v0.5 with the water use parameters of Schymanski et al. (2015).